The Essentiality of DivIVA$_{Ef}$ Oligomerization for Proper Cell Division in *Enterococcus faecalis* and Interaction with a Novel Cell Division Protein

A Thesis Submitted to the

College of Graduate Studies and Research

in partial fulfillment of the requirements for the

Master of Science Degree in the

Department of Microbiology and Immunology

University of Saskatchewan

Saskatoon

By

Cherise E. Hedlin

PERMISSION TO USE

In presenting this thesis in partial fulfillment of the requirements for a postgraduate degree from the University of Saskatchewan, I agree that the libraries of the university may make it freely available for inspection. I further agree that permission to copy this thesis in any way, for scholarly purposes only, may be granted by the professor of professors who supervised my thesis work, or in their absence, by the Head of the Department of Microbiology and Immunology or the Dean of the College of Graduate Studies and Research. It is understood that any copying or publication or use of this thesis or parts thereof for financial gain shall not be allowed without written permission. It is also understood that due recognition shall be given to me and the University of Saskatchewan in any scholarly use which may be made of any materials in my thesis.

All requests for permission to copy or to make use of material in this thesis in part or whole should be addressed to:

Head of the Department of Microbiology and Immunology

University of Saskatchewan

Saskatoon, Saskatchewan

S7N 5E5

ABSTRACT

DivIVA is a Gram-positive cell division protein involved in chromosome segregation, midcell placement of the cell division machinery, complete septum closure, and polar growth and morphogenesis. Although well conserved across various Gram-positive species, DivIVA is believed to be relatively species specific. One similarity among DivIVA homologues is the ability to oligomerize through coiled-coil interaction into complexes comprising 10-12 monomers. To date, the importance of DivIVA oligomerization and the N-terminal coiled-coil for its proper function in bacterial cell division has not been reported. This study examined the biological significance of DivIVA oligomerization and the N-terminal coiled-coil in bacterial cell division. This research provides evidence that the N-terminal coiled-coil and oligomerization is essential for the proper biological function of $DivIVA_{Ef}$ in *E. faecalis* cell division. Introduction of point mutations into chromosomal $divIVA_{Ef}$ known to disrupt either the N-terminal coiled-coil or the two central coiled-coils, involved in oligomerization, were found to be lethal unless rescued by *in trans* expression of wild type $DivIVA_{Ef}$. Using this rescue method, the N-terminal $divIVA_{Ef}$ mutant strain, *E. faecalis* MWMR5, and the mutant strain with partial disruption of oligomerization, *E. faecalis* MWMR10, were successfully rescued. Differential Interference Contrast (DIC) and Transmission Electron Microscopy (TEM) were utilized to determine the phenotypes of $divIVA_{Ef}$ mutant strains *E. faecalis* MWMR5 and MWMR10. Both these strains showed asymmetrical division, loss of normal lancet shape, and irregular chains. Full disruption of oligomerization with point mutations in both central coiled-coils resulted in a dominant lethal phenotype. These results demonstrate the essentiality of the N-terminal coiled-coil and oligomerization of $DivIVA_{Ef}$ for its proper biological function in *E. faecalis* cell division.

Previous detection of DivIVA interaction with a novel cell division protein, MLJD1, by screening a Yeast Two-Hybrid (Y2H) was weak. GST-pulldown and immunoprecipitation did indicate $DivIVA_{Ef}$ interaction with MLJD1, but another *in vivo* assay was required to support these results. In this study I demonstrate a strong interaction, using an *in vivo* Bacterial Two-Hybrid (B2H) assay, between $DivIVA_{Ef}$ and a fragment of MLJD1 containing two cystathionine-beta-synthase (CBS) domains. The *in vitro* and *in vivo* results thus confirm interaction between $DivIVA_{Ef}$ and MLJD1.

Another objective of this study was to determine the localization of DivIVA and MLJD1 in *E. faecalis*. Localization of $DivIVA_{Ef}$ in *E. faecalis* was found to be similar to DivIVA localization in *B. subtilis* and *Streptococcus pneumoniae*. $DivIVA_{Ef}$ was diffused along the cell membrane and, as chromosome replication and segregation and cell division proceeded, $DivIVA_{Ef}$ migrated to the cell poles and then concurrently to the division site. Intriguingly, MLJD1 was found to localize in the same pattern as $DivIVA_{Ef}$ in *E. faecalis*, further implicating MLJD1 as a bacterial cell division protein.

Since MLJD1 has potential DNA binding capabilities a proposed model of its role in cell division has been proposed. I hypothesize that MLJD1 could be forming a bridge between $DivIVA_{Ef}$ and the chromosome to aid in proper chromosomal replication and segregation. This model could explain how $DivIVA_{Ef}$ is involved in chromosome replication. This model is similar to the role of RacA in sporulation in *B. subtilis* where RacA directs the chromosome during sporulation through direct interaction with $DivIVA_{Bs}$ and Spo0J.

This study has set some important and essential ground work for developing a novel model of cell division for the elusive Gram-positive coccal bacterial strains.

ACKNOWLEDGEMENTS

I would first like to show my deepest gratitude to Dr. Jo-Anne Dillon for giving me the opportunity to study under her supervision. I have gained a wealth of knowledge and have become a proficient scientist with a wide skill set due to the unique variety of techniques performed in the Dillon laboratory and great respect and attention to detail. I would also like to say a special thanks to Dr. Nelson Eng, whom patiently taught me a lot of what I know today, despite being the champion of the Gigolo Award. I suppose in this way he also taught me mistakes do happen and letting the whole lab know ensures you will not make the same mistake twice. I could not have made it through the past three years without the support of Mingmin Laio and Monique Horbay (aka Dr. Moe) who were always willing to answer my questions or just listen to me think out loud to get the ideas flowing. I also have to thank my partner in crime, Monica Wang; I could have never finished without her microscopy prowess. Special thanks to the staff at VIDO for creating a warm friendly environment to work in and I greatly appreciate the help and support the VIDO family provides. Thanks must also go out to employees at PBI for their DNA sequencing support as well as Dr. M. Chen at the Electron Microscopy Unit, Surgical Medical Research Institute, University of Alberta (Edmonton, Alberta) for undertaking the daunting task of electron microscopy for this project. I would also like to thank Marc Rigden, whose previous research set the ground for my project and headed the way for my first publication. Finally I would like to acknowledge my committee members, Dr. Peter Howard, Dr. Vikrarm Misra, and Dr. Sean Hemmingson, for their guidance and support during the past three years.

Last, but not least I would like to acknowledge my parents Heidi and Pius Baier, my brother Mitchell, sister Chantelle, and my husband Peter. It was only with their love and support I was able succeed and become what I am today. Thank you.

TABLE OF CONTENTS

LIST OF FIGURES

LIST OF TABLES

LIST OF ABBREVIATIONS

Amp	Ampicillin
ATP	Adenosine-5'-triphosphate
β-gal	β-galactosidase
BSA	Bovine Serum Albumin
Ccp	Catabolite Control Protein
CCR	Carbon Catabolite Repression
DAPI	4'-6-Diamidino-2-phenylindole: stains chromosomal DNA
Div	division
dcw	Division and Cell Wall synthesis gene cluster
ddH_2O	Double Distilled water
DIC	Differential Interference Contrast Microscopy
$DivIVA_{Bs}$	DivIVA protein from *Bacillus subtilis*
$DivIVA_{Ef}$	DivIVA protein from *Enterococcus faecalis*
$DivIVA_{Sp}$	DivIVA protein from *Streptococcus pneumoniae*
DNA	DoxyriboNucleic Acid
EDTA	Ethylenediamine tetra-acetic acid
Ery	Erythromyocin
EtBr	Ethidium Bromide
GFP	Green Fluorescent Protein
h	hour (s)
IgG	Immunogolbulin G
IPTG	Isopropyl-β-D-thiogalactopyranoside
Kan	Kanamyocin
LB	Luria Bertani bacterial culture medium
M	Molar
Min	Minicell gene cluster
min	minutes (s)
MR5	$DivIVA_{Ef\ E37P,\ N43P,\ L46D,\ L50E,\ L57F}$
MR10	$DiviVA_{Ef\ L143P}$
MR15	$DivIVA_{Ef\ L104P,\ I115P,\ I125P}$
MR16	$DivIVA_{Ef\ L104P,\ I115P,\ I125P,\ L143P}$
OD	Optical Density
PBS	Phosphate Buffered Saline
PBST	Phosphate Buffered Saline plus Tween 20
PCR	Polymerase Chain Reaction
rpm	Revolutions per minute
sec	second (s)
SDS	Sodium dodecyl sulfate
SDS-PAGE	Sodium dodecyl sulfate polyacrylamide gel electrophoresis
TAE	Tris-Acetate-EDTA buffer
TBS	Tris-buffered saline
TG	Tris-Glycine buffer
TTBS	Tris-buffered saline with 0.05% Tween-20

TEM	Transmission Electron Microscopy
UV	Ultraviolet light
V	Volt
W	Watts

1.0 Introduction

1.1 Bacterial Cell Division Initiation and Regulation

1.1.1 The Bacterial Division and Cell Wall (*dcw*) Gene Cluster

Bacterial cell division has been most extensively studied in the Gram-negative bacillus *Escherichia coli* and the Gram-positive bacillus *Bacillus subtilis*. Proteins involved in cell division were first described in *E. coli* as having a filamentous temperature sensitive (Fts) phenotype when mutated (Bi & Lutkenhaus, 1991). Mutations in these Fts proteins caused the *E. coli* cells to become filamentous at the non-permissive temperature (Bi & Lutkenhaus, 1991). Fts division proteins and other proteins involved in cell division and cell wall synthesis have been located on the *E. coli* chromosome in what is called the division and cell wall synthesis (*dcw*) cluster (Rothfield & Justice, 1997, Margolin, 2001, Margolin, 2003, Vicente & Errington, 1996). The *dcw* cluster is highly conserved in bacterial species as found in *E. coli*, *B. subtilis*, *Staphylococcus aureus*, *Enterococcus faecalis*, *Streptococcus pyogenes*, and *Streptococcus pneumoniae* (Fig 1.1) as well as in *Neisseria gonorrhoeae* (Francis *et al.*, 2000, Real & Henriques, 2006, Fadda *et al.*, 2003, Ramirez-Arcos *et al.*, 2005, Massidda *et al.*, 1998). Genes within the *dcw* cluster, such as *ftsZ* and *ftsA*, are highly conserved between Gram-negative and Gram-positive bacteria (Fig 1.1), but there are some significant differences between the two. The major difference seems to be the organization of the genes within the *dcw* cluster. As seen in Fig 1.1, the *dcw* cluster in *S. pyogenes* and *S. pneumoniae* are in two or three segments, respectively, which are located on separate sections of the chromosomes (Massidda *et al.*, 1998). The involvement of all the known and putative division proteins transcribed by these *dcw* genes is very complex and beyond the scope of this study. However, knowing the function of key cell division proteins is imperative for understanding bacterial cell division.

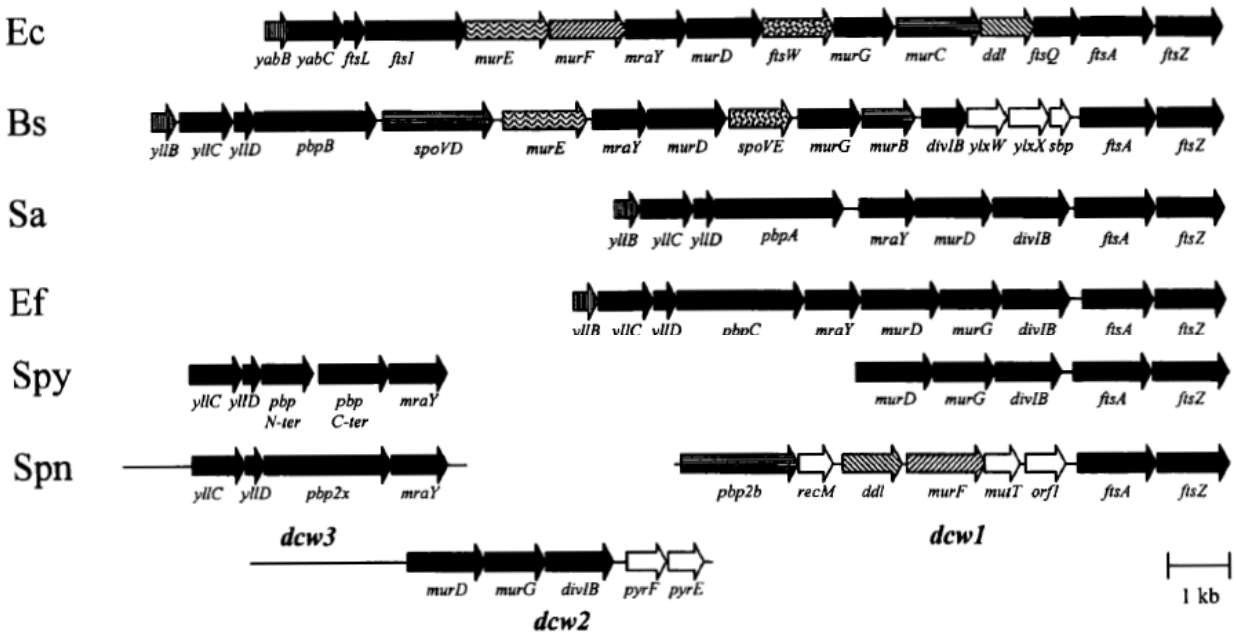

Figure 1.1: **The division and cell wall (*dcw*) clusters of *Escherichia coli* (Ec), *Bacillus subtilis* (Bs), *Staphylococcus aureus* (Sa), *Enterococcus faecalis* (Ef), *Streptococcus pyogenes* (Spy), and *Streptococcus pneumoniae* (Spn)**. The arrows point in the direction of transcription. Black arrows indicate genes common to all the *dcw* clusters shown, while identical patterns in different *dcw* clusters represent functional or structural homologues. White arrows represent open reading frames (ORF) unrelated to the *dcw* genes. This figure was modified from (Massidda *et al*., 1998).

Studying the genes and corresponding proteins involved with the *dcw* clusters has given researchers an understanding of bacterial cell division initiation and regulation.

1.1.2 Initiation of Bacterial Cell Division and the Proteins Involved in Divisome Formation

The most conserved division protein across bacterial species is FtsZ (Margolin, 2000). FtsZ is a tubulin homolog which has GTPase activity and self oligomerization capabilities that allow it to form a dynamic ring along the inner membrane of bacterial cells before septum formation (Bi & Lutkenhaus, 1991, Mukherjee & Lutkenhaus, 1998, Addinall & Holland, 2002). The formation of the Z-ring is the vital first step in bacterial cell division initiation and is known to form before the replicating chromosome is completely segregated (Bi & Lutkenhaus, 1991). A hierarchy of division proteins, including FtsA, ZipA, FtsK, FtsQ, FtsL, FtsW, FtsI, and FtsN in *E. coli*, are recruited after Z-ring formation is established. The recruitment of these proteins forms a complex known as the divisome or septosome (Margolin, 2005, Goehring & Beckwith, 2005, Weiss, 2004, Di Lallo *et al.*, 2003). The divisome works at the leading edge of the septum and contracts to divide into two daughter cells (Margolin, 2005, Harry, 2001).

1.1.3 Regulation of Bacterial Cell Division: The Min System in Gram-negative Bacteria *Escherichia coli* and *Neisseria gonorrhoeae*

The most important aspect of bacterial cell division initiation is placement of the FtsZ-ring in the center of the cell, the midcell site. Therefore, midcell site selection is vital for proper symmetrical division. Without regulation mechanisms FtsZ can form a ring and constrict anywhere at the cellular membrane forming minicells, which contain no DNA, and elongated filaments that eventually end up as unhealthy cells, leading to cell death (Begg & Donachie, 1985). The mechanisms utilized for proper placement of the Z-ring have been

extensively studied in the Gram-negative rod *Escherichia coli* (*E. coli*). *Escherichia coli* utilizes the Min (minicell gene cluster) proteins to ensure midcell placement of the Z-ring (Harry, 2001). There are three Min proteins, MinC, MinD, and MinE, which are all transcribed from the *minB* operon (de Boer *et al.*, 1989). MinC acts as a Z-ring inhibitor by depolymerizing FtsZ (Hu *et al.*, 1999, Shiomi & Margolin, 2007). MinD activates MinC by forming a reversible complex with MinC, which anchores MinC to the cell membrane (Fig 1.2) (Pichoff & Lutkenhaus, 2001, Hu *et al*., 1999). With MinC concentrated at the cell membrane Z-ring formation is inhibited at that location (Pichoff & Lutkenhaus, 2001, Hu *et al*., 1999). MinE oscillates from one end of the cell to the other and stimulates the ATPase activity of MinD, which causes MinCD to dissociate (Fig 1.2) (Shih *et al.*, 2003, Rothfield *et al.*, 2001). Dissociated MinC and MinD oscillate down the concentration gradient to the opposite end of the cell where it can form a complex once more (Fig 1.2) (Hu & Lutkenhaus, 2001). This dynamic oscillation results in the concentration of MinCD complex being least at the midcell site and highest at the cell poles (Fig 1.2) (Hu & Lutkenhaus, 2001, Ramirez-Arcos *et al*., 2001a, Ramirez-Arcos *et al*., 2001b, Ramirez-Arcos *et al*., 2004). This amazing process ensures division at the midcell site and prevents division at the cell poles, resulting in symmetrical division.

The Min system in the coccal shaped Gram-negative bacterium *Neisseria gonorrhoeae* (*N. gonorrhoeae*) should be more complex due to the lack of an obvious midcell site. *N. gonorrhoeae* does utilize the Min system to control FtsZ placement (Ramirez-Arcos *et al*., 2001b, Ramirez-Arcos *et al.*, 2002, Ramirez-Arcos *et al*., 2001a, Ramirez-Arcos *et al*., 2004). The Min proteins from *N. gonorrhoeae* have been shown to also function in Gram-negative bacilli (Ramirez-Arcos *et al.*, 2002), suggesting the Min proteins retain their function despite cell shape.

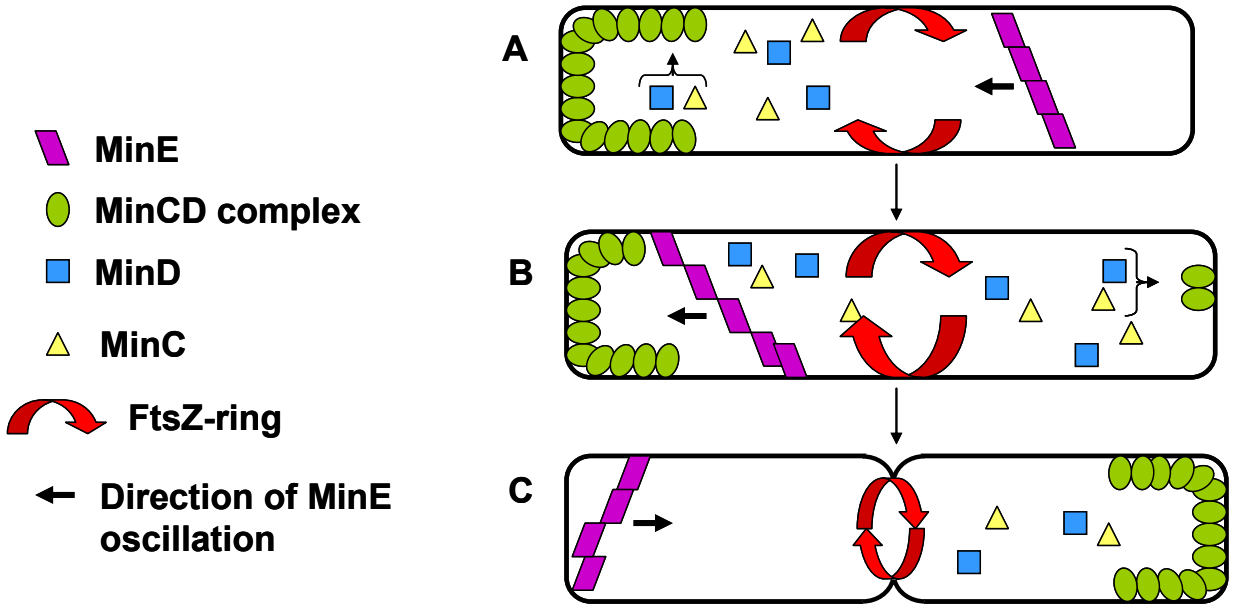

Figure 1.2: **Schematic diagram of the *E. coli* Min system for midcell site selection.**

A) MinC and MinD form a complex, capable of inhibiting Z-ring formation, at the cell membrane at one end of the cell. Forming a dynamic ring near midcell, MinE oscillates towards the MinCD complexes formed. B) As MinE reaches the other end of the cell it dissociates the MinCD complex. C) Free MinC and MinD oscillate down a concentration gradient to the opposite end of the cell where they form a MinCD complex once more. The dynamic oscillation of MinE, MinD and, by association, MinC results in a MinCD free zone at the midcell site allowing Z-ring formation and symmetrical division.

Although the Min system prevents division at the cell poles, some research suggests there is another mechanism involved in defining the midcell site. This other mechanism for midcell site selection in both *B. subtilis* and *E. coli* is called nucleoid occlusion (Woldringh *et al.*, 1991). Nucleoid occlusion occurs when replicating and segregating nucleoids prevent Z-ring formation in the vicinity of higher DNA concentrations (Harry, 2001). As chromosomal segregation nears completion, the chromosomes move apart leaving an area with decreased DNA concentration at the midcell where the Z-ring can then form (Wu *et al.*, 1995, Mulder & Woldringh, 1989, Den Blaauwen *et al.*, 1999, Marston & Errington, 1999, Sun *et al.*, 1998). Nucleoid occlusion thus prevents septum formation and closing before the chromosomes have completely segregated. The mechanism of nucleoid occlusion in *B. subtilis* involves the Noc protein, which non-specifically associates with the segregating chromosomes and prevents divisome assembly in the vicinity of the nucleoid (Wu & Errington, 2004). The nucleoid occlusion protein SlmA in *E. coli* functions in a similar mannar (Bernhardt & de Boer, 2005). It is the combination of nucleoid occlusion and the Min system which provides midcell site selection for Z-ring formation (Yu & Margolin, 1999, Margolin, 2000).

1.1.4 Division in the Gram-positive Rod Shaped Bacterium: *Bacillus subtilis*

Bacillus subtilis is a Gram-positive bacillus bacterium that also utilizes Min proteins to regulate midcell placement of the Z-ring. *Bacillus subtilis* contains MinC and MinD homologues, but does not possess a MinE homologue. In 1973 Reeve *et al*. created mutations in the *B. subtilis* chromosome using nitrosoguanidine mutagenesis (Reeve *et al.*, 1973). Mutations which caused misplacement of the division site in *B. subtilis* were found in the *divIVA* gene that codes for the $DivIVA_{Bs}$ (*B. subtilis* DivIVA) protein. This mutated $DivIVA_{Bs}$ resulted in division close to the cell poles causing the formation of DNA absent minicells

(Reeve *et al*., 1973). It was not until later on that the topological function of DivIVA was found to be similar to MinE (Cha & Stewart, 1997, Edwards & Errington, 1997). DivIVA and MinE share no sequence similarity, but perform the same topological function of midcell site selection for symmetrical division (Marston *et al.*, 1998). There is, however, a difference between the mechanisms used by $DivIVA_{Bs}$ and MinE to perform midcell site selection. While MinE stimulates oscillation of the Min proteins (Fig 1.2), $DivIVA_{Bs}$ sequesters MinCD to the cell poles, thus preventing division at either pole (Fig 1.3) (Marston *et al*., 1998, Marston & Errington, 1999). In the absence of $DivIVA_{Bs}$, MinD was diffused throughout the entire cell and localized to the cell poles only in the presence of functional $DivIVA_{Bs}$ (Marston *et al*., 1998). Without the dynamic oscillation of MinD, a MinCD free zone is created at the midcell site by the elongation of dividing *B. subtilis* cells. Therefore, MinCD concentrations decrease at the midcell to allow Z-ring formation (Fig 1.3) (Edwards & Errington, 1997, Marston & Errington, 1999). After the Z-ring has stabilized and it becomes insensitive to MinCD inhibition, $DivIVA_{Bs}$ is recruited to the division site where it eventually forms the new cell poles of the daughter cells (Edwards & Errington, 1997, Perry & Edwards, 2004). MinD and MinC do not directly interact with $DivIVA_{Bs}$. Instead, $DivIVA_{Bs}$ interacts with a protein named MinJ, which was discovered in *B. subtilis* and was found to interact with MinD as well (Bramkamp *et al.*, 2008, Patrick & Kearns, 2008). Thus, MinJ completes a bridge between $DivIVA_{Bs}$ and the MinCD complex in order to control midcell placement of the cell division machinery by preventing division at the cell poles (Patrick & Kearns, 2008, Bramkamp *et al*., 2008).

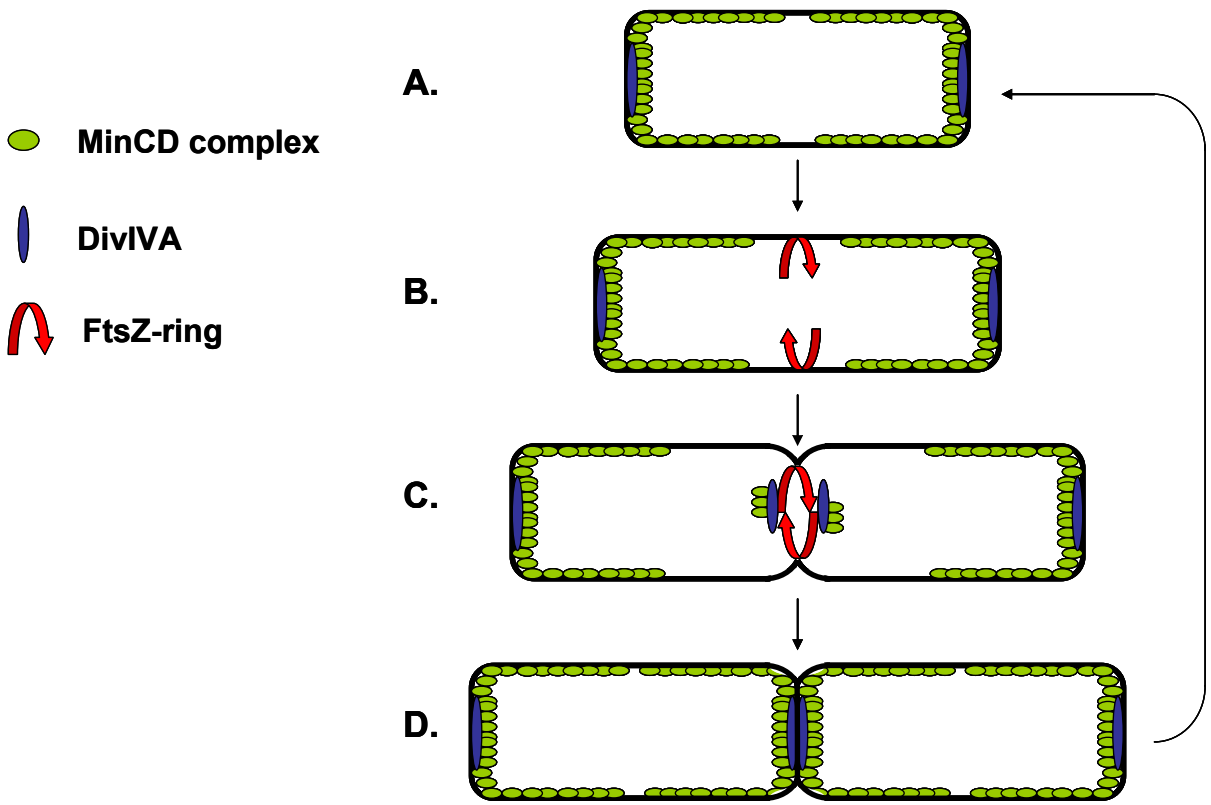

Figure 1.3: Midcell site selection in *Bacillus subtilis*. A) $DivIVA_{Bs}$ sequesters the MinCD complex to the cell poles. B) As the cell elongates a MinCD free zone appears where the Z-ring and divisome can form. C) Once the divisome forms it begins to constrict and $DivIVA_{Bs}$ is recruited to the division site. D) $DivIVA_{Bs}$ remains at the new cell poles of the daughter cells along with MinCD.

1.1.5 Gram-positive Coccal Cell Division Mechanisms

Gram-positive coccal bacteria such as *Enterococcus faecalis*, *Streptococcus pneumoniae*, and *Staphylococcus aureus* are similar to *B. subtilis* in that they contain DivIVA homologues. They do not, however, contain homologues of any of the three Min proteins (Ramirez-Arcos *et al*., 2005, Pinho & Errington, 2004, Flardh, 2003a). These round cells lack an obvious midcell site and research has not yet illuminated the mechanisms used by these cells for proper midcell placement.

For these reasons, research on the mechanisms used to regulate cell division have focused on the function of the division protein DivIVA in *B. subtilis* and various Gram-positive coccal bacteria including *E. faecalis* (Ramirez-Arcos *et al*., 2005), *S. pneumoniae* (Fadda *et al.*, 2007), and *S. aureus* (Pinho & Errington, 2004). Although most commonly found in Gram-positive bacterial species, a DivIVA homologue, named FruD, was found in the Gram-negative bacterial species *Myxococcus xanthus* (Akiyama *et al.*, 2003). Mutations in FruD caused *M. xanthus* cells to become filamentous demonstrating that FruD is required for proper cell division (Akiyama *et al*., 2003). In the cyanobacterium *Synechococcus elongatus* there are both MinE and DivIVA present in the cells (Miyagishima *et al.*, 2005). Filimentus cells result from disruptions in *minE* and disruption of *divIVA* resulted in misplacement and reduced frequency of the septum and elongated cells, implying both *minE* and *divIVA* play a role in cell division (Miyagishima et al., 2005).

1.2 DivIVA : A Gram-positive Cell Division Protein

1.2.1 *divIVA* Chromosomal Location

The focus of bacterial cell division in Gram-positive coccal cells has not only been on DivIVA, but also on the protein products of genes in the *dcw* cluster. The chromosomal localization of *divIVA* typically appears downstream *ftsZ* with four to five ORFs of various *ylm*

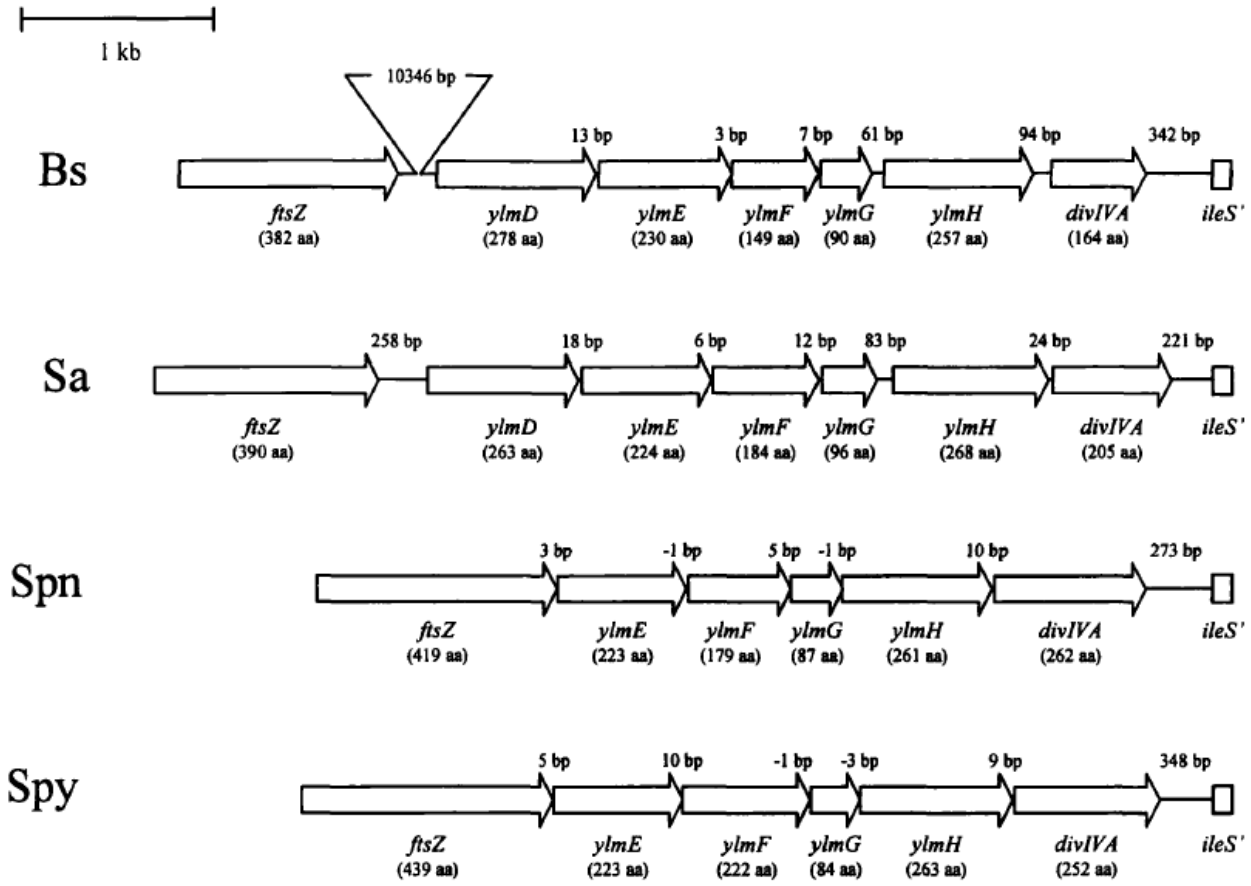

Figure 1.4: **Region downstream *ftsZ* in *B. subtilis* (Bs), *Staph. aureus* (Sa), *Streptococcus pneumoniae* (Spn), and *Streptococcus pyogenes* (Spy).** Arrows indicate direction of transcription. The names of genes and size of transcribed proteins are indicates under each open reading frame (ORF). Figure modified from (Massidda *et al*., 1998).

genes in between (Fig 1.4) (Massidda *et al*., 1998). The genes *ylmE*, *ylmF*, *ylmG*, and *ylmH* in *S. pneumoniae* were found to be involved in cell division and/or chromosomal segregation, as their disruption resulted in altered cell shape, cells in chains or tetrads, thinner or incomplete septum formation, and/or decrease or absent nucleoids (Fadda *et al*., 2003). Disrupting *divIVA* in *S. pneumoniae* has the most detrimental effect on cell growth rates, incomplete septum formation, and chromosomal distribution (Fadda *et al*., 2003). In bacteria which possess DivIVA homologues, *divIVA* is found on the chromosome immediately upstream the isoleucyl tRNA synthetase gene and is considered as part of the *dcw* cluster (Fig 1.4) (Cha & Stewart, 1997, Massidda *et al*., 1998, Ramirez-Arcos *et al*., 2005, Ramos *et al.*, 2003). Bioinformatic analysis confirmed that *divIVA* is part of the *Enterococcal dcw* cluster, thus implicating DivIVA as a cell division protein (Fig 1.5) (Ramirez-Arcos *et al*., 2005). In particular, *E. faecalis divIVA* (*divIVA*$_{Ef}$) is potentially co-transcribed with six up-stream division proteins due to the placement of three ρ-independent transcriptional terminators, one immediately downstream *divIVA*$_{Ef}$ (Fig 1.5; (Ramirez-Arcos *et al*., 2005)). Transcription of *divIVA* in *E. faecalis* and other Gram-positive bacteria is controlled by a *divIVA* promoter and its transcription is not effected by mutations in genes upstream in the *dcw* gene cluster (Cha & Stewart, 1997, Fadda *et al*., 2003, Ramirez-Arcos *et al*., 2005). *divIVA*$_{Ef}$ transcription may also be controlled by the *ftsA* promoter upstream in the *dcw* cluster (Ramirez-Arcos *et al*., 2005).

1.2.2 Multiple Biological Functions of DivIVA

DivIVA is a multifunctional protein, essential in chromosome segregation and cell division in *E. faecalis* (Ramirez-Arcos *et al*., 2005) as in *B. subtilis* in which it also plays a role in sporulation (Edwards & Errington, 1997, Thomaides *et al.*, 2001, Errington, 2001).

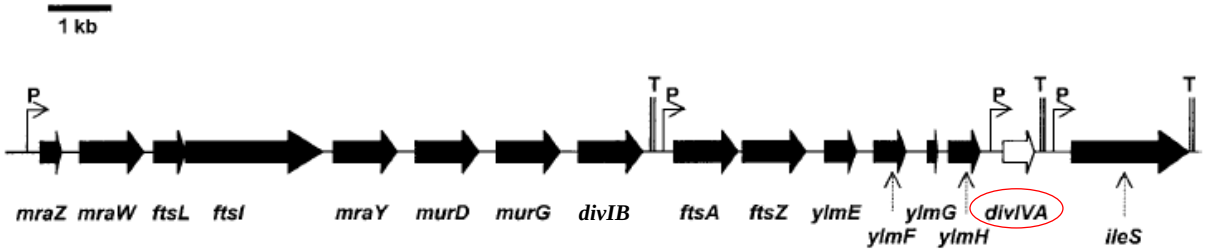

Figure 1.5: ***Enterococcus faecalis* V583 division and cell wall synthesis (*dcw*) cluster.** The gene organization and transcriptional direction running the same way for every gene. The *divIVA*$_{Ef}$ gene is circled in red. T- putative ρ-independent transcriptional terminator; P- putative σ70 promoter (Ramirez-Arcos *et al*., 2005).

In *S. pneumoniae*, *Streptomyces coelicolor*, and *Brevibacterium lactofermentum* DivIVA is also essential for polar growth and morphogenesis (Flardh, 2003a, Flardh, 2003b, Fadda *et al*., 2007, Ramos *et al*., 2003). Disruption or overexpression of *divIVA* causes a variety of cell division and morphology defects including misplacement of the divisome, incomplete formation of the septum, filamentation, and swelling of the cells depending on the host species (Cha & Stewart, 1997, Ramos *et al*., 2003, Ramirez-Arcos *et al*., 2005, Fadda *et al*., 2007). Although DivIVA is capable of performing similar functions such as those involved in cell division and chromosome segregation in *B. subtilis*, *E. faecalis*, and *S. pneumoniae*, the protein does appear to have species-specific functions. Ramirez-Arcos *et al*. (2005) demonstrated the species specificity of DivIVA through the inability of DivIVA from *E. faecalis* ($DivIVA_{Ef}$) to complement DivIVA null mutants of *B. subtilis* and *S. pneumoniae*. The species specificity of DivIVA may imply the ability to interact with specific proteins within individual species has evolved and adapted in order for DivIVA to carry out its multiple functions within specific species (Ramirez-Arcos *et al*., 2005).

1.2.3 Cellular Localization of DivIVA

Among the multiple functions of DivIVA there are similar localization patterns among Gram-positive species. DivIVA in *Streptococcus pneumoniae* ($DivIVA_{Sp}$) localized to the cell poles and concurrently to the site of cell division (Fadda *et al*., 2007). $DivIVA_{Sp}$ localized to the cell division site after FtsZ ring formation had been initiated (Fadda *et al*., 2007, Edwards *et al.*, 2000). In *B. subtilis*, a $DivIVA_{Bs}$–GFP (green fluorescent protein) fusion protein localized to the cell poles and site of cell division (Edwards & Errington, 1997). $DivIVA_{Bs}$ also targeted the site of cell division in *B. subtilis* after FtsZ ring formation where it remained at the new poles of the daughter cells (Edwards & Errington, 1997). Furthermore, $DivIVA_{Bs}$ was still able to localize to previous cell division sites in outgrowing *B. subtilis* spores (Hamoen & Errington,

2003, Harry & Lewis, 2003). This indicated $DivIVA_{Bs}$ localization to previous and new cell division sites was independent. Expression of *divIVA*$_{Bs}$*~gfp* heterologously in *E. coli* demonstrated $DivIVA_{Bs}$ could still target the cell poles and division site in the heterogonous host background (Edwards *et al*., 2000).

Similarities between DivIVA homologues and a fission yeast division protein Cdc 8p lead Edwards and colleagues (2000) to study localization patterns of $DivIVA_{Bs}$ in *Schizosaccharomyces pombe*, a eukaryotic fission yeast species. Intriguingly, $DivIVA_{Bs}$ was able to target the growth zones and the division septum of *S. pombe* indicating the conservation of DivIVA target specificity across an extreme evolutionary distance (Edwards *et al*., 2000). However, little is known of the precise mechanism utilized by DivIVA to localize to new and nascent division sites.

The amazing ability of DivIVA to localize to cell poles (nascent cell division sites) and sites of current cell division in homologous, heterologous, and eukaryotic hosts suggests that a marker is conserved across bacterial species and eukaryotes (Edwards *et al*., 2000, Fadda *et al*., 2007, Edwards & Errington, 1997). The marker recognized by DivIVA homologues for localization at nascent and new division sites is yet unknown, but the key to the answer may lie in the structure of DivIVA and interaction with a hierarchy of division proteins (Edwards *et al*., 2000).

1.2.4 DivIVA Structure and Complex Formation

DivIVA homologues have a significant degree of sequence similarity in their N-terminal (Fig 1.6) and in each of *B. subtilis*, *E. faecalis*, and *S. pneumoniae*, DivIVA can self interact to form oligomer structures comprised of 10-12 monomers *in vitro* and *in vivo* (Rigden *et al.*, 2008, Fadda *et al*., 2007, Edwards *et al*., 2000). Conservation of the N-terminal and complex oligomer formations could mean the N-terminal and oligomer formation are essential for proper

Figure 1.6: Multiple sequence alignment (MSA) of DivIVA homologues. MSA was performed using ClustalWand the Jalvieweditor (http://www.ebi.ac.uk/Tools/clustalw, last accession September 26, 2007) (Rigden *et al*., 2008). Twenty-seven sequences were selected from 27 bacterial species representing 70 *divIVA* loci annotated in the TIGR database (http://cmr.tigr.org/tigr-scripts/CMR/CmrHomePage.cgi, last accession on September 25, 2007). The deduced amino acid sequences were obtained from NCBI database (http://www.ncbi.nlm.nih.gov/sites/entrez, last accession on September 25, 2007). Shadowed boxes indicate residues with an identity of ≥70% across the sequences. Black bars represent the positions of predicted coiled-coils of *E. faecalis* (Ef) DivIVA. Black arrows indicate conserved residue R18 and G19. Star indicates conserved residue A78, and dashed arrow shows L120 in *B. subtilis* DivIVA and L143 of DivIVA$_{Ef.}$ This figure is from Supplementary Material (Rigden *et al*., 2008)

Ef: *Enterococcus faecalis*, V583, AAO80808
Bs: *Bacillus subtilis*, CAB06818
Ba: *Bacillus anthracisAmes*, AAP2776
Bce: *Bacillus cereus*, ATCC10987, NP_980236
Bcl: *Bacillus clausii*, KSM-K16, BAD64878
Bh: *Bacillus halodurans*, C-125, BAB06265
Bl: *Bacillus licheniformis*, ATCC 14580, YP_091349
Bt: *Bacillus thuringiensis konkukian*, 97-27, AAT61098
Cp: *Clostridium perfringens*, 13, NP_562767
Ch: *Cytophaga hu chinsonii*, ATCC33406, YP_677387
Dv: *Desulfovibrio vulgaris Hildenborough*, YP_010592
Gk: *Geobacillus kaustophilus*, HTA426, BAD75420
La: *Lactobacillus acidophilus*, NCFM, P_193709
Lp: *Lactobacillus plantarum*, WCFS1, NP_785685
Lsal: *Lactobacillus salivarius*, UCC118, YP_535731
Lsak: *Lactobacillus sakei* 23K, P_395369
Li: *Listeria innocua* CAC97358
Lm: *Listeria monocytogenes* CAD00098
Mx: *Myxococcus xanthus* DK1622, YP_631315
Oi: *Oceanobacillusi heyensis* HTE831, BAC13439
Sa: *Staphylococcus aureus* BAB42539
Sm: *Streptococcus mutans* UA159, NP_720993
Spn: *Streptococcus pneumoniae* AAC95445
Spy: *Streptococcus pyogenes* MGAS315, AAM79774
St: *Streptococcus thermophilus* CNRZ1066, YP_141148
Syt: *Symbiobacteriumthermophilum*IAM 14863, YP_075059
Tm: *Thermoanaerobactertengcongensis*, NP_623196.

Figure 1.6 continued

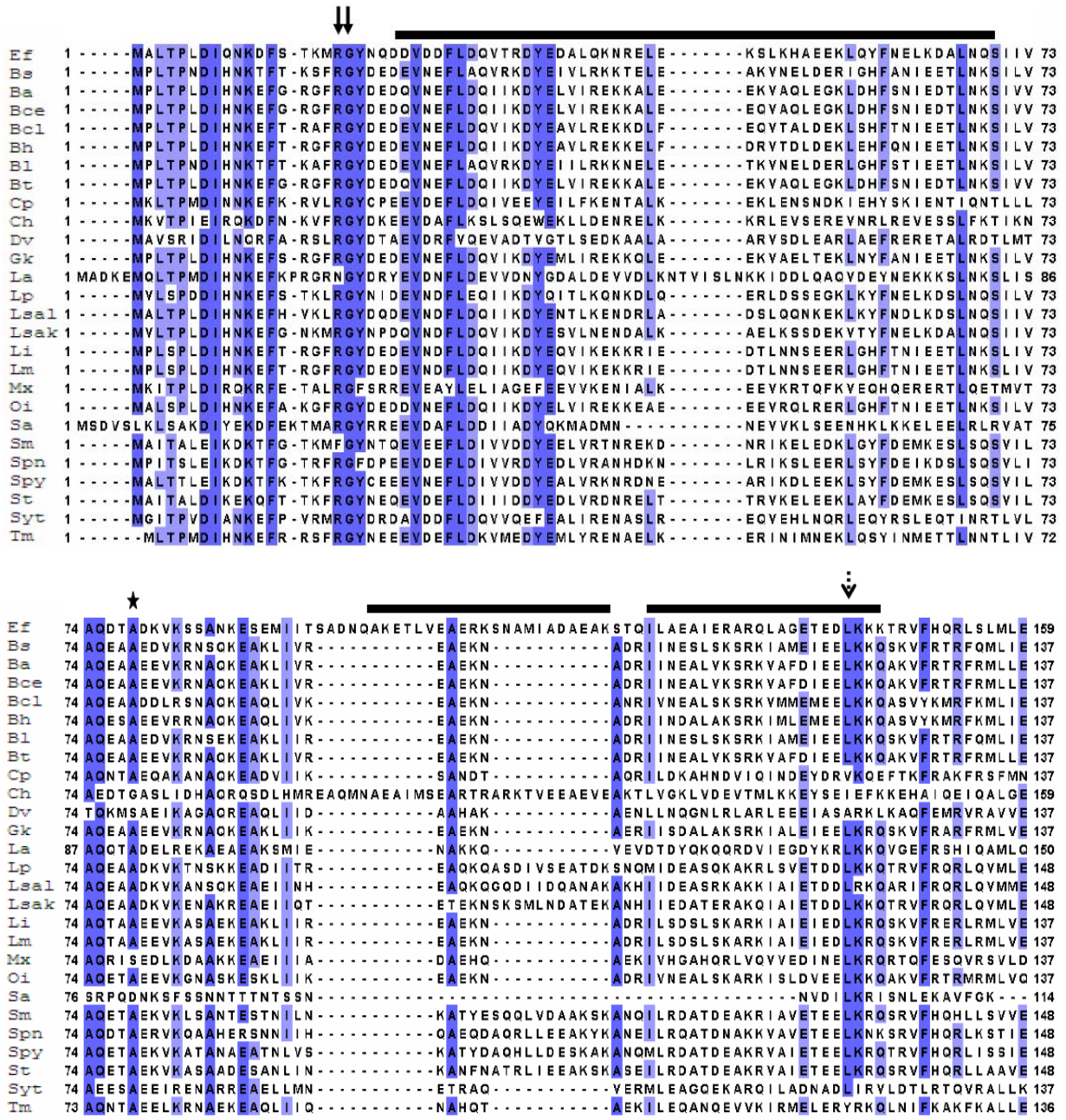

Figure 1.6 continued

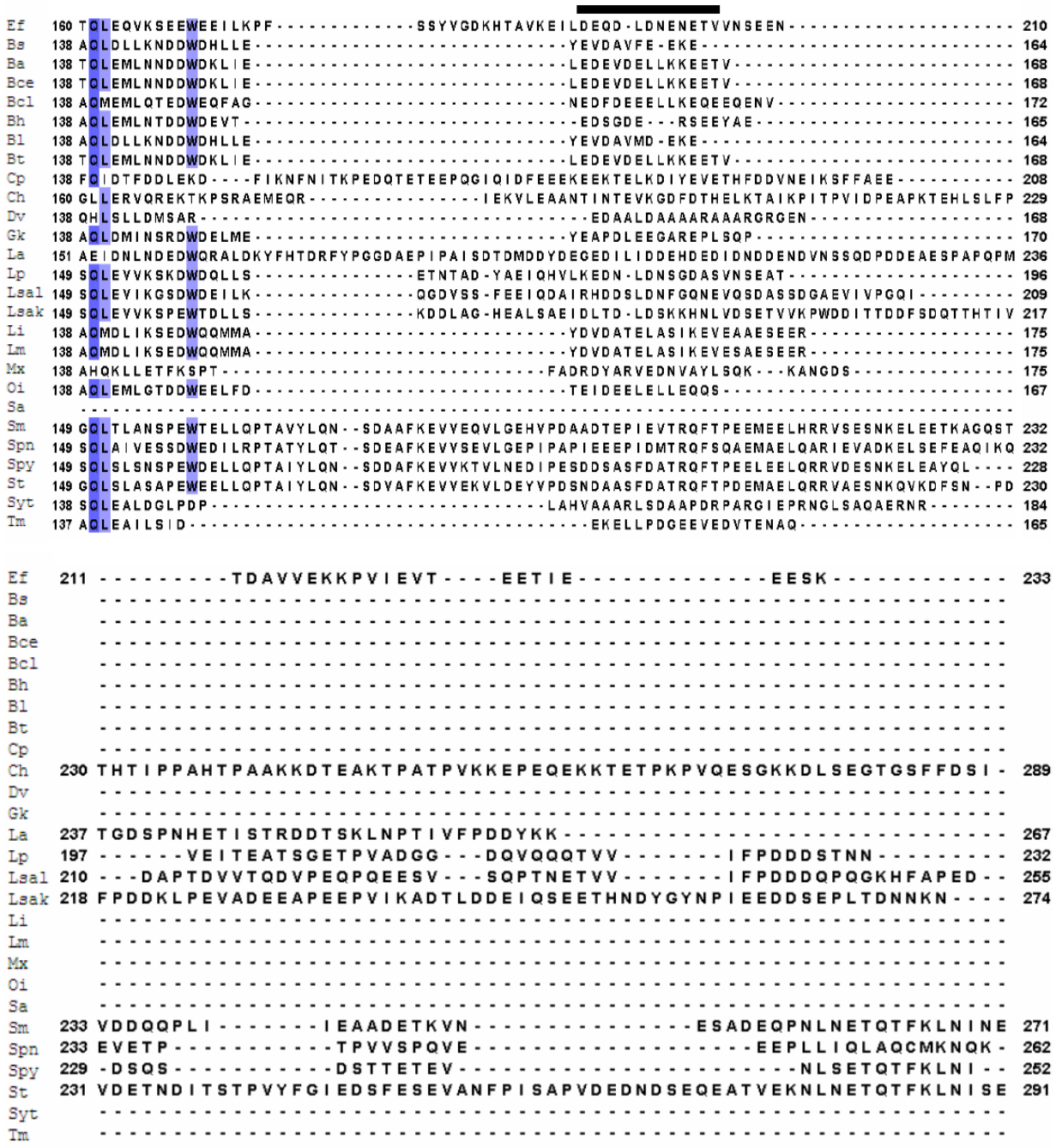

functions of DivIVA (Rigden *et al*., 2008, Fadda *et al*., 2007, Edwards *et al*., 2000). While the DivIVA N-terminal is well conserved across DivIVA homologues the C-terminal is much more variable (Edwards *et al*., 2000, Rigden *et al*., 2008). Additional bioinformatic analysis has shown *B. subtilis*, *S. pneumoniae*, and *E. faecalis* DivIVA to have a high propensity to form coiled-coil structures (Edwards *et al*., 2000, Rigden *et al*., 2008, Fadda *et al*., 2007, Rigden, 2005). *Bacillus subtilis* $DivIVA_{Bs}$ has a short C-terminal and is comprised of two predicted coiled-coils, one at the N-terminal and one at the central region (Muchova *et al.*, 2002b, Muchova *et al.*, 2002a, Rigden *et al*., 2008, Rigden, 2005). A mutation in the central coiled-coil of $DivIVA_{Bs}$ from leucine to proline at residue 120 (L120P) reduced oligomer complex formation by 50% (Muchova *et al*., 2002b). DivIVA from *E. faecalis* ($DivIVA_{Ef}$), by contrast has four predicted coiled-coils, one at the N-terminus, two in the central region, and one at the C-terminus (Rigden, 2005). It has recently been determined, by creating point mutations at conserved residues, that the central coiled-coils in $DivIVA_{Ef}$ are required for oligomerization, as these mutations largely reduced oligomer formation (Table 1.1) (Rigden, 2005). The point mutation in *E. faecalis* $DivIVA_{Ef}$ L143P, corresponding to the L120P mutation in *B. subtilis* $DivIVA_{Bs}$, was one of the mutations which decreased oligomerization (Table 1.1) (Rigden *et al*., 2008). Point mutations disrupting the N-terminal and C-terminal coiled-coils of $DivIVA_{Ef}$ did not result in decreased oligomerization (Table 1.1) (Rigden, 2005).

1.3 *Enterococcus faecalis* $DivIVA_{Ef}$ Interaction with a Novel Putative Division Protein – MLJD1

1.3.1 $DivIVA_{Ef}$ Interaction with a Novel Putative Division Protein

A novel, putative division protein was discovered in the Dillon Laboratory by screening an *E. faecalis* DNA library using a Yeast Two-Hybrid (Y2H) assay with $DivIVA_{Ef}$ as the bait. Tentatively named MLJD1, this novel division protein was shown to interact with $DivIVA_{Ef}$

Table 1.1: DivIVA$_{Ef}$ mutations and their effects on oligomerization

divIVA$_{Ef}$ mutations[a]	Complex Mass [kDa]/ Number of monomers[b]	Point Mutation Locations and their effect on DivIVA$_{Ef}$ oligomerization
MR5: E37P, N43P, L46D, L50E, L57F	1003.38 / 37.16	N-terminal point mutations: oligomerization conserved
MR10: L143P	841.1 / 31	Point mutation in second central coiled coil: partial disruption of oligomerization
MR15: L104P, I115P, I125P	27 / 1.0	Point mutations in first central coiled-coil: full disruption of oligomerization
MR16: L104P, I115P, I125P, L143P	40.4 / 1.5	MR10 and MR15 mutations combined: complete disruption of oligomerization
Wild type *divIVA*$_{Ef}$	1011.83 / 37.47	Normal oligomerization

a The *divIVA* mutations were created by site directed mutagenesis (Rigden, 2005). *E. coli* XL-1Bule and *E. coli* DH5α were used for cloning purposes.

b Gel-filtration (superose-6) was used to determine the molecular mass in kilodaltons (kDa) and determine the number of monomers in each complex (Rigden, 2005). Native gel-electrophoresis (data not shown) was also used to determine molecular weight (Rigden, 2005).

using co-immunoprecipitation, GST-pulldown, and quantitative Y2H assays (Liao *et al*., manuscript in preparation).

MLJD1 is a 209 amino acid protein with a predicted molecular weight of 23.41 kDa (Liao *et al*., manuscript in preparation). It has a putative DNA binding helix-turn-helix (HTH_11) motif at the N-terminal and two cystathionine-beta-synthase (CBS) domains, one in the central region and the second in the C-terminal end (Fig 1.7). The HTH_11 superfamily of winged helix DNA binding proteins is mostly found in bacterial proteins, such as BirA, which regulate transcription of the biotin operon in *E. coli* (Wilson *et al.*, 1992). *E. coli* BirA acts as a transcription factor and an enzyme capable of catalyzing the reaction involving ATP and biotin to produce biotinyl-5'-adenylate (Eisenberg *et al.*, 1982, Eisenberg & Hsiung, 1982). HTH_11 DNA binding domains are also found in proteins involved in regulating amino acid biosynthesis, such as LysM, and carbohydrate metabolism as with LicR and FryR (Tobisch *et al.*, 1999, Reizer *et al.*, 1994). Sporulation in *B. subtilis* requires interaction of RacA with DNA and DivIVA in an Spo0J/ Soj dependent manner to draw the origin of one chromosome into the forespore (Ben-Yehuda *et al.*, 2003). During sporulation RacA displaces MinCD from being sequestered at the cell poles by $DivIVA_{Bs}$ and is sequestered to the cell poles itself (Ben-Yehuda *et al*., 2003). The MLJD1 equivalent in *B. subtilis*, YqzB or CcpN, binds to the promoter regions of *pckA* and *gapB* to repress transcription and subsequently production of PckA and GapB, enzymes required for gluconeogenic growth, when grown in the presence of preferred carbon sources, like glucose (Servant *et al*., 2005, Tannler *et al.*, 2008).

CBS domains are found in many proteins with different functions including: chloride channels (Lloyd *et al.*, 1997), inosine-monophosphate dehydrogenase (Sintchak *et al.*, 1996), and cystathionine-beta-synthase (Bateman, 1997). CBS domains typically occur in pairs

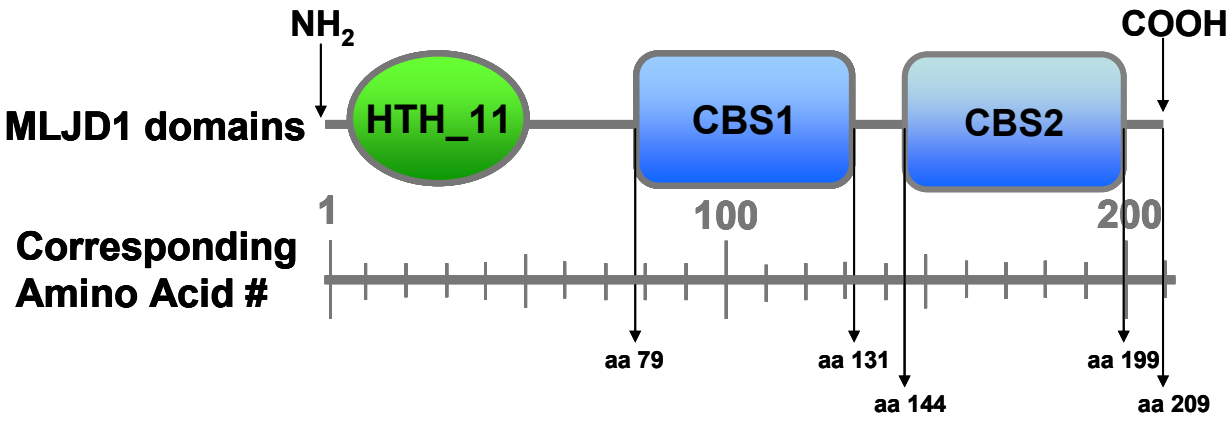

Figure 1.7: Diagram of predicted MLJD1 domains. HTH_11: potential DNA binding domain; CBS: cystathionine beta-synthase domain; NH_2: N-terminal; COOH: C-terminal. Domains determined by bioinformatic analysis with Pfam (http://pfam.sanger.ac.uk/) and an Entrez protein blast (http://www.ncbi.nlm.nih.gov/sites/gquery). Both programs were used with default settings. Program used to creat image to scale: http://ca.expasy.org/cgi-bin/prosite/mydomains/

forming a stable globular domain called a Bateman domain (Ponting, 1997, Kemp, 2004, Bateman, 1997). Mutations in CBS domains of various human proteins cause genetic disorders including homocystinuria, retinitis pigmentosa, and congenital myotonia (Kemp, 2004). In bacteria, CBS domains have been identified in proteins such as ABC transporters and inosine-5'-monophosphate dehydrogenase (IMPDH), which is involved in GTP synthesis, as well as in proteins of unknown function (Biemans-Oldehinkel *et al.*, 2006, Zhang *et al.*, 1999). CBS domains are also capable of binding adenosyl compounds ATP, AMP or S-AdoMet, depending on the protein (Kemp, 2004). The protein similar to MLJD1 in *B. subtilis*, CcpN (or YqzB) has been found to bind ATP and ADP (Licht *et al.*, 2008). CcpN also has a different secondary structure depending on which ligand it is bound to (ATP or ADP) (Licht *et al.*, 2008). ATP along with an acidic environment induce *pckA* and *gapB* repression capabilities of CcpN, while ADP seems to relieve CcpN of this repression function (Licht *et al.*, 2008).

1.3.2 Predicted Domains Involved in $DivIVA_{Ef}$ Interaction with MLJD1

Deletional mutations and truncation in $DivIVA_{Ef}$ and MLJD1 were used to elucidate potential points of interaction between these two proteins. It was previously determined that a fragment of MLJD1, amino acids 78-209 containing the CBS domains (Fig 1.7), interacted with the second coiled-coil (amino acids 60-130) of $DivIVA_{Ef}$ (Liao *et al.*, manuscript in progress). The second coiled-coil of $DivIVA_{Ef}$ is also implicated in self interaction, which may elucidate the function of MLJD1 in cell division (Rigden *et al.*, 2008, Rigden, 2005).

1.3.3 MLJD1 is an Essential Division Protein

Expression of MLJD1 was confirmed through RT-PCR and was purified for subsequent development of rabbit polyclonal antibody to detect MLJD1 in Western-blots (Liao *et al.*, manuscript in progress). The gene encoding MLJD1, *mljd1*, is conserved in Gram-positive bacteria (Liao *et al.*, manuscript in progress). No MLJD1 homologues have been identified in

Gram-negative organisms. Attempts were made to knockout *mljd1* in the *E. faecalis* chromosome by insertion of a kanamycin resistance cassette. The knockout proved lethal as no viable cultures could be obtained. A marker rescue method, previously developed in the our laboratory (Ramirez-Arcos *et al*., 2005), was used to express wild type MLJD1 *in trans*. Expression of wild type MLJD1 was minimized, as previously done (Ramirez-Arcos *et al*., 2005), to determine the MLJD1 knockdown phenotype. The knockdown resulted in retarded growth of the cells, morphological aberrations, and cell death (Liao *et al*., manuscript in progress). The *in trans* complementation was also unable to fully restore the cells back to the wild type phenotype further confirming the essentiality of MLJD1 (Liao *et al*., manuscript in progress).

Escherichia coli has previously been identified as a useful model organism to study the effects of *divIVA*$_{Ef}$ overexpression, which resulted in filamentous cells caused by incomplete septation and shorter cells caused by division close to the cell poles (Ramirez-Arcos *et al*., 2005). Overexpression of *mljd1* in *E. coli* inhibited cell growth (Liao *et al*., manuscript in progress). The essentiality of *mljd1* in *E. faecalis*, interaction of MLJD1 with DivIVA$_{Ef}$ and its effects on *E. coli* cell division implicate MLJD1 as a putative division protein.

1.4 Rational for using *Enterococcus faecalis* as a Model Organism and Studying DivIVA$_{Ef}$ and MLJD1 Cell Division Proteins

Enterococcus faecalis was chosen as a model organism for studying Gram-positive coccal cell division because very little is known about the mechanisms it utilizes for cell division. *E. faecalis* is an important bacterium in the medical world, as it is known to cause nosocomial infections (Clewell, 1981). Multiple drug resistant bacteria, such as vancomycin resistant *Enterococci* (VRE) (Cetinkaya *et al.*, 2000), also exist and *Enterococci* may be capable of transferring their multiple antibiotic resistances to other bacterial species (Jones *et*

al., 1987). Vancomycin is a drug of last resort when other antibiotics are ineffective. A rise in resistance to vancomycin could result in incurable bacterial infections. Also, because of the danger of nosocomial infection to hospital patients and this increasing concern of multiple drug resistant bacteria, studying cell division in *E. faecalis* could help develop more effective antibiotics, potential vaccines, and/or strategies for controlling drug resistance and nosocomial infections.

Due to the species specific functions of the Gram-positive cell division protein DivIVA, it is useful to study DivIVA in a number of representative Gram-positive species. DivIVA from *B. subtilis*, *S. pneumoniae*, and *E. faecalis* are known to contain coiled-coils and oligomeriz into complexes of 10-12 monomers (Fadda *et al*., 2007, Edwards *et al*., 2000, Rigden, 2005, Rigden *et al*., 2008). Previous research in our laboratory identified the two central coiled-coils of $DivIVA_{Ef}$ to be essential for oligomerization (Rigden, 2005). However, the biological significance of DivIVA oligomerization had not yet been determined for any DivIVA homologues.

Understanding DivIVA oligomerization is just part of a greater picutre. While *B. subtilis* utilizes MinCD to direct midcell placement of the septum, no proteins have yet been identified in Gram-positive cocci that direct midcell placement. Research has shown that DivIVA in *S. pneumoniae* to interact with FtsZ, FtsA, ZapA, FtsK, FtsL, and Spo0J (Fadda *et al*., 2007). Our laboratory has recently found $DivIVA_{Ef}$ to interact with FtsZ, FtsA, DivIB and FtsW in *E. faecalis* (Dillon *et al*., manuscript in progress). All of these proteins are involved in divisome formation or chromosome segregation. To develop a novel model for *E. faeclalis* cell division the function of DivIVA should be researched along with how it interacts with other division proteins to perform its functions. Once developed in *E. faecalis*, the information might be applicable to other Gram-positive coccal species.

1.5 Hypothesis and Objectives

Previous research on *E. faecalis* $DivIVA_{Ef}$ and MLJD1 inspired my thesis work. Biochemical experiments identified four coiled-coils in $DivIVA_{Ef}$: one at the N-terminal, two in the central region, and one at the C-terminal. $DivIVA_{Ef}$ was also determined to form oligomer complexes of 10-12 monomers (Rigden, 2005). Complex formation was driven by interaction of the two central coiled-coils of $DivIVA_{Ef}$ (Rigden, 2005). However, the biological significance of $DivIVA_{Ef}$ oligomerization in *E. faecalis* cell division was not determined. Interaction between $DivIVA_{Ef}$ and MLJD1 had also been determined using *in vitro* and *in vivo* methods, but required further *in vivo* experiments to confirm the interaction due to weak interaction in the Y2H experiments (Liao *et al*., manuscript in progress). Finally, the localization patterns of DivIVA and MLJD1 in *E. faecalis* had not yet been determined and potential co-localization of $DivIVA_{Ef}$ and MLJD1 could further implicate MLJD1 as a bacterial cell division protein.

My work was motivated by two hypotheses:

1) $DivIVA_{Ef}$ oligomerization is essential for proper biological function in cell division

2) MLJD1 is a cell division protein in *E. faecalis*, which interacts with $DivIVA_{Ef}$

To test these hypothesizes, I established the following objectives:

1. Introduce various point mutations into chromosomal $divIVA_{Ef}$ known to disrupt oligomerization and analyze the biological effects by Differential Interference Contrast (DIC) Microscopy and Transmission Electron Microscopy (TEM).
2. Confirm $DivIVA_{Ef}$/MLJD1 interaction and identify specific domains involved in that interaction using a Bacterial Two-Hybrid (B2H) system.
3. Determine the localization of $DivIVA_{Ef}$ and MLJD1 in *Enterococcus faecalis* using immunofluorescence microscopy.

2.0 Materials and Methods

2.1 Bacterial Strains and Growth Conditions

Bacterial strains and plasmids used in this study are listed in Table 2.1. *Escherichia coli* XL1-Blue was used as a host strain for cloning experiments and *E. coli* R721 as a reporter strain for Bacterial Two-Hybrid (B2H) protein interaction studies. *Enterococcus faecalis* JH2-2 was used for immunofluorescence microscopy and for creation of *E. faecalis* CBWT and the *divIVA* mutant strains *E. faecalis* MWMR5 and MWMR10. *Escherichia coli* XL1-Blue strain was grown at 37 ^{o}C in Luria-Bertani (LB) medium (Difco, Detroit, MI) supplemented with 100 μg/ml ampicillin (Amp) and/or 50 μg/ml kanamycin (Kan). *Escherichia coli* R721 was grown in LB broth (Difco) supplemented with 50 μg/ml Amp and/or 30 μg/ml Kan at 34 ^{o}C with shaking at 200 rpm. *Enterococcus faecalis* strains were grown in Brain Heart Infusion (BHI) medium (Difco) supplemented with 125 μg/ml erythromycin (Ery), 500 μg/ml Kan, or 1000 μg/ml Kan, as required.

All bacterial strains were stored in cryogenic tubes in BHI broth (Difco) supplemented with 20% glycerol in a -80 ^{o}C freezer (Revco).

2.2 Plasmid Construction

2.2.1 General Polymerase Chain Reaction Amplification Conditions

Primers used in this study are listed in Table 2.2. All primers were designed based on the *E. faecalis* V583 NC_004668 genome available on the NCBI Entrez website (http://www.ncbi.nlm.nih.gov/sites/gquery) and produced by Invitrogen (Carlsbad, CA). Primers used for cloning experiments were designed to incorporate appropriate digestion sites, as indicated in Table 2.2.

Table 2.1: Bacterial strains used in this study

Strains	Relevant Genotype	Source
E. coli XL1-Blue	*hsdR17*, *supE44*, *recA1*, *endA1, gyrA46*, *thi relA1*, *lac*/F' [*proAB*$^{+}$, *lacI*^{q}, *lacZ*DM15::Tn*10*(Tet^{r})]	Stratagene
E. coli R721	71/18 *glpT* :: O-$P_{434/P22}$ *lacZ*	(Di Lallo *et al.*, 2001)
E. faecalis JH2-2	wild type, Rif^{R}, Fus^{R}	ATCC 29212 (Jacob & Hobbs, 1974)
E. faecalis JH2-2+R	JH2-2 carrying pMSPSRDiv-2 (P_{divIVA}-*divIVA*$_{Ef}$)	(Ramirez-Arcos *et al*., 2005)
E. faecalis CBWT	Kan^{R}	this study
E. faecalis MWMR5	JH2-2 *divIVA*$_{Ef}$ mutations (E37P, N43P, L46D, L50E, L57F) carrying pMSPSRDiv-2 (P_{divIVA}- *divIVA*$_{Ef}$); kan^{R} Ery^{R}	this study
E. faecalis MWMR10	JH2-2 *divIVA*$_{Ef}$ point mutation (L143P) carrying pMSPSRDiv-2 (P_{divIVA}- *divIVA*$_{Ef}$); kan^{R} Ery^{R}	this study

Table 2.2: Oligonucleotide primers used in this study

Primer	Sequence (5'- 3')[1]	Restriction Endonucleae Site	Product
CBdivIVA-F	GCGTCGACTATGGCATTAAC	SalI	*divIVA*$_{Ef}$
CBdivIVA-R	GCGGATCCCTATTTTGATTC[2]	BamHI	*divIVA*$_{Ef}$
CBmljd1-F	GCGTCGACGATGAAATTAAG	SalI	*mljd1*
CBmljd1-R	GCGGATCCTTATCTGTTTTG[2]	BamHI	*mljd1*
CBS1-F	GCGTCGACGGAGATCATGAGTCCAC CA	SalI	sequence coding for CBS1 or CBS1CBS2 domains of *mljd1*
CBS2-R	GCGGATCCCTACGTAATATAGGTTAA AATTTTCGT[2]	BamHI	sequence coding for CBS2 or CBS1CBS2 domains of *mljd1*
CBkan-up	GCGCTCTAGAGTGGTTTCAAAATCGG CTCCG	XbaI	P_{aphA-3} ~ *aphA-3*
CBkan-down	GCGCGTCGACTAGGTACTAAAACAA ATCATC[2]	SalI	P_{aphA-3} ~ *aphA-3*
AFdiv-up	GCGCGTCGACATAGACAGAACGTTT AATGTTTATT	SalI	500 base pair sequence after *divIVA*$_{Ef}$
AFdiv-down	GCGCCTGCAGGAATATTTCCGTTTGC ATACGG[2]	PstI	500 base pair sequence after *divIVA*$_{Ef}$
IVA-5	GCGCGGATCCATGGCATTAACTCCAT TAGA	BamHI	*divIVA*$_{Ef}$
CBIVA-2	GAGATCTAGACTATTTTGATTCTTCTT CAA[2]	XbaI	*divIVA*$_{Ef}$
CH-F	TTCATTCAGACGAAGTTGTG	N/A	*divIVA*$_{Ef}$ and 117 bp upstream *divIVA*$_{Ef}$
CH-R	GAACTGCATCTAGGATAGTG[2]	N/A	*divIVA*$_{Ef}$ and 102 bp downstream *divIVA*$_{Ef}$

[1]Restriction endonuclease sites are underlined
[2]Anneals to complementary strand

PCR reactions were carried out in a Perkin-Elmer Gene Amp 9600 Thermocycler (Perkin Elmer, Wellesly, MA) as follows: 5 min at 94 ^{o}C; 35 amplification cycles comprising denaturation at 94^{o}C for 15 seconds, annealing at temperature appropriate to primer for 15 seconds (sec), and extension at 72 ^{o}C for 45 sec to one min depending on sequence length. For the final extension, after completion of cycles, samples were incubated at 72 ^{o}C for 10 min and held at 4 ^{o}C until samples were removed from the thermocycler. PCR products were purified with a PCR Purification Kit (Qiagen Mississauga, ON) before being used for DNA sequencing and/or cloning.

2.2.2 Cloning for Bacterial Two-Hybrid to Study Protein-Protein Interactions

The self-interaction of $DivIVA_{Ef}$ and interaction between $DivIVA_{Ef}$ and MLJD1, $DivIVA_{Ef}$ and the fragment of MLJD1 incorporating the CBS domains, and between $DivIVA_{Ef}$ containing point mutation L104P, I115P, I125P, and L143P (collectively named MR16) and the MLJD1 CBS domain fragment were studied using a Bacterial Two-Hybrid (B2H) system (described in Appendix A). To perform the B2H assay, the genes of the proteins under study, *divIVA*$_{Ef}$ (wild type and mutant), *mljd1*, and the *mljd1* fragment which comprises the sequence encoding the CBS domains (a.a. 79-199), had to be cloned into the expression vectors designed for the B2H system (pcI_{434} and pcI_{P22}; see Table 2.3) (Di Lallo *et al*., 2001). The vectors sent by Di Lallo *et al.* (2001) were p434ftsZ and p22minC (pcI_{434} and pcI_{P22} with *ftsZ* and *minC* cloned in; Table 2.3). I was not interested in studying FtsZ or MinC, so the *ftsZ* and *minC* were digested out of the plasmids p434ftsZ and p22minC, respectively.

Table 2.3: Plasmids used in this study

Plasmid	Relevant Genotype	Source
p434ftsZ	pcI_{434} derivative carrying *ftsZ*	(Di Lallo *et al*., 2001)
p22minC	pcI_{P22} derivative carrying *minC*	(Di Lallo *et al*., 2001)
linear pcI_{434}	pACYC177 derivative carrying N-terminal end of phage 434 repressor	This study
linear pcI_{P22}	pACYC177 derivative carrying N-terminal end of phage P22 repressor	This study
pMR16	Kan^R P_{T7}::*divIVA*$_{Ef}$ (L104P, I115P, I125P, L143P) – 6xHis	(Rigden *et al*., 2008)
pdivIVA434	p434minE derivative with *minE* replaced with wt *divIVA*$_{Ef}$	This study
pdivIVA22	p22minE derivative with *minE* replaced with wt *divIVA*$_{Ef}$	This study
pcI_{434}~linker	pcI_{434} derivative carrying an extra linker	GeneArt
pcI_{P22}~linker	pcI_{P22} derivative carrying an extra linker	GeneArt
p434L-mljd1	pcI_{434}~linker derivative carrying *mljd1*	This study
p22L-mljd1	pcI_{P22}~linker derivative carrying *mljd1*	This study
p434L-CBS1CBS2	pcI_{434}~linker derivative carrying *mljd1* sequence that encodes a.a. 79-199 of MLJD1 containing CBS domains	This study
p22L-CBS1CBS2	pcI_{P22}~linker derivative carrying *mljd1* sequence that encodes a.a. 79-199 of MLJD1 containing CBS domains	This study
p434L-MR16	pcI_{434}~linker derivative carrying mutant *divIVA*$_{Ef}$ (L104P, I115P, I125P, L143P)	This study
p22L-MR16	pcI_{P22}~linker derivative carrying mutant *divIVA*$_{Ef}$ (L104P, I115P, I125P, L143P)	This study
p3ERM	Ery^R P_{lac}::*lacZ*	(Callegan *et al*., 1999)
pTCV-*lac*	Ery^R Kan^R::*lacZ*	(Poyart & Trieu-Cuot, 1997)
p3ERM-kan	Kan^R p3ERM::P_{aphA}::*aphA-3*	This study
p3ERM-kan500	p3ERM-kan::500bp sequence immediately downstream *divIVA*$_{Ef}$	This study
pMR5	Kan^R P_{T7}::*divIVA*$_{Ef}$ (E37P, M43P, L46D, L50D, L57F) – 6xHis	(Rigden *et al*., 2008)
pMR10	Kan^R P_{T7}::*divIVA*$_{Ef}$ (L143P) – 6xHis	(Rigden *et al*., 2008)

pMR15	Kan^R P_{T7}::*divIVA*$_{Ef}$ (L104P, I115P, I125P) – 6xHis	(Rigden *et al*., 2008)
pCBWT	p3ERM-kan500:: wild type *divIVA*$_{Ef}$	This study
pMWMR5	p3ERM-kan500::*divIVA*$_{Ef}$ (E37P, M43P, L46D, L50D, L57F)	This study
pMWMR10	p3ERM-kan500::*divIVA*$_{Ef}$ (L143P)	This study
pCBMR15	p3ERM-kan500:: *divIVA*$_{Ef}$ (L104P, I115P, I125P)	This study
pCBMR16	p3ERM-kan500:: *divIVA*$_{Ef}$ (L104P, I115P, I125P, L143P)	This study
pMSPSRDiv-2	Ery^R P_{nisA} $P_{divIVAEf}$-*divIVA*$_{Ef}$	(Ramirez-Arcos *et al*., 2005)

To do so, p434ftsZ and p22minC were double digested with SalI and BamHI (all restriction endoneucleases were purchased from MBI Fermentas Burlington, ON) as follows: 10 u (units) of BamHI, 20 u of SalI, 4 µl of plasmid DNA, 2 µl of 10x BamHI special buffer (MBI Fermentas), and 11 µl of ddH_2O. Manufacturer's recommendations described SalI as only 50% active in BamHI Special buffer, so the units (u) of SalI added to the reaction was doubled (MBI Fermenta). The samples were run on a 1% agarose gel containing 0.2 mg/ml ethidium bromide (EtBr) at 100 V for 1 hr in TAE buffer (40 mM Tris base, 0.1% acetic acid, 1 mM EDTA). The band in the gel comprising linear plasmid DNA, linear pcI_{434} and pcI_{P22} (Table 2.3), was isolated by gel extracted using a Gel Extraction Kit (Qiagen Mississauga, ON). The bands comprising the *ftsZ* and *minC* genes, now digested out of the plasmid, were discarded with the remaining gel.

In the next step, $divIVA_{Ef}$ was PCR amplified using *E. faecalis* JH2-2 genomic DNA and primers CBdivIVA-F and CBdivIVA-R with an annealing temperature of 53 ^oC and extension time of 1 min. The primers incorporated 5' SalI and 3' BamHI restriction sites. $divIVA_{Ef}$ was digested with SalI and BamHI using 20 u of SalI, 10 u of BamHI, 8 µl of insert ($divIVA_{Ef}$), 2 µl of BamHI special buffer, and 7 µl of ddH_2O. $divIVA_{Ef}$ was cloned into the previously gel extracted linear pcI_{434} and pcI_{P22} using the following ligation reaction: 3 u of T4 DNA ligase (MBI Fermentas Burlington, ON), 3 µl of ATP, 10 µl of insert DNA ($divIVA_{Ef}$), 2 µl of linear vector DNA (pcI_{434} or pcI_{P22}), 2µl of 10x T4 DNA ligase buffer (MBI Fermentas), and 3 µl of ddH_2O with incubated at room temperature for 2 hr. Amounts of insert and vector DNA used in the ligation reaction varied depending on their concentration.

Competent *E. coli* XL1-Blue (Table 2.1) cells were prepared by treatment of log phase culture with sterile 0.1 M $CaCl_2$ (Sambrook, 2001). Competent cells were stored in 0.1 M $CaCl_2$ with 17.5% glycerol at -80 ^oC. The $divIVA_{Ef}$ / plasmid ligation reaction, discussed above,

was transformed into *E. coli* XL1-Blue competent cells as follows: 100 µl aliquot of competent cells and the *divIVA*$_{Ef}$ ligation reaction was incubated on ice for 30 min and 10 µl of the ligation reaction was added to the *E. coli* XL1-Blue cells. After incubating on ice for 30 more min, the cells were then incubated at 42 ^{o}C for 45 sec and once again on ice for 2 min. Nine hundred µl of LB broth was added and the cells were incubated at 37 ^{o}C with shaking at 200 rpm for 2-3 hr. After incubation, cells were collected by centrifuging for 5 min at 5000 rpm in a bench top Microfuge 18 Centrifuge (Beckman Coulter, Mississauga, ON) and resuspended in 200 µl of LB broth. Transformed cells were grown on LB agar supplemented with either 50 µg/ml Kanamycin (Kan^{50}) or 100 µg/ml Ampacylin (Amp^{100}). Screening for positive colonies was performed using a cracking method as follows: after streaking out isolated colonies and o/n incubation, cells from each colony were resuspended in 25 µl of ddH_2O and 25 µl of - 9 parts cracking buffer (11 mM EDTA, pH 8.0, 11% glycerol, 38.5 mM bromophenol blue) with 1 part 1 M NaOH. After incubation at room temperature for 15 min cells were spun for 10 min at 12, 000 rpm and 25 µl loaded onto a 1% agarose gel and run as previously mentioned. DNA samples run by agarose gel electrophoresis were visualized with a MultiImage Light Cabinet (Alpha Innotech Corporation, San Leandro, CA) using the Alpha Imager v5.5 software. All plasmid constructs were isolated and purified (Qiagen Miniprep Kit) and sent to the Plant Biotechnology Institute (PBI Saskatoon, SK) for sequencing as described in Section 2.2.4. Plasmid resulting from the *divIVA*$_{Ef}$ insertion into linear pcI$_{434}$ and pcI$_{P22}$ were named pdivIVA434 and pdivIVA22, respectively (Table 2.3).

Attempts were made to clone *mljd1* into the linear pcI$_{434}$ and pcI$_{P22}$, but this was unsuccessful. Initial cloning of *divIVA*$_{Ef}$ and *mljd1* into the B2H plasmids was difficult because *ftsZ* and *minC* genes had to be digested out of the plasmids to produce the linear pcI$_{434}$ and pcI$_{P22}$, so *divIVA*$_{Ef}$ and *mljd1* could be cloned. The digestion and gel extraction of the vector

DNA resulted in low concentrations of linear pcI_{434} and pcI_{P22}, decreasing the efficiency of the cloning of *divIVA*$_{Ef}$ and *mljd1* into the vectors. Insertion of *divIVA*$_{Ef}$ into linear pcI_{434} and pcI_{P22} was successful, but attempts for cloning in *mljd1* failed. To resolve this cloning issue, plasmids p434ftsZ and p22minC were sent to GeneArt (BioPark, Germany) who removed *ftsZ* and *minC* from the vectors, added a linker (highlighted in Fig 2.1) to incorporate additional digestion sites, and re-circularized the plasmids to create pcI_{434}~linker and pcI_{P22}~linker (Fig 2.1). With pcI_{434}~linker and pcI_{P22}~linker there was no need to digest out any unwanted genes (i.e. *ftsZ* and *minC*) or perform gel extraction. Plasmids pcI_{434}~linker and pcI_{P22}~linker could be digested with SalI and BamHI, as previously described, purified using a PCR purification kit (Qiagen), and directly used in ligations. This resulted in a higher concentration of linear pcI_{434}~linker and pcI_{P22}~linker, which greatly improved the efficiency of cloning as described below.

Enterococcus faecalis JH2-2 genomic DNA was used as a template to PCR amplify *mljd1* using primers CBmljd1-F and CBmljd1-R (Table 2.2) with an annealing temperature of 53 ^{o}C and extension time of 45 sec. These primers incorporated the same 5' SalI and 3' BamHI digestion site as the primers used to amplify *divIVA*$_{Ef}$. Digested, with SalI and BamHI, *mljd1* was cloned into similar treated pcI_{434}~linker and pcI_{P22}~linker using the ligation reaction described for the pdivIVA434 and pdivIVA22 constructs. The ligation reactions were transformed into *E. coli* XL1-Blue and colonies were screened for plasmid as performed previously. The resulting plasmids were named p434L-mljd1 and p22L-mljd1. The 434 and 22 number indicates which phage repressor N-terminal gene sequence is in the plasmid (discussed in Appendix A) and the "L" indicates the B2H plasmids with the linker were used for cloning (pcI_{434}~Linker and pcI_{P22}~Linker).

A.

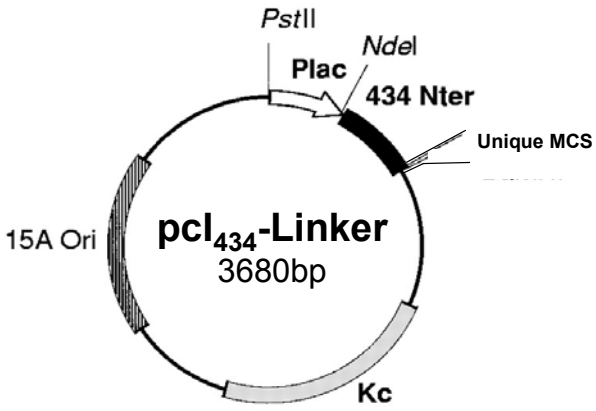

Unique Multiple Cloning Site (MCS) Sequence

SalI

5'- TT AGC ATG GTT AGA GCT GGT TCG TGG TAT GAA GCT TGT GAA CCC TAC GAT ATC AAG TCG ACT **TGG AAT**
Ser Met Val Arg Ala Gly Ser Trp Tyr Glu Ala Cys Glu Pro Tyr Asp Ile Lys Ser Thr Trp Asn

BglII *BamHI*

TCA ATA GAT CTG GAC ATA TGG TTC TCG AGT TAC TGC AGA ATC CCG GGT ATG GAT CCT CCG GCG TTC AGC
Ser Ile Asp Leu Asp Ile Trp Phe Ser Ser Tyr Cys Arg Ile Pro Gly Met Asp Pro Pro Ala Phe Ser

CTG TGC CAC AGC CGA CAG GAT GGT GAC CAC CA **-3'**
Leu Cys His Ser Arg Gln Asp Gly Asp His

B.

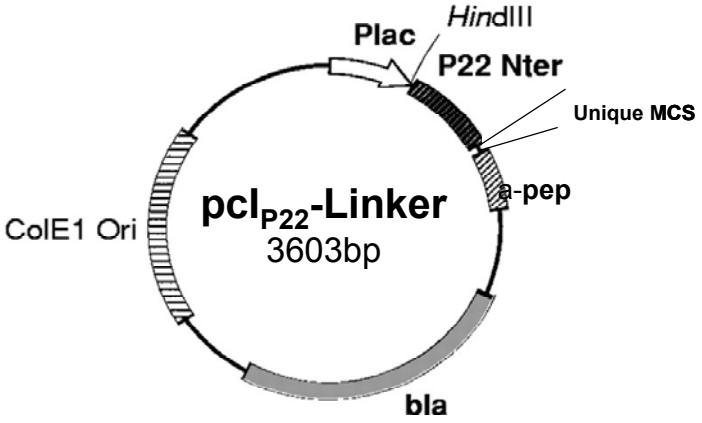

Unique Multiple Cloning Site (MCS) Sequence

SalI *BglII*

5'- A TTG ATT AGC ATG GTT AGA GCT GGT TCG TGG TCG ACT **TGG AAT TCA ATA GAT CTG GAC ATA TGG**
Leu Ile Ser Met Val Arg Ala Gly Ser Trp Ser Thr Trp Asn Ser Ile Asp Leu Asp Ile Trp

XhoI *PstI* *SmaI* *BamHI*

TTC TCG AGT TAC TGC AGA ATC CCG GGT ATG GAT CCC CGG GAA TTC ACT GGC CGT CGT TTT ACA A **-3'**
Phe Ser Ser Tyr Cys Arg Ile Pro Gly Met Asp Pro Arg Glu Phe Thr Gly Arg Arg Phe Thr

Figure 2.1: Modified Bacterial Two-Hybrid vectors. A) pcI_{434}~Linker and B) pcI_{P22}~Linker from Gene Art added a linker (sequence in bold) containing extra digestion sites for cloning purposes.

A gene fragment of *mljd1* incorporating the two CBS domains MLJD1 (encoding amino acids 79-199) were PCR amplified from *E. faecalis* JH2-2 using primers CBS1-F and CBS2-R with an annealing temperature of 53 ^{o}C and an extension time of 45 sec. The fragment was purified, digested with SalI and BamHI, cloned into pcI_{434}~linker and pcI_{P22}~linker, and screened for as performed for *mljd1*. The resulting plasmids were named p434L-CBS1CBS2 and p22L-CBS1CBS2 (Table 2.3).

divIVA$_{Ef}$ $MR16_{L104P,\ I115P,\ I125P,\ L143P}$, which completely disrupts $DivIVA_{Ef}$ oligomerization (Rigden, 2005), were PCR amplified from pMR16 using primers CBdivIVA-F and CBdivIVA-R as performed for wild type *divIVA*$_{Ef}$. The PCR fragment was cloned into pcI_{434}~linker and pcI_{P22}~linker as performed for *mljd1*. The resulting plasmids were named p434L-MR16 and p22L-MR16. MR16 indicates *divIVA*$_{Ef}$ containing the L104P, I115P, I125P, and L143P point mutations.

2.2.3 Cloning *Enterococcus* Suicide Plasmid to Create Point Mutations in *divIVA*$_{Ef}$ on the *Enterococcus faecalis* Chromosome

To test the hypothesis that the N-terminal coiled-coil region and oligomerization of $DivIVA_{Ef}$ are required for its proper biological function in cell division, key point mutations disrupting the N-terminal coiled-coil and oligomerization were introduced into *divIVA*$_{Ef}$ on the *E. faecalis* chromosome. A common method used to introduce mutations into chromosomal genes is to use a suicide plasmid such as p3ERM (Table 2.3). To achieve point mutations in chromosomal *divIVA*$_{Ef}$, the p3ERM constructs required *divIVA*$_{Ef}$, carrying point mutations $MR5_{E37P,\ M43P,\ L46D,\ L50D,\ L57F}$, $MR10_{L143P}$, $MR15_{L104P,\ I115P,\ I125P}$, or $MR16_{L104P,\ I115P,\ I125P,\ I143P}$ (Table 1.1) and a 500 bp sequence of homology with the *E. faecalis* chromosome immediately downstream *divIVA*$_{Ef}$ to facilitate homologous recombination. For screening purposes, a kanamycin cassette was also required in the p3ERM constructs.

To clone the kanamycin cassette into p3ERM, the kan cassette was first PCR amplified from pTCV-*lac* (Table 2.3) using primers CBkan-up and CBkan-down (Table 2.2) with an annealing temperature of 54 ^{o}C and 1.5 min extension. The primers incorporated 5' XbaI and 3' SalI restriction digestion sites. The PCR product was purified and digested with XbaI and SalI as in section 2.2.2, but with 10x Tango buffer (2x) to optimize for these different enzymes. Plasmid p3ERM (Table 2.3) was isolated (Qiagen Miniprep Kit) and digested with XbaI and SalI. The digested Kan cassette and p3ERM (vector) were ligated as mentioned in section 2.2.2. The ligation reaction of the kan cassette with p3ERM was transformed into competent *E. coli* XL1-Blue as in section 2.2.2. Cells were then plated on LB agar supplemented with 125 µl/ml Ery (Ery^{125}) plus 50 µl/ml Kan (Kan^{50}) and incubated over night (o/n) at 37 ^{o}C. Between 16-32 colonies were re-grown on a fresh LB plate containing Ery^{125} Kan^{50} for screening using the cracking method previously described in section 2.2.2 (Fig 2.2 A). Recombined plasmids suspected of containing the kan cassette were isolated and the kan cassette was amplified using the CBkan-up and CBkan-down primers (Table 2.2) to confirm the presence of the cassette. The resulting amplification confirmed insertion of the kan cassette into p3ERM with a band at approximately 1000 bp (Fig 2.2 B). The p3ERM plasmid with the kan cassette insert was named p3ERM-kan (Fig 2.3 B; Table 2.3). The next step in the creation of suicide vector p3ERM-kan500 (Fig 2.3 C) was to insert the 500 bp sequence, sequence from immediately downstream of chromosomal $divIVA_{Ef}$, to the 3' end of the kan cassette insert in p3ERM-kan. The 500 bp sequence was PCR amplified from *E. faecalis* JH2-2 genomic DNA using primers AFdiv-up and AFdiv-down with an annealing temperature of 57 ^{o}C (Table 2.2).

The primers introduced 5' SalI and 3' PstI restriction digestion sites onto the 500 bp sequence. Using p3ERM-kan as vector, restriction digestion, ligation, and transformation procedures were performed as described in section 2.2.2.

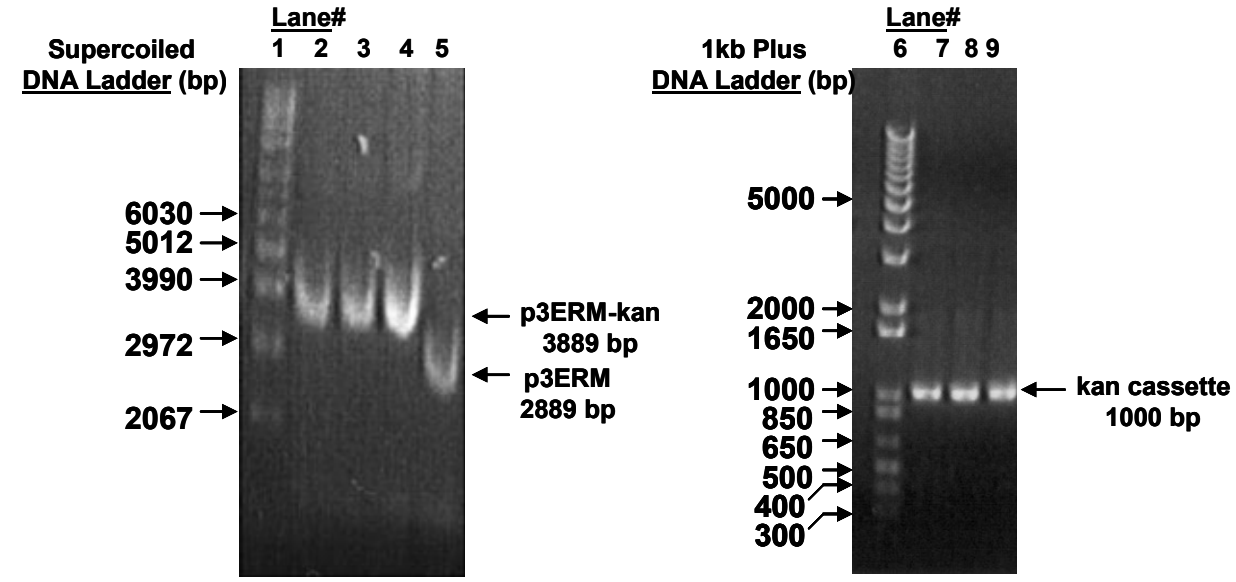

Figure 2.2: Gel electrophoresis of screening for p3ERM-kan plasmid construct. A) Cracking results of p3ERM-kan plasmid constructs. Cell extracts from three colonies, lanes 2, 3, and 4, showed plasmids potentially carrying the kan cassette insert. Lane 5 is cell extract showing p3ERM. B) Plasmids isolated from cell samples from lanes 2, 3, and 4 were confirmed to contain the kan cassette through using the plasmids as templates to PCR amplify the kan-cassette (lanes 7, 8, and 9 respectively). DNA ladders are from Invitrogen.

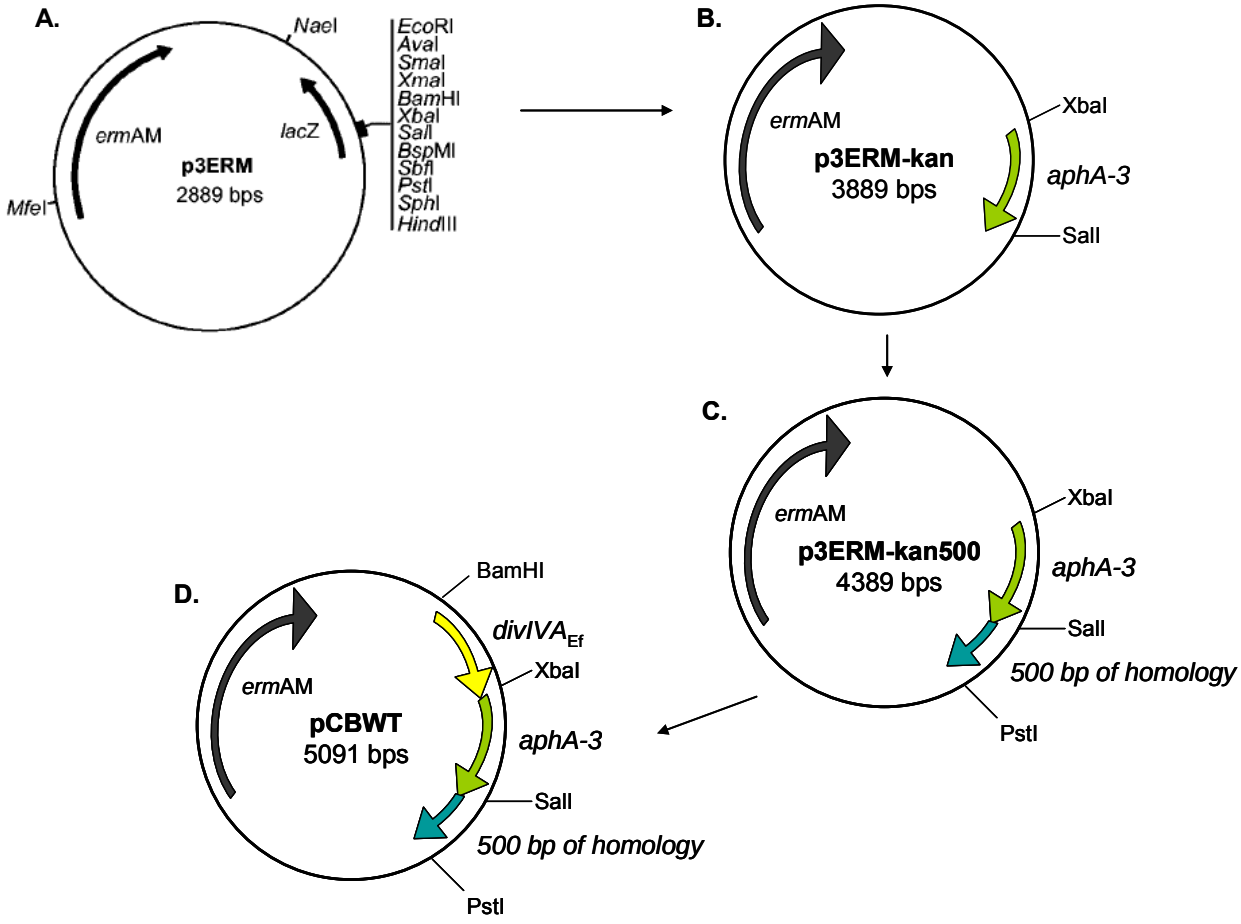

Figure 2.3: Maps of plasmids constructed for creating *Enterococcus faecalis divIVA*$_{Ef}$ mutant strains. A) p3ERM- an *Enterococcus* suicide vector (Callegan *et al*., 1999). B) p3ERM with the kanamycin cassette cloned into the XbaI/ SalI digestion site. C) A 500 bp DNA sequence homologous to the DNA sequence immediately downstream *divIVA*$_{Ef}$ on the *E. faecalis* chromosome. This sequence was cloned into p3ERM-kan to facilitate homologous recombination of cloned *divIVA*$_{Ef}$ with *divIVA*$_{Ef}$ on the *E. faecalis* JH2-2 chromosome. D) The suicide vector pCBWT includes *divIVA*$_{Ef}$~kan cassette~500 bp of homology. Mutant *divIVA*$_{Ef}$ could be cloned in place of wild type *divIVA*$_{Ef}$ using p3ERM-kan500 as the vector.

To screen for potential positive colonies cracking was utilized as for p3ERM-kan (Fig 2.4 A). The plasmid p3ERM-kan potentially carrying the 500 bp sequence was used as template for PCR using AFdiv-up and AFdiv-down to check for the 500 bp insert (Fig 2.4 B). The resulting plasmid was named p3ERM-kan500 (Fig 2.3 C; Table 2.3).

The p3ERM-kan500 vector was then used to clone wild type *divIVA*$_{Ef}$ or *divIVA*$_{Ef}$ containing MR5$_{E37P, M43P, L46D, L50D, L57F}$, MR10$_{L143P}$, MR15$_{L104P, I115P, I125P}$, or MR16$_{L104P, I115P, I125P, L143P}$ point mutations (Table 1.1) upstream of the kan cassette. Wild type *divIVA*$_{Ef}$ and mutant *divIVA*$_{Ef}$ were PCR amplified using primers IVA-5 and CBIVA-2 at an annealing temperature of 50 ^{o}C (Table 2.2). The template for the PCR amplification of wild type *divIVA*$_{Ef}$ was *E. faecalis* JH2-2 genomic DNA. The templates for *divIVA*$_{Ef}$ with mutations MR5$_{E37P, M43P, L46D, L50D, L57F}$ was pMR5, point mutation MR10 (L143P) was pMR10, point mutations MR15$_{L104P, I115P, I125P}$ was pMR15, and for point mutations MR16$_{L104P, I115P, I125P, L143P}$ was pMR16 (Table 2.3). Digestion sites introduced were 5' BamHI and 3' XbaI which were utilized to clone *divIVA*$_{Ef}$ into the p3ERM-kan500 vector. Digestion of p3ERM-kan500 and the *dvIVA*$_{Ef}$ PCR product with BamHI and XbaI and subsequent ligation would result in a construct comprising *divIVA~kan cassette~500 bp of homology* cloned into the p3ERM suicide vector (Fig 2.5 A). Cracking was utilized for screening and positive colonies were used to isolate the cloned vectors. The vector containing wild type *divIVA*$_{Ef}$ was named pCBWT (Fig 2.3 D; Table 2.3), whereas pMWMR5 contains *divIVA*$_{Ef}$ point mutation construct MR5$_{E37P, M43P, L46D, L50D, L57F}$, pMWMR10 contains point mutation construct MR10$_{L143P}$, pCBMR15 contains MR15$_{L104P, I115P, I125P}$, and pCBMR16 contains MR16$_{L104P, I115P, I125P, L143P}$ (Table 2.3). All plasmids were sequenced using primers IVA-5 and CBIVA-2 to check for *divIVA*$_{Ef}$ gene integrity and conservation of the desired point mutations.

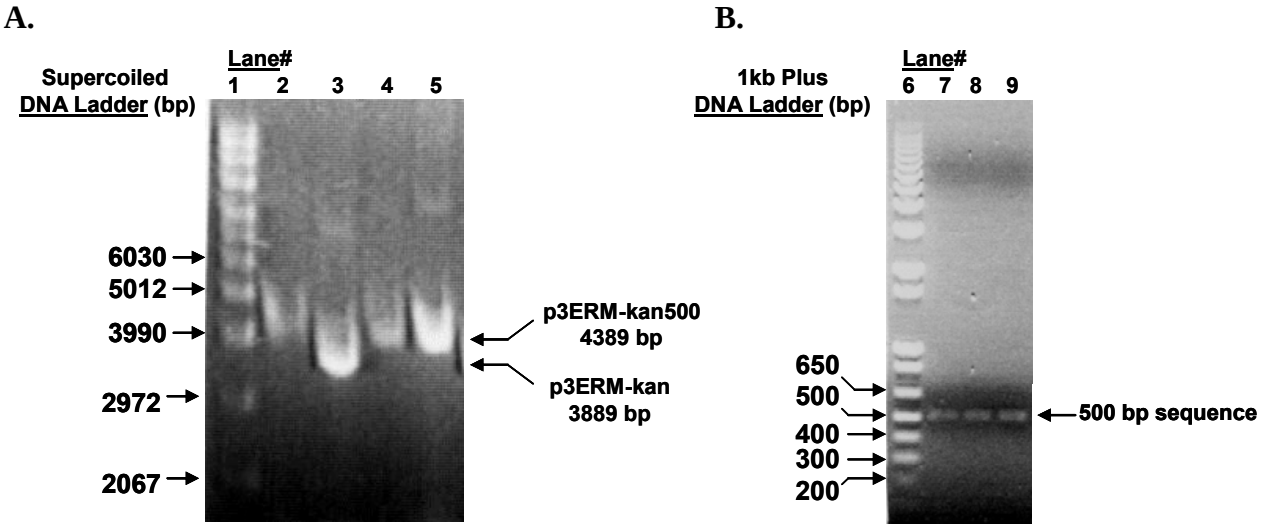

Figure 2.4: Gel electrophoresis of screening for p3ERM-kan500 plasmid construct: A) Cracking results of screening for colonies positive for p3ERM-kan500. Plasmids in Lanes 2, 4, and 5 were suspected to have the 500 bp insert while Lane 3 was suspected to contain p3ERM-kan without the 500 bp insert. B) PCR amplification of the 500 bp insert, using isolated plasmids from sample in lane 2, 4 and 5 as template, confirmed the presence of the 500 bp insert in all three isolates.

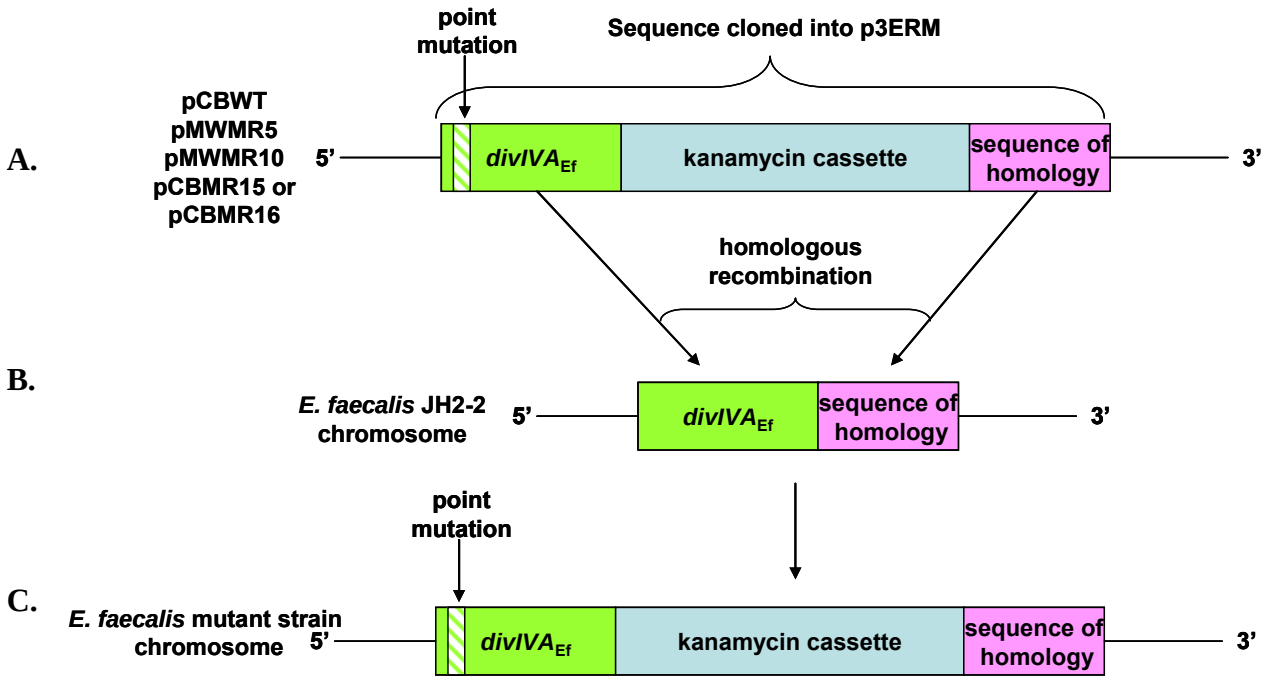

Figure 2.5: Diagram of allelic replacement of chromosomal wild type *divIVA*$_{Ef}$ with plasmid *divIVA*$_{Ef}$ carrying various point mutations. How the suicide vectors pCBWT (no point mutations in *divIVA*$_{Ef}$), pMWMR5 (*divIVA* with point mutations E37P, N43P, L46D, L50E, L57F), pMWMR10 (*divIVA* with point mutation L143P), pCBMR15 (*divIVA* with point mutations L104P, I115P, I125P) or pCBMR16 (*divIVA* with point mutations L104P, I115P, I125P, L143P) was used to replace chromosomal wild type *divIVA*$_{Ef}$ with *divIVA*$_{Ef}$ carrying the indicated point mutations. A) *divIVA* cloned into p3ERM-kan500; where the sequence of homology assists in homologous recombination between B) the *divIVA*$_{Ef}$ and 500 bp sequence of homology in the vector and the same sequence in the *E. faecalis* JH2-2 chromosome. C) The result is allelic replacement in the *E. faecalis* chromosome of wild type *divIVA*$_{Ef}$ with the mutated *divIVA*$_{Ef}$ and insertion of the kanamycin cassette.

Once constructed, the modified p3ERM was transformed into *E. faecalis* JH2-2 (Table 2.1) to allow allele exchange to occur between $divIVA_{Ef}$ in the chromosome and mutated $divIVA_{Ef}$, from the vector (Fig 2.5 C).

2.2.4 Sequencing of Plasmid Constructs and PCR Products

The DNA sequence of all genes, cloned into plasmid constructs (the entire gene) and their respective PCR products, were obtained at the Plant Biotechnology Institute (PBI Saskatoon, SK) to check gene integrity. Forward and reverse sequences were analyzed using an NCBI web page program BLAST 2 Sequences (http://blast.ncbi.nlm.nih.gov/bl2seq/wblast2.cgi) to align the sequencing data with the wild type sequence on default settings. All DNA sequence chromatographs were also manually analyzed to check any miss matched bases.

2.3 Creation of *Enterococcus faecalis divIVA* Mutants

2.3.1 Creation of Electrocompetent *Enterococcus faecalis* Cells

To create *E. faecalis divIVA* mutants, *E. faecalis* JH-2-2 (Table 2.1) cells were made electrocompetent. Using the protocol of Shepard *et al.* (Shepard & Gilmore, 1995), *E. faecalis* JH2-2 was grown in M17 broth (Difco) overnight at 37 ^{o}C without shaking. One ml of the overnight culture was added to 100 ml of fresh sterile M17 broth (Difco) supplemented with 0.5 M sucrose and 4% glycine (SGM17 broth) at pH 6.8-7.0 (Shepard & Gilmore, 1995). Initially SGM17 broth containing 2%, 4%, or 8% glycine was tested. Growth in glycine weakens the Gram-positive cell wall allowing entrance of plasmid DNA upon exposure to an electric pulse (Shepard & Gilmore, 1995). A higher percentage of glycine increases the transformation efficiency (Shepard & Gilmore, 1995). However, cells grown in 8% glycine did not grow up to the required OD_{560} of about 0.6 within 24 hr. Growth in 4% glycine did work well, so this concentration was used to create all electrocompetent *E. faecalis* JH2-2 cells. After growth

reached OD_{560} 0.6 (log phase), cells were collected by centrifuging at 5000 rpm for 10 min in a Sorvall RC 5C Plus centrifuge in a GSA rotor. Cells were washed with ice cold electroporation buffer (0.5 M sucrose and 10% glycerol) three times (Shepard & Gilmore, 1995). The cells were resuspended in electroporation buffer to a volume one one-hundredth of the original volume and 40 µl aliquots dispensed in microcentrifuge tubes for storage in the -80 ^{o}C freezer (Shepard & Gilmore, 1995).

2.3.2 Electroporation of *Enterococcus faecalis* JH2-2 Electrocompetent Cells for the Creation of Mutant *divIVA*$_{Ef}$ Strains

Plasmid DNA (pCBWT, pMWMR5, pMWMR10, pCBMR15 or pCBMR16 (Table 2.3)) and a 40 µl aliquot of the electrocompetent *E. faecalis* JH2-2 cells were incubated on ice for 30 min. An electroporation cuvette with a gap width of 0.2 cm was also chilled on ice for at least 5 min (Shepard & Gilmore, 1995). The volume of plasmid DNA added to *E. faecalis* cells depended on the concentration of the plasmid preparation, which was eluted in ddH_2O. Generally, no more than 3.5 µl of plasmid DNA was added to 40 µl of electrocompetent cells (Shepard & Gilmore, 1995). A higher volume used could reduce the transformation efficiency and/or result in arching of the electrical pulse due to higher salt concentrations associated with a higher volume. The concentration of each plasmid transformed into *E. faecalis* is discussed below. A pulse of 2.5 kV, 25 mF capacitance, and 200 W was applied to the cuvette containing cell/plasmid mixture (Shepard & Gilmore, 1995). One ml of ice cold M17 broth supplemented with 0.5 M sucrose, 10 mM $MgCl_2$, and 10 mM $CaCl_2$ (SM17MC broth) was added to the cells in the cuvette and the cuvette was incubated on ice for a minimum of 10 min and at 37 ^{o}C for 3 hr (Shepard & Gilmore, 1995). Cells were collected by centrifuging at 5000 rpm for 5 min and resuspended in 100 µl of SM17MC broth (Shepard & Gilmore, 1995). Cells were plated on SR agar containing either Kan^{500} or Kan^{500} plus Ery^{125} depending on the plasmids transformed.

The plasmid pCBWT (Table 2.3) was transformed into *E. faecalis* JH2-2 to ensure the insertion of the kan cassette into the chromosome did not affect cell growth. The ideal amount of plasmid DNA required for efficient transformation into electrocompetent *E. faecalis* was determined to be between 150-1000 ng, however, the volume of DNA added to the cells could not exceed one-tenth the volume of the cells (as discussed above). So, in a 40 µl aliquot of cells no more than 4 µl of DNA could be added. To obtain high concentrations of plasmid DNA, two 50 µl plasmid preparations were run through a single PCR purification column and eluted with 50 µl of ddH_2O to obtain a concentration of 400 ng/µl for pCBMR15, 240 ng/µl of pCBMR16 (Fig 2.6 A), and 200 ng/µl of pCBWT (Fig 2.6 B). After electroporation and incubation, the transformed cells were plated on SR Kan^{500} agar and incubated at 37 ^{o}C for 18-24 hr. Electroporation of pMWMR5 and pMWMR10 was performed in the same manner. Colonies were isolated for the pCBWT transformation by streaking on a fresh SR Kan^{500} [the minimal inhibitory concentration (MIC) for *E. faecalis* JH2-2 was found to be 500 µg/ ml Kan (Ramirez-Arcos *et al*., 2005)] plate and incubated for 18 hr at 37 ^{o}C. Upon 4-5 attempts no viable cells giving rise to *E. faecalis* JH2-2 colonies were obtained after transforming the pMWMR5, pMWMR10, pCBMR15 or pCBMR16 plasmid constructs. For screening colonies transformed with pCBWT a small amount of cells was resuspended in ddH_2O to use as a template for screening with PCR. For screening, PCR using primers that bind 117 bp upstream $divIVA_{Ef}$, CH-F (Table 2.2) and 102 bp downstream $divIVA_{Ef}$, CH-R (Table 2.2) on the chromosome were used to check if allelic exchange was successful. After transformation with pCBWT, wild type $divIVA_{Ef}$ was present and the kan cassette was integrated into the chromosome immediately downstream $divIVA_{Ef}$ (stain named *E. faecalis* CBWT; Table 2.1). This strain had a PCR fragment of about 1921 bp (Fig 2.7) containing $divIVA_{Ef}$, the kan

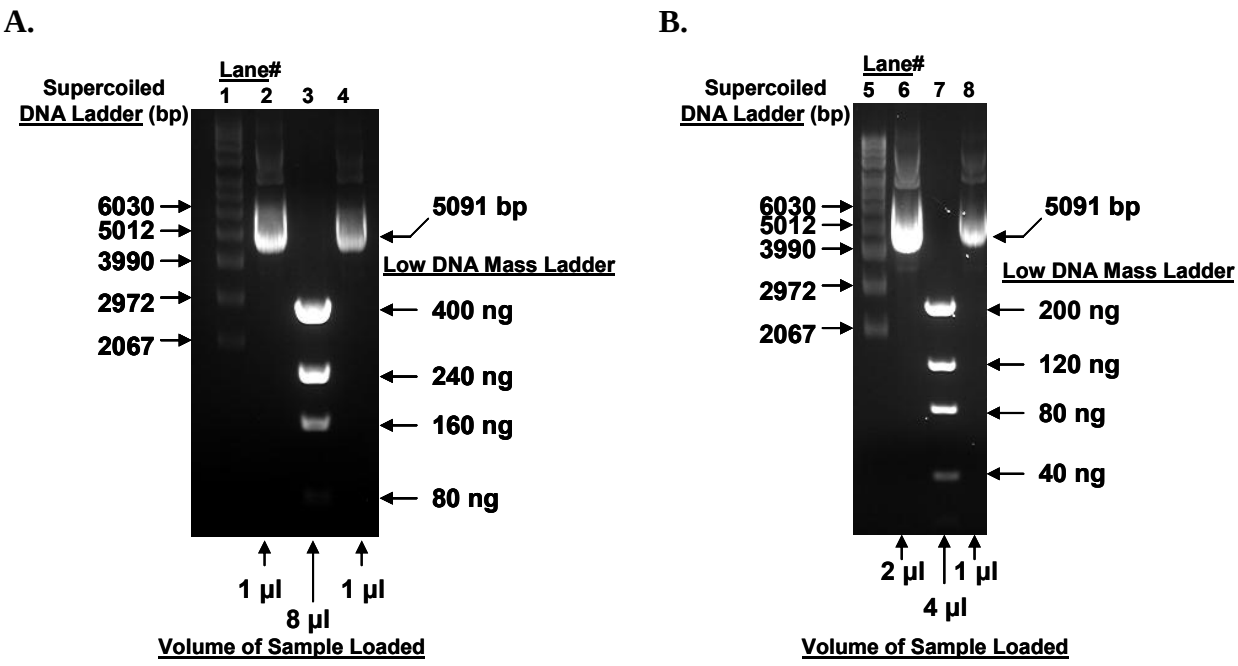

Figure 2.6: Gel electorphoresis for determining plasmid concentrations for *Enterococcus faecalis* JH2-2 electroporation. A) Lane 2: pCBMR15 with a concentration of approximately 400 ng/µl; Lane 4: pCBMR16 with an approximate concentration of 240 ng/µl. B) Lanes 6 and 8 are the same sample of pCBWT with an approximate concentration of 200 ng/µl. Lane 3 and 7: Low Mass DNA Ladder (Invitrogen).

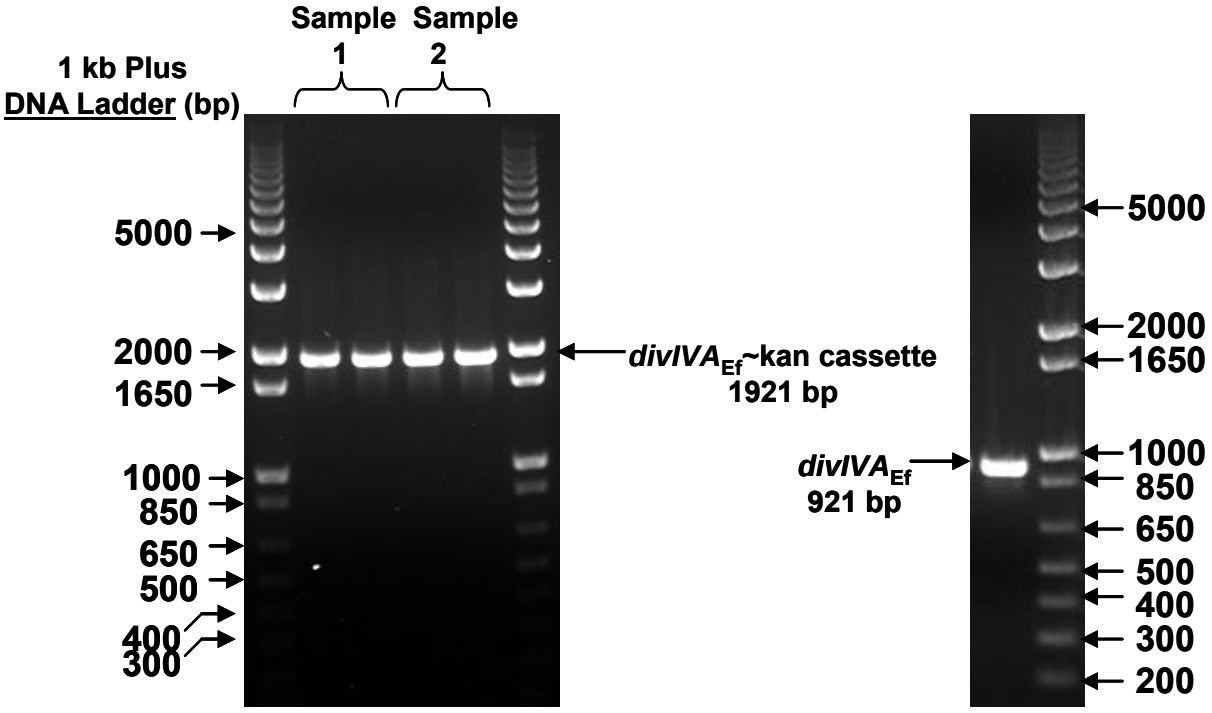

Figure 2.7: Gel electrophoresis of PCR amplification used to screen *Enterococcus faecalis* for the kanamycin cassette insert. *E. faecalis* cells transformed with pCBWT was used as template to PCR screen for the *divIVA*::kan cassette insert, using chromosomal primers CH-F and CH-R, into the *E. faecalis* JH2-2 chromosome. Sample 1 and sample 2 were positive for the *divIVA*~kan insert with an expected fragment including 117 bp upstream *divIVA*$_{Ef}$, *divIVA*$_{Ef}$, the kan cassette, and 102 bp downstream *divIVA*$_{Ef}$ resulting in the band at ~1921 bp. The picture on right is a negative control for primers CH-F and CH-R showing *divIVA*$_{Ef}$ PCR amplified from *E. faecalis* JH2-2, which did not contain the kanamycin insert.

cassette, and 117 bp upstream and 102 bp downstream *divIVA*$_{Ef}$, respectively, due to the binding sites of primers CH-F and CH-R on the *E. faecalis* chromosome. Those colonies negative for homologous recombination resulted in a PCR fragment of the 117 bp upstream bases, *divIVA*$_{Ef}$, and the 102 bases downstream *divIVA*$_{Ef}$ to give a fragment size of 921 bp (Fig 2.7). The 1921 bp fragments PCR amplified from positive colonies were sent for sequencing (PBI) using primers CH-F, CH-R, IVA-5, CBIVA-2, CBkan-up, and CBkan-down to check gene integrity of *divIVA*$_{Ef}$ and the kan cassette (as mentioned in section 2.2.4). Since no colonies were recovered upon transformation with pMWMR5, pMWMR10, pCBMR15, or pCBMR16, the *divIVA*$_{Ef}$ mutations MR5$_{I37P,\ M43P,\ L46D,\ L50D,\ L57D}$, MR10$_{L143P}$, MR15$_{L104P,\ I115P,\ I125P,}$ and MR16$_{L104P,\ I115P,\ I125P,\ L143P}$ (Table 1.1) were probably lethal. For this reason the rescue method developed by Ramirez-Arcos *et al* was employed (Ramirez-Arcos *et al*., 2005). The rescue plasmid pMSPSRDiv-2 (Table 2.3), which expressed wild type *divIVA*$_{Ef}$ *in trans*, was co-transformed with pMWMR5, pMWMR10, pCBMR15, or pCBMR16. Colonies resulting from pMWMR5 and pMWMR10 double transformed with pMSPSRDiv-2 were isolated from growth on SR Kan^{500} Ery^{125} agar plates and screened using the CH-F and CH-R primers as was done for screening with pCBWT. The use of SR agar helped to reduce background growth observed when plated on BHI agar after electroporation of *E. faecalis* JH2-2 to transform in plasmid DNA. SR agar contains per liter: 10 g trypton, 200 g sucrose, 5 g yeast extract, 25 g gelatin, 10 g glucose, 2.5 mM $MgCl_2$, 2.5 mM $CaCl_2$. Colonies were screened for positive homologous recombination as was performed with *E. faecalis* CBWT. Introduction of the MR5$_{E37P,\ N43P,\ L46D,\ L50E,\ L57F}$ and MR10$_{L143P}$ point mutations was successful. The *E. faecalis* JH2-2 strain with the *divIVA*$_{Ef}$ MR5 (E37P, N43P, L46D, L50E, L57F) point mutations was named *E .faecals* MWMR5 and *E. faecalis* MWMR10 carrying the *divIVA*$_{Ef}$ MR10 (L143P) point mutation (Table 2.1). Sequencing of the 1921 bp PCR fragment amplified from *E.*

faecalis MWMR5 and *E. faecalis* MWMR10 confirmed the presence of the required point mutations.

Three attempts to introduce $MR16_{L104P,\ I115P,\ I125P,\ L143P}$ were unsuccessful with no colonies isolated. One colony isolated from a transformation with pCBMR15 (containing $divIVA_{Ef}$ MR15 $_{L104P,\ I115P,\ I125P}$) did have the appropriate 1921 bp PCR amplicon, but DNA sequencing showed that only the I125P point mutation was present in the chromosome. Additional attempts to introduce MR15 point mutations into $divIVA_{Ef}$ were unsuccessful, so were probably lethal.

2.4 Western Blots

Enterococcus faecalis JH2-2, *E. faecalis* CBWT and *E. coli* R721 (carrying various B2H plasmids) cell extracts were analyzed using sodium dodecyl sulphate polyacrylamide gel electrophoresis (SDS-PAGE) as developed by Sambrook *et al*. (1980). To extract protein from log phase *E. faecalis*, cells were first treated with 20 mg/ml lysozyme (Sigma, Oakville, ON) and incubated at 37 ^{o}C for 1 hr. Then glass beads (Sigma, Oakville, ON) were added followed by 5 min of vigorous mixing with a vortex (all *E. faecalis* strains were treated the same). For *E. coli* and *E. faecalis* protein loading buffer (62.5mM Tris-HCl; pH 6.8, 2% SDS, 25% glycerol, 0.01% bromophenol blue) was added, in a 1:5 ratio, to each sample (Sambrook, 1980). Samples were then boiled for 10 min., vortexed again for 2 min., and spun down at 14,000 rpm for a few seconds. For *E. coli* and *E. faecalis,* whole cell extracts were run on an SDS-PAGE gel consisting of a 5% stacking gel and 12% resolving gel. For electrophoresis, 10 µl of Precision Plus Protein dual color standard marker (Bio-Rad, Hercules, CA) and 30 µl of each sample was loaded on the SDS-PAGE gel and run in running buffer (5 mM Tris-HCl, 50 mM glycine and 0.1% SDS, pH 8.3) at 100V for 1.6 hr (until loading dye ran off the gel). The gel was then stained with Coomassie brilliant blue (Sambrook, 1980) for an hr and distained using

45% methanol (CH_3OH) and 10% acetic acid solution. Spot densitometry was performed using the MultiImage Light Cabinet (Alpha Innotech Corporation, San Leandro, CA) and Alpha Imager v5.5 software to determine approximate protein concentrations for normalized loading of Western blots.

After protein electrophoresis with standardized loading, the separated proteins in the SDS-PAGE gel were transferred to an Immobilon transfer membrane with a pore size of 0.45 um (Millipore, Bedford, MA) for 90 min at 100V in transfer buffer (20% CH_3OH, 10% TG buffer). The membrane was blocked for 1 hr at room temperature with 3% skim milk in 1x TBS (4x TBS: 200 mM Tris, 5M NaCl). After blocking, the membrane was washed with TTBS (1x TBS with 0.05% Tween 20). The membrane was then incubated o/n at 4 ^oC with primary $DivIVA_{Ef}$ polyclonal antibody (Ramirez-Arcos *et al*., 2005) diluted 1:1000, 1:2000, and 1:4000 in TTBS. The next day the membrane was washed in TTBS three times and treated with secondary anti rabbit IgG antibody (BioRad) diluted 1:3000 in TTBS. It was incubated for 1 hr at room temperature, washed three times in TTBS, and washed once in 1x TBS. Autophos was added to the membrane and viewed with the MultiImage Light Cabinet (Alpha Innotech Corporation, San Leandro, CA) using the Alpha Imager v5.5 software.

2.5 Bacterial Two-Hybrid Assay

The Bacterial Two-hybrid system used in this study is discussed in Appendix A. *E. coli* R721 cells were double transformed with pcI_{434}~linker and pcI_{22}~linker each containing gene inserts of proteins under study (Table 2.4). For interaction studies between $DivIVA_{Ef}$ and full length MLJD1 *E. coli* R721 was double transformed with pdivIVA434 / pdivIVA22 (to check $DivIVA_{Ef}$ self interaction), pdivIVA434 / p22L-mljd1, and p434L-mljd1 / pdivIVA22 (Table 2.4). Each plasmid mentioned was also transformed into *E. coli* R721 alone to check background repression induced by each plasmid alone (negative control). *E. coli* R721 with no

Table 2.4: The combination of plasmids transformed into *Escherichia coli* R721 for Bacterial Two-Hybrid experiments.

B2H Plasmid Constructs	pdivIVA434	p434L-mljd1	p434L-CBS1CBS2	p434L-MR16
pdivIVA22	+	+	+	-
p22L-mljd1	+	-	-	-
p22L-CBS1CBS2	+	-	-	+
p22L-MR16	-	-	+	-

Note: Plasmid combinations used to study the interaction capabilities between $DivIVA_{Ef}$ and full length MLJD1, $DivIVA_{Ef}$ and the CBS containing fragment of MLJD1, and $MR16_{L104P, I115P, I125P, L143P}$ mutant $DivIVA_{Ef}$ with the CBS containing fragment of MLJD1.

+ indicates plasmids that were double transformed
- indicates plasmids that were not double transformed

plasmid transformed was also used in each assay as a base measure for maximum β-galactosidase activity. The same was performed when studying the interaction between $DivIVA_{Ef}$ and the fragment of MLJD1 containing the two CBS domains, with plasmids pdivIVA434, pdivIVA22, p434L-CBS1CBS2, and p22L-CBS1CBS2 (Table 2.4). Interaction between the $MR16_{L104P,\ I115P,\ I125P,\ L143P}$ $DivIVA_{Ef}$ mutant and the fragment containing the two CBS domains of MLJD1 was also studied, using plasmids p434L-MR16, p22L-MR16, p434L-CBS1CBS2, and p22L-CBS1CBS2 (Table 2.3). Each assay was performed in triplicates.

To prepare cultures for the B2H assay, 3 ml of LB broth supplemented with $Kan^{30}Amp^{50}$, Kan^{30}, or Amp^{50} and 30 μg/ml chloramphenicol (Cm^{30}) for *E. coli* R721 with no plasmid, were inoculated from frozen stock and grown o/n at 37 ^{o}C and 200 rpm. The following morning o/n culture was diluted 1:100, for cultures with normal growth rates, or 1:50, for cultures with slower growth rates, into 4 ml of fresh LB broth supplemented with appropriate antibiotics and 1.0 x 10^{-4} M IPTG. Cultures were grown for 2.5-3 hr or until OD_{600} = 0.4-0.7. Cells were then incubated on ice for 20 min and then spun down at 6000 rpm for 10 min. After the supernatant was discarded, cells were resuspended in 1.5 ml of cold Z-buffer (0.06 M Na_2HPO_4, 0.04 M NaH_2PO_4 H_2O, 0.002 M KCl, 0.004 M $MgSO_4$ $7H_2O$, and 10.28% β-mercaptoethanol). The OD_{600} of the cell suspension was measured with an Ultrospec 3100 Pro (Fisher Scientific, Ottawa, ON) using 1 ml cuvettes (VWR, Mississauga, ON). Each sample was diluted 1:10 to make triplicates with a final volume of 1 ml. Cells were permeabilized by the addition of 0.1 ml chloroform and 0.05 ml of 0.1% SDS, vortexed and incubated for 5 min at 28 ^{o}C. To start the β-galactosidase assay 4 mg/ ml of ONPG was added to each tube consecutively every 10 seconds and the tubes vortexed. Once the reaction reached sufficient yellowing the reaction was stopped with 0.5 ml of 1 M Na_2CO_3, vortexed, and the stop time recorded. Samples were centrifuged at 14,000 rpm to pull cell debris and chloroform

to the bottom of the tube and 1 ml of the supernatant was dispensed into a cuvette. The OD_{420} and OD_{550} were recorded and Miller units were determined using the following equation: Miller units = 1000 x [(OD_{420} – 1.75) x OD_{550}] / (T x V x OD_{600}) where T = reaction time in min and V = volume of culture used in assay tubes in ml. The percentage of reduced β-galactosidase activity was calculated as in the following sample calculation: % reduction = ((R721 control (Miller Units) -$DivIVA_{Ef}$~$DivIVA_{Ef}$ (Miller Units) / R721 control) x 100 = ((1842.74 – 884.06) / 1842.74) x 100 = 52%. The threshold for determining protein-protein interaction was 50%, where >50% reduction in β-gal activity indicates positive interaction and <50% reduction indicates no or uncertain interaction (Di Lallo *et al.*, 2003, Fadda *et al*., 2007).

2.6 Microscopy of *Enterococcus faecalis* Strains JH2-2, JH2-2+R, CBWT, MWMR5 and MWMR10

2.6.1 Differential Interference Contrast Light Microscopy

For Differential Interference Contrast (DIC) light microscopy *E. feacalis* strains JH2-2, JH2-2+R (JH2-2 with rescue vector pMSPSRDiv-2 containing *divIVA*$_{Ef}$ and its own promoter (Table 2.1)), CBWT, MWMR5, and MWMR10 were cultured over night for stationary cultures or for 6-7 hr (or until the culture reached OD_{560} 0.6) for log phase cultures (Shepard & Gilmore, 1995) in BHI broth supplemented with no antibiotics, 1000 μg/ml Kan, 125 μg/ml Ery, or 1000 μg/ml Kan plus 125 μg/ml Ery. Cells were fixed with 0.2% gluteraldehyde and 6% formaldehyde and transferred to 0.1% Poly-L-Lysine (Sigma-Aldrich Co., St. Louis, MO) coated cover slips (Ramirez-Arcos *et al*., 2001b). To stain chromosomal DNA, about 3 μl of 0.2 μg/ ml of 4',6-diamidino-2-phenylindole (DAPI) stain was incubated on the cover slips for 1.5-2 min and then rinsed off with 1x PBS. Cover slips containing fixed cells were placed on glass slides containing a drop of 50% glycerol (Ramirez-Arcos *et al*., 2001b) and the edges of the cover slip were sealed with clear nail polish to prevent the sample from drying out. Over

500 cells were examined for each strain and with an Olympus BX61 microscope. Images were taken using a Photometrics CoolSnap ES camera with ImagePro Version 5 Software (Media Cybernetics, Bethesda, MD) and In Vitro (Media Cybernetics) software. The experiment was performed twice for each strain (Rigden *et al*., 2008).

2.6.2 Transmission Electron Microscopy

To prepare *E. faecalis* JH2-2, CBWT, MWMR5 and MWMR10 for transmission electron microscopy, cultures were first grown over night to stationary phase at 37 ^{o}C, with no shaking, in BHI broth supplemented with 1000 μg/ml Kan, 125 μg/ml Ery, or 50 μg/ml Kan plus 125 μg/ml Ery (for strains CBWT, MWMR5 and MWMR10). *E. faecalis* JH2-2 required no antibiotic supplementation. Cells were grown to log phase (6-7 hr) and 3 ml were pellated by centrifuging at 5,000 rpm for 5 min. Collected cells were washed in 0.01 M Na-cacodylate buffer and 38 μl of 25% glutaraldehyde was added. Cells were left at 4 ^{o}C overnight to fix. Cells were washed in 0.01 M Na-cacodylate buffer twice more, resuspended in 0.01 M Na-cacodylate buffer and shipped on ice to the Electron Microscopy Unit, Surgical Medical Research Institute, University of Alberta (Edmonton, Alberta). Dr. Ming Chen further processed the samples and performed Transmission Electron Microscopy (TEM) using a Hitachi Transmission Electron Microscope H-7000 and mailed the negatives back to our laboratory for analysis.

2.6.3 Statistical Analysis of DIC and TEM Micrographs of *Enterococcus faecalis* JH2-2, JH2-2+R, CBWT, MWMR5 and MWMR10

Wild type *Enterococcus faecalis* JH2-2 cells were defined as diplococci with a characteristic lancet shape in DIC and TEM micrographs. For DIC microscopy, 500 or more cells were counted in consecutive microscopy fields and defined as either normal (diplococci lancet shaped) or aberrant (enlarged spheres, short chains, and irregular shapes) (Rigden *et al*.,

2008). Using the chi-square test comparing *E. faecalis* JH2-2+R, CBWT, MWMR5 and MWMR10 to *E. faecalis* JH2-2, P-values were determined. P-values were considered significant if they were < 0.05.

For the TEM micrographs a lancet shape was identified as the ratio of pole-to-pole length (x) versus the length between the two edges at the division site (y) to be $x/y \geq 1.50$ (Rigden *et al*., 2008). Cells with an $x/y \leq 1.50$ were considered spherical (Rigden *et al*., 2008). Again, lancet shaped diplococci were considered normal while spherical shape, short chains, and asymmetrical division were counted as aberrant (Rigden *et al*., 2008). Counting 40-60 cells, *E. faecalis* CBWT, MWMR5 and MWMR10 were compared to *E. faecalis* JH2-2 using the chi-square test to determine the P-values (Rigden *et al*., 2008). P-values of <0.05 were considered significant. *Enterococcus faecalis* JH2-2+R were previously defined as having the normal lancet shaped diplococci phenotype as compared to *E. faecalis* JH2-2 in TEM micrographs (Ramirez-Arcos *et al*., 2005).

2.6.4 Immunoflorescence Microscopy for Determining DivIVA$_{Ef}$ and MLJD Localization in *Enterococcus faecalis* JH2-2

Enterococcus faecalis JH2-2 were fixed as described by Morlot *et al*. (2003). Briefly, cells were grown in 3 ml of BHI broth (Difco) at 37 ^{o}C o/n without agitation. The following day an o/n culture was diluted 1:100 into 5 ml of fresh BHI broth and grown to an $OD_{600} \sim 0.6$ (approximately 5 hr to log phase). Cells were collected by centrifuging at 10,000 g for 15 min at 4 ^{o}C. Collected cells were washed with 30 mM phosphate buffer (pH 7.0) three times. Cells were then fixed in 1 ml of 2.5% paraformaldehyde and 0.03% glutaraldehyde for 15 min at room temperature and 2 hr on ice (Morlot *et al.*, 2003). Cells were washed three more times in 1x PBS and stored in 0.5 ml 1x PBS at 4 ^{o}C. Cells were stained as in Fadda *et al*. (2007). Fixed cells were first transferred to 0.1% Poly-L-Lysine coated cover slips. Cover slips were

washed twice with 1x PBS, air dried, and dipped in -20 ^{o}C CH_3OH for 10 min. They were then blocked for 1 hr at room temperature with BSA-PBST (2% BSA and 0.2% TritanX-100 in 1x PBS). Next, slides were incubated with 1:50 and 1:200 dilutions of primary anti-$DivIVA_{Ef}$ rabbit antibody (Ramirez-Arcos *et al*., 2005) for 4 hr. Slides were washed 4-5 times with PBST and incubated with 1:600 dilution of secondary anti-rabbit IgG Alexa Fluor 488 (Sigma) for 45 min at room temperature in the dark. Cells were stained with DAPI as in section 2.6.1.

3.0 Results

3.1 Phenotype Determination of *divIVA*$_{Ef}$ Mutant *Enterococcus faecalis* Strains MWMR5 and MWMR10

Disruption of the DivIVA$_{Ef}$ N-terminal coiled-coil and oligomerization was shown to be lethal, as introduction of the MR5$_{E37P, N43P, L46D, L50E, L57F}$ and MR10$_{L143P}$ point mutations into *E. faecalis* JH2-2 chromosomal *divIVA*$_{Ef}$ resulted in no bacterial growth. d*ivIVA*$_{Ef}$ MR5 $_{E37P, N43P, L46D, L50E, L57F}$ and MR10$_{L143P}$ were successfully introduced into *E. faecalis* JH2-2 chromosomal *divIVA*$_{Ef}$ when rescued by *in trans* expression of wild type *divIVA*$_{Ef}$ by the pMSPSRDiv-2 rescue vector.

Expression of wild type DivIVA$_{Ef}$ from the rescue vector in *E. faecalis* MWMR5 was unable to fully restore the wild type phenotype, described as being lancet shaped diplococci (Ramirez-Arcos *et al*., 2005). Differential Interference Contrast (DIC) microscopy showed *E. faecalis* MWMR5 cells with aberrant growth, characterized by spherical cells (arrows, Fig 3.1 B), short chains, and cells with irregular shapes (arrowheads, Fig 3.1 B) as compared to wild type *E. faecalis* JH2-2 (Fig 3.1A). Statistical analysis comparing 549 cells of *E. faecalis* MWMR5 to 580 cells of *E. faeclis* JH2-2 demonstrated that a significant percentage (ie: 50% with a P-value of <0.01 being significant) of *E. faecalis* MWMR5 cells had aberrant morphology (black bars, Fig 3.1 D). Transmission Electron Microscopy (TEM) of *E. faecalis* MWMR5 also showed a significant percentage, about 80% of the cells, with aberrant morphology (black bars, Fig 3.2 D), with a P-value of <0.05 being significant. The aberrant morphology was defined as asymmetrical septum placement in ~1-2% of cells (arrowheads, Fig 3.2 B), spherical shape in ~70% of cells, or aberrant septation resulting in irregular short chains in ~8% of cells (arrows, Fig 3.2 B).

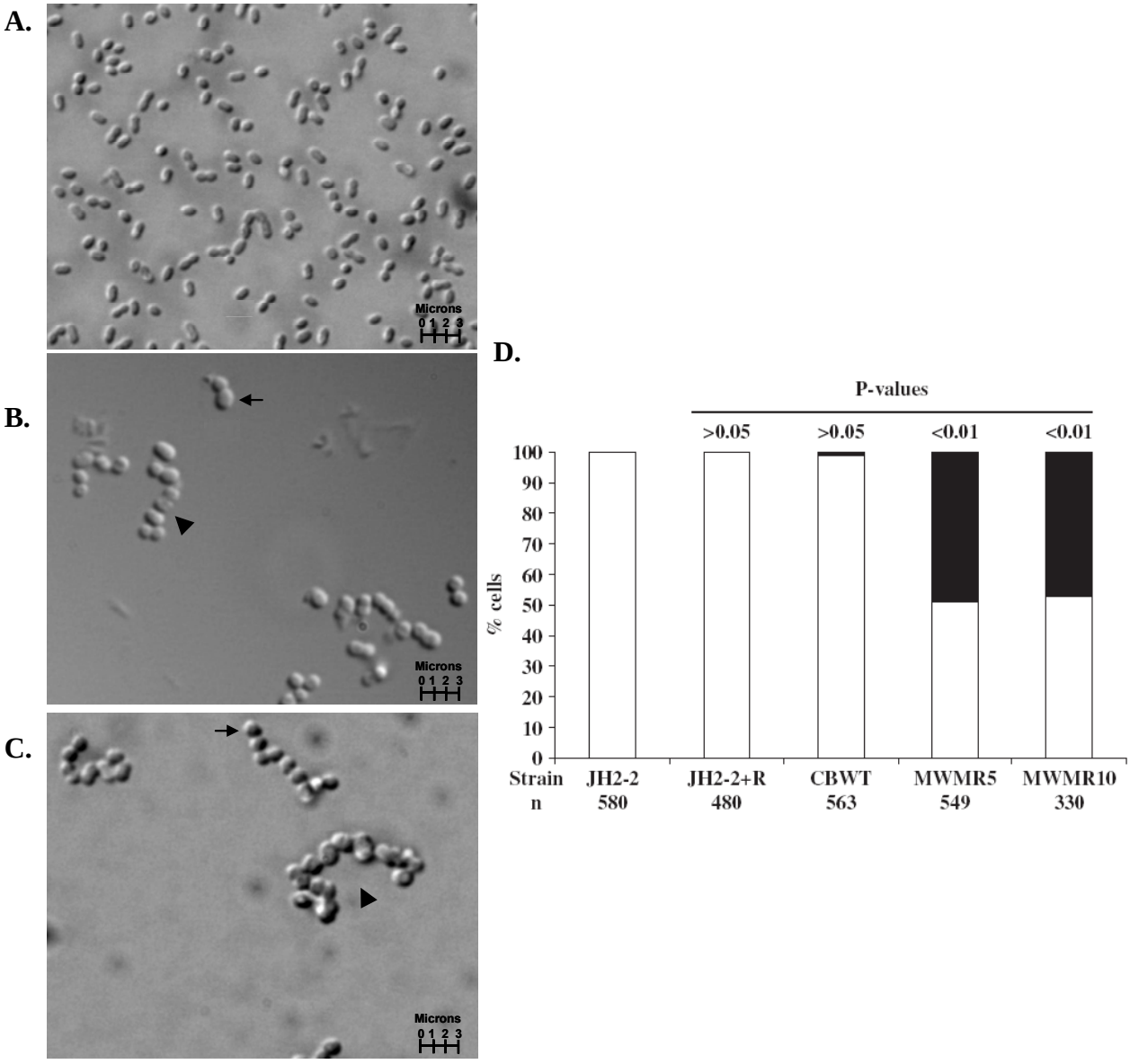

Figure 3.1: Differential Interference Contrast microscopy of *Enterococcus faecalis* JH2-2, MWMR5, and MWMR10 strains. A) *E. faecalis* JH2-2, B) *E. faecalis* MWMR5, and C) *E. faecalis* MWMR10. A, B, and C are of the same magnification. Arrows indicate enlarged round cells while the arrow heads indicate irregular cells in chains. D) Percentage of *E. faecalis* strains; white bars- % of normal lancet shaped cells; black bars- % of cells with aberrant morphology (enlarged spheres, irregular shape, and short chains). "n" is the number of cells counted for each strain.

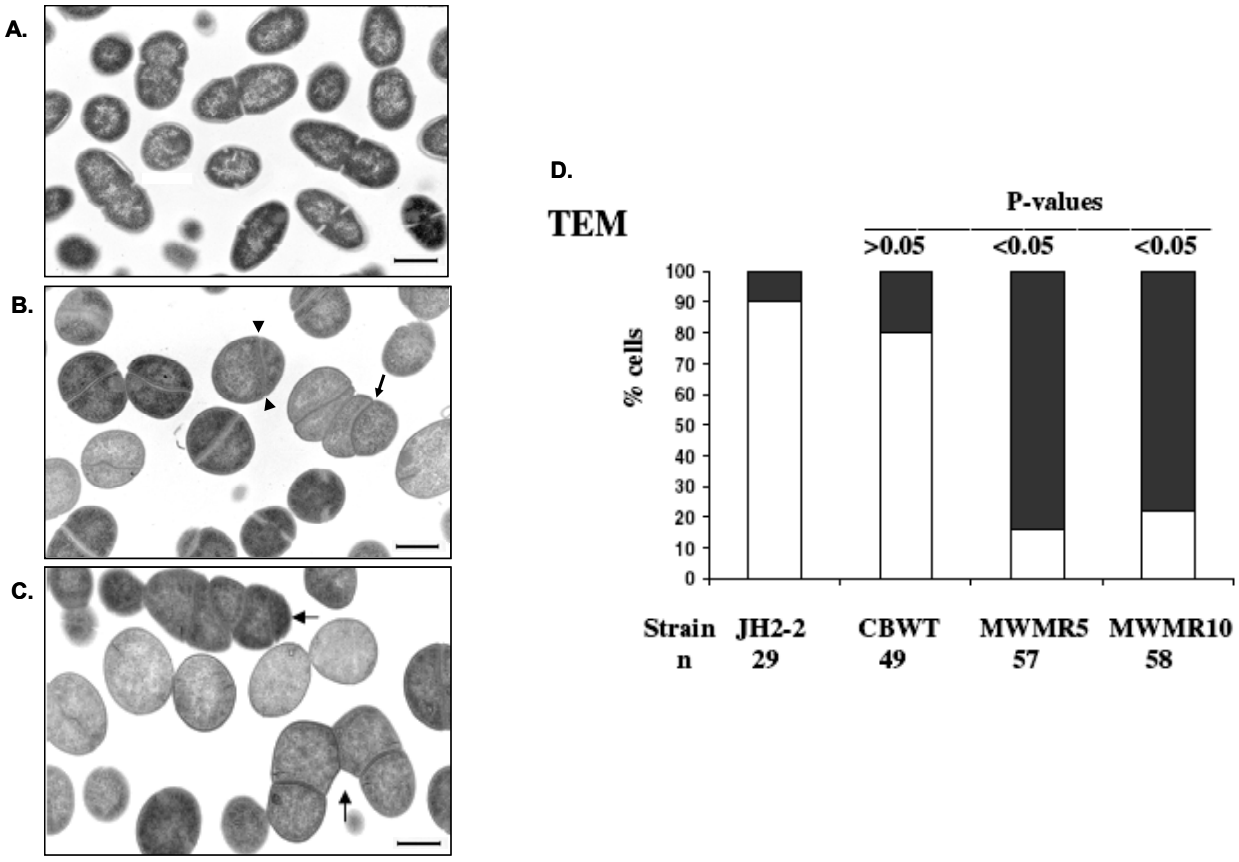

Figure 3.2: Transmission electron microscopy of *Enterococcus faecalis* strains JH2-2, MWMR5, and MWMR10. A) *E. faecalis* CBWT, B) *E. faecalis* MWMR5, and C) *E. faecalis* MWMR10. The scale bar in (bottom right corner) represents 1 micron and images (A), (B), and (C) are of the same magnification. Arrowheads in (B) indicate asymmetrical septum placement while arrows in (B) and (C) indicates short chains of irregular cells. D) Percentage of cells with wild type lancet dipplococci (white bars) and percentage of cells with aberrant cell morphology (spherical, asymmetrical division, and irregular short chains; black bars). P values were calculated using the chi-square test comparing *E. faecalis* CBWT, MWMR5 and MWMR10 to JH2-2. A P value of <0.05 is considered significant. "n" represents the number of cells counted.

Similar results were found in the case of *E. faecalis* MWMR10, where wild type $DivIVA_{Ef}$ expressed from the rescue vector was again unable to fully restore the wild type phenotype. The DIC micrographs showed *E. faecalis* MWMR10 cells (Fig 3.1 C) had aberrant growth defined by spherical cells (arrows, Fig 3.1 C), short chains and cells with irregular shapes (arrowheads, Fig 3.1 C) as compared to *E. faecalis* JH2-2 (Fig 3.1 A). The TEM micrographs of *E. faecalis* MWMR10 (Fig 3.2 C) demonstrated that $DivIVA_{Ef}$ carrying $MR10_{L143P}$ resulted in a significant percentage of cells with aberrant morphology (black bars, Fig 3.2 D) defined as asymmetrical division, spherical shape, and irregular cells in short chains (arrows, Fig 3.2 C) as compared to *E. faecalis* JH2-2 (Fig 3.2 A) with a normal lancet shape and midcell septum placement (white bars, Fig 3.2 D) (Rigden *et al*., 2008).

By comparison of *E. faecalis* MWMR5 and *E. faecalis* MWMR10, *E. faecalis* JH2-2+R (Table 2.1) and *E. faecalis* CBWT had a significant number of lancet shaped cells with symmetrical division (Fig 3.1 D; Fig 3.2 D). These results demonstrated that the rescue vector in *E. faecalis* JH2-2+R and the kanamycin cassette in *E. faecalis* CBWT did not affect bacterial cell division in these strains (Rigden *et al*., 2008, Ramirez-Arcos *et al*., 2005). The results thus implicate the essentiality of the N-terminal coiled-coil region and oligomerization of $DivIVA_{Ef}$ in *E. faecalis* cell division.

3.2 Localization of $DivIVA_{Ef}$ and MLJD1 in *Enterococcus faecalis*

3.2.1 Localization of $DivIVA_{Ef}$

Five stages of cell division were defined for *E. faecalis* cells in log phase growth (Fig 3.3). The first stage was defined as a single cell with a central chromosome. Stage two was represented as the single chromosome appearing larger and elongated as the single cell began to divide, seen by a small indentation at the midcell site (Fig 3.3). The third stage of cell division was defined as when two newly replicated and segregated chromosomes were evident. At this

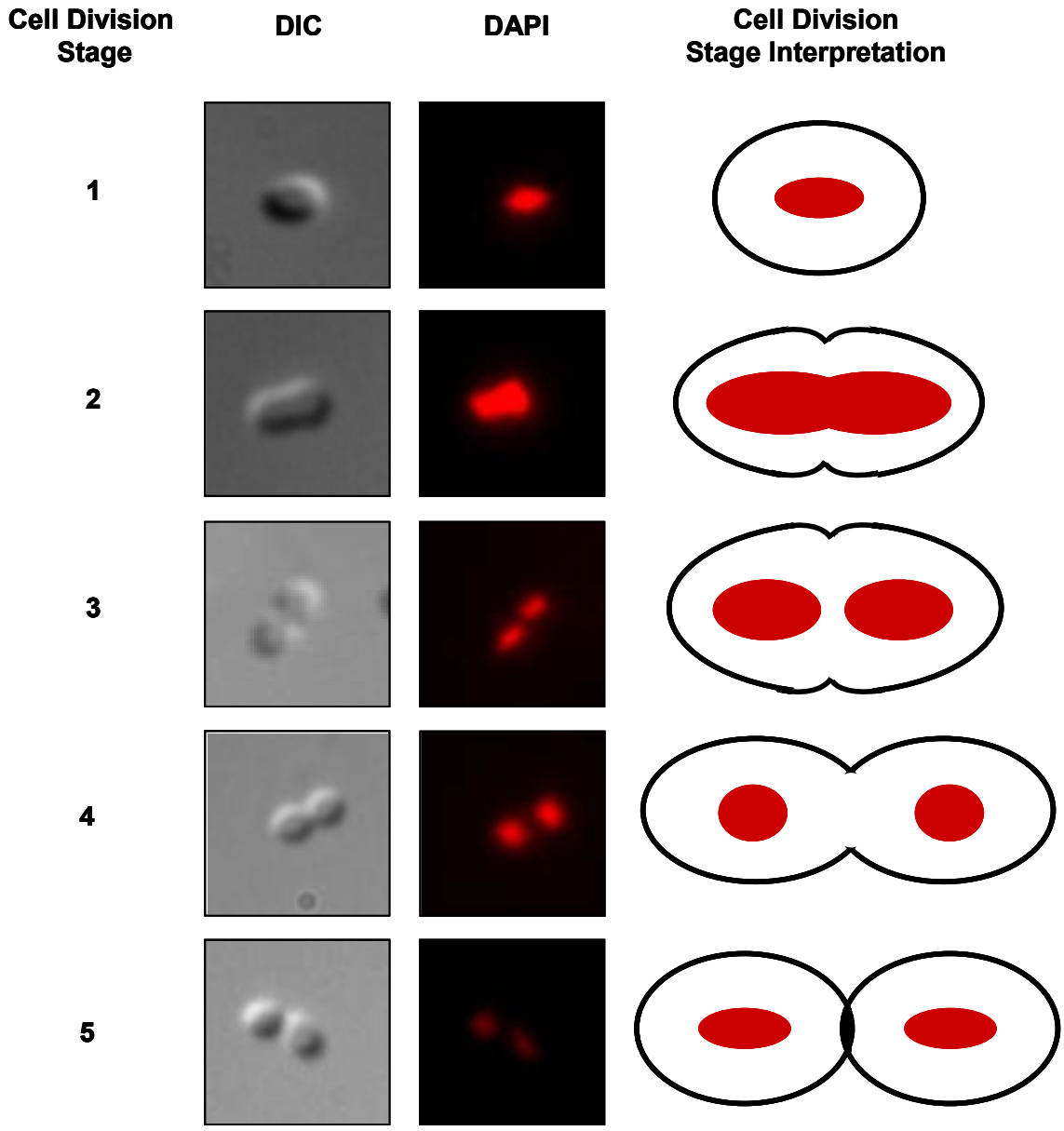

Figure 3.3: Representation of five stages of *Enterococcus faecalis* JH2-2 cell division. Stages were defined by interpretation of DIC micrographs, DAPI staining of the chromosome, and $DivVIA_{Ef}$ and MLJD1 localization patterns. Diagram on the right is not to scale.

stage the septum at the midcell site was more constricted, as seen by greater indentation at this site. As the septum further constricted and the chromosomal DNA condensed, the cells reached Stage 4. In Stage 5 the two daughter cells appeared to be separated by the septum, but remained attached together as diplococci (Fig 3.3). The chromosome of each new daughter cell was also beginning to elongate to initiate the next round of cell division.

For $DivIVA_{Ef}$ localization in *E. faecalis* JH2-2, out of 273 cells counted, the percentage of cells at each stage of cell division was calculated (Fig 3.4). To determine the localization of $DivIVA_{Ef}$ in *E. faecalis* JH2-2 cells, immunofluorescence using primary anti-$DivIVA_{Ef}$ antibody and Aluxa Fluor 488 secondary antibody was utilized. In Stage 1 of cell division, 20.5% of the cells counted, $DivIVA_{Ef}$ appeared equally distributed along the entire inner membrane (Fig 3.4 Stage 1). As the cells began to divide, 16.1% of the cells counted, $DivIVA_{Ef}$ started to concentrate to the cell poles (Fig 3.4 Stage 2). 26.4% of the cells counted were in Stage 3 where $DivIV_{Ef}$ appeared as caps at the "cell poles" (Fig 3.4 Stage 3). Stage 2 and 3 were very similar, the main difference being the state of chromosomal segregation. In Stage 4 of cell division $DivIVA_{Ef}$ was localized to both the "cell poles" and concurrently at the division site, which represented 16.8% of the cells counted (Fig 3.4 Stage 4). A diagram depicting $DivIVA_{Ef}$ localization is in Figure 3.5.

3.2.2 Localization of MLJD1

Immunofluorescence was performed to determine the localization of MLJD1 in *E. faecalis* JH2-2 cells similar to $DivIVA_{Ef}$, but with primary antibi-MLJD1 primary antibody. Cells were again counted and separated into five stages of cell division. MLJD1 appeared to localize differently from $DivIVA_{Ef}$ at stages 2 and 3 of cell division. 38.1% of cells were in Stage 1 of cell division and showed MLJD1 to be dispersed throughout the inner membrane of

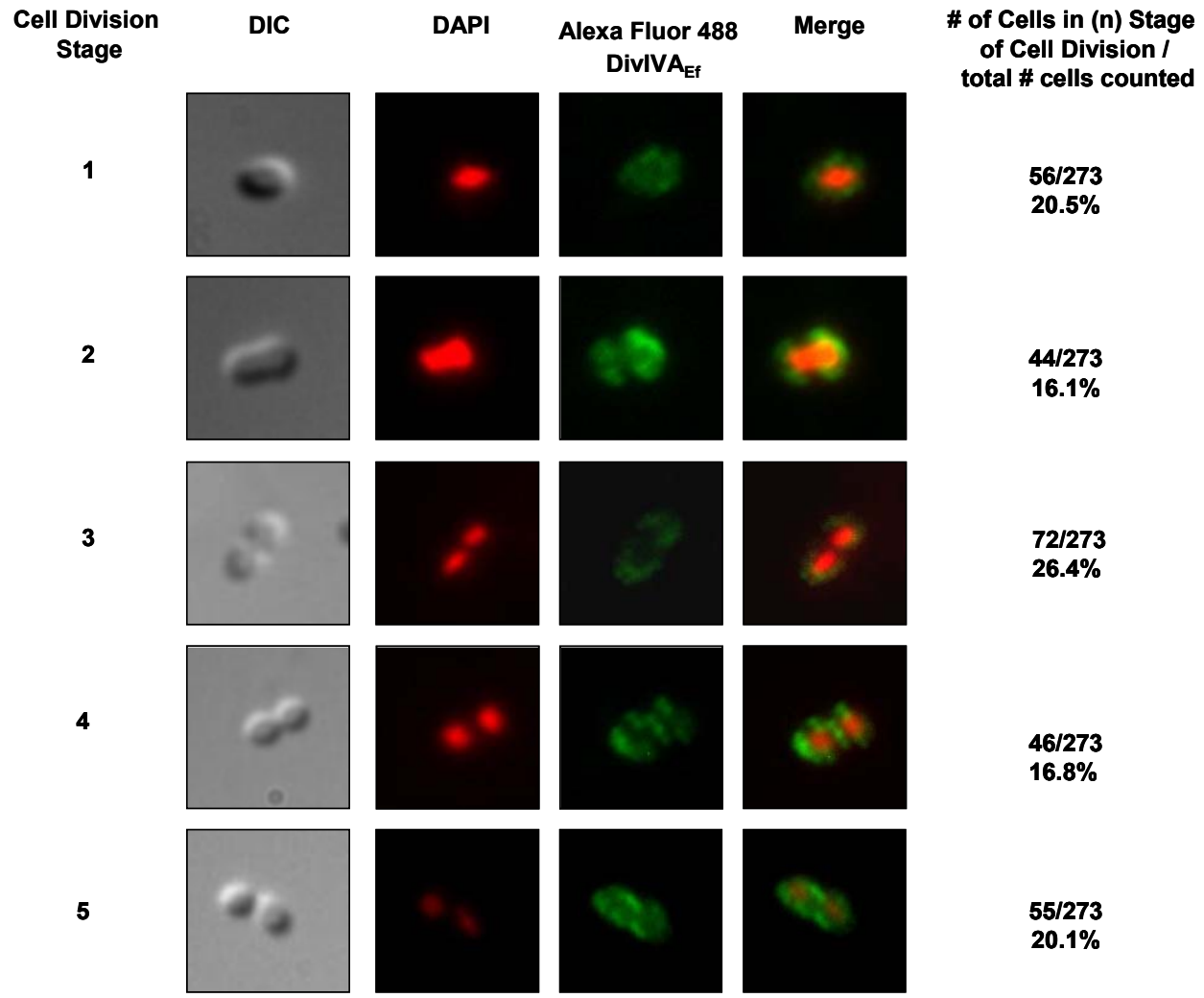

Figure 3.4: Immunoflorescence localization of DivIVA$_{Ef}$ in *Enterococcus faecalis* JH2-2. Differential Interference Contrast (DIC) microscopy; 4'-6-diamidino-2-phenylindole (DAPI) staining of chromosomal DNA; Alexa Fluor 488 secondary anti-rabbit antibody bound to primary anti-DivIVA$_{Ef}$ antibody fluoresced green to detect localization of DivIVA$_{Ef}$. Log phase cells (273) were counted and the percentage of cells in each stage of cell division determined.

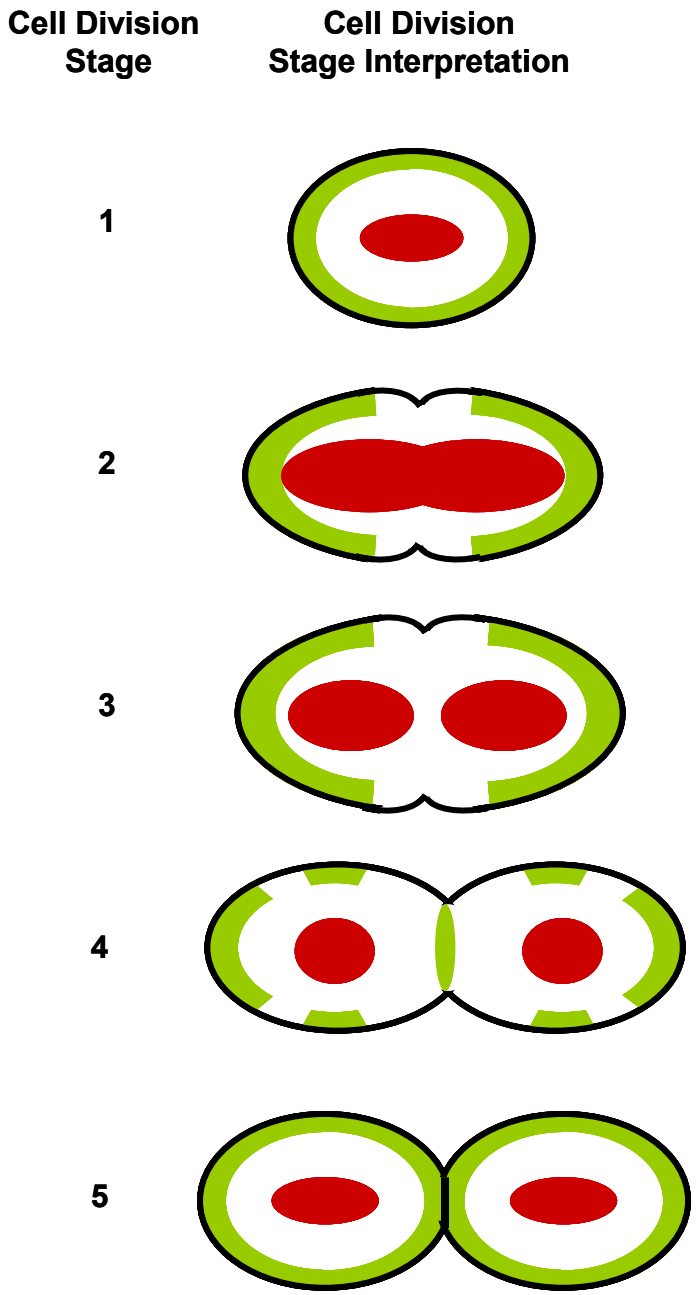

Figure 3.5: Interpretation of DivIVA$_{Ef}$ localization in *E. faecalis* JH2-2. Green represents DivIVA$_{Ef}$, while red represents the chromosome.

the cells, similar to $DivIVA_{Ef}$ (Fig 3.6 Stage 1). As the cells progressed through Stage 2 and 3 of cell division, 27.4% of the cells counted, MLJD1 appeared to localize along the length of the cell rather than to the cellular poles (Fig 3.6 Stage 2 and 3). In 22.8% of the cells counted, the chromosomes were completely segregated (appearing as two separate entaties) and the septum was more defined and constricted. In this stage, Stage 4, MLJD1 localized to the cell poles or along the cell length (difficult to distinguish) and concurrently at the division site (Fig 3.6 Stage 4), as was the case with $DivIVA_{Ef}$ (Fig 3.4 Stage 4). As cell division completed in Stage 5, 11.7% of the cells, MLJD1 became dispersed along the inner membrane once more (Fig 3.6 Stage 5). These results suggest MLJD1 may co-localizes with $DivIVA_{Ef}$ in *E. faecalis* during later stages of cell division.

3.2.3 Potential Co-localization of $DivIVA_{Ef}$ and MLJD1 in *Enterococcus faecalis* JH2-2

The localization patterns of $DivIVA_{Ef}$ and MLJD1 in *E. faecalis* JH2-2 were somewhat different. For each localization study, cells were grown to log phase (6-7 hr or until the culture reached OD_{560} 0.6 (Shepard & Gilmore, 1995)). A percentage of cells in Stage 1 of cell division were more than double the percentage of cells in Stage 5 of cell division for MLJD1 localization studies (Table 3.1). This indicates the culture was in log phase growth (Haeusser & Levin, 2008). For the cultures used for $DivIVA_{Ef}$ localization there was an equal amount of cells in Stage 1 and Stage 5, indicating they may have not been in mid-log phase at the time the cells were fixed. For future studies using Immunofluorescense in *E. faecalis* it would be useful to determine the actual replication time in a particular media with consistent growth conditions (temperature). It would also be useful to utilize synchronized cell cultures for use in future co-localization studies for MLJD1 and $DivIVA_{Ef}$ in *E. faecalis* (see Discussion).

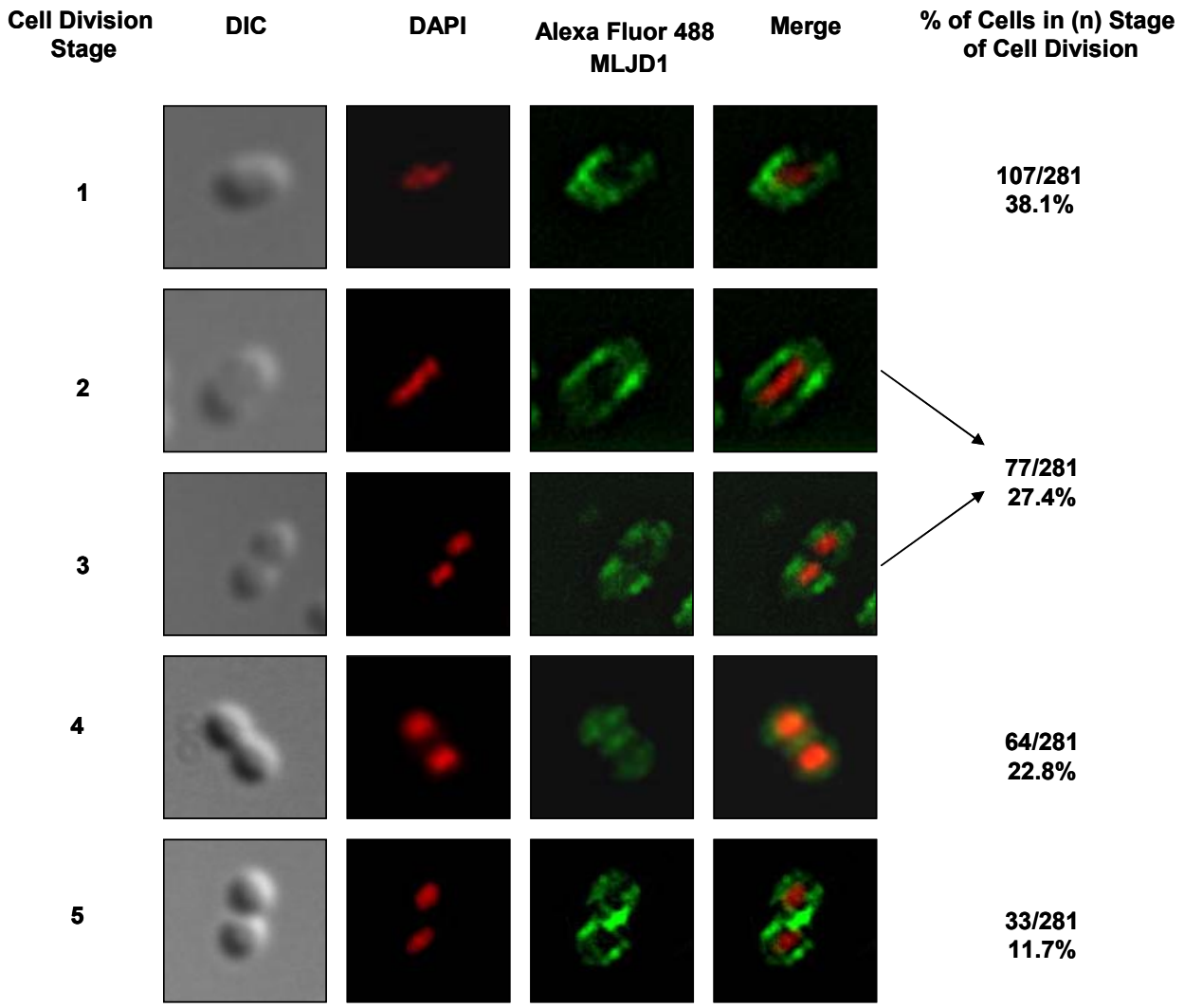

Figure 3.6: Immunofluorescence of MLJD1 localization in *Enterococcus faecalis* JH2-2. Differential Interference Contrast (DIC) microscopy; 4'-6-diamidino-2-phenylindole (DAPI) staining of chromosomal DNA; Alexa Fluor 488 secondary anti-rabbit antibody bound to primary anti-MLJD1 antibody fluoresced green to detect localization of MLJD1. 281 log phase cells were counted and the percentage of cells in each stage of cell division determined.

Table 4.1: Percentage of cells in each of five cell division stages for $DivIVA_{Ef}$ and MLJD1 localization studies in *Enterococcus faecalis*

Stage of Cell Division	% of Cells Counted in $DivIVA_{Ef}$ Localization Study	% of Cells Counted in MLJD1 Localization Study
1	20.5%	38.1%
2 and 3	42.5%	27.4%
4	16.8%	22.8%
5	20.1%	11.7%

3.3 $DivIVA_{Ef}$ Self-Interaction and Interaction with MLJD1, a Novel Division Protein, using a Bacterial Two-Hybrid System

3.3.1 $DivIVA_{Ef}$ Interaction with Full Length MLJD1

The interaction between full length MLJD1 and $DivIVA_{Ef}$ was very weak in the Yeast Two-Hybrid (Y2H) studies used to screen the *E. faecalis* JH2-2 genomic library (Liao *et al*., manuscript in preparation). Instead, a fragment of MLJD1, containing the two CBS domains, demonstrated interaction capabilities with $DivIVA_{Ef}$ (Liao *et al*., manuscript in preparation). The Bacterial Two-Hybrid (B2H) system has been determined to detect interaction between bacterial proteins previously undetected in the Y2H system (Di Lallo *et al*., 2001). For this reason, $DivIVA_{Ef}$ self interaction and $DivIVA_{Ef}$ interaction with full length MLJD1 were examined using the B2H developed by Di Lallo (Di Lallo *et al*., 2001). Figure 3.7 shows the average of 3-4 B2H assays, as indicated, each of which was done in triplicate. Interaction was positive if there was 50% or greater reduction of β-galactosidase (β-gal) activity as compared to the *E. coli* R721 control (without plasmid). *E. coli* R721 without plasmid represented the maximum β-gal activity (Fig 3.7). Reading Fig 3.7 from left to right, the data represented in the first bar indicates a positive $DivIVA_{Ef}$ self interaction which reduced β-gal activity by 52%. The data represented by the second and third bars in Fig 3.7 were examining the interaction capabilities between $DivIVA_{Ef}$ and MLJD1, representing both plasmid combinations. The data represented in the second bar suggests $DivIVA_{Ef}$ does not interact with full length MLJD1, with a 35% reduction in β-gal activity. Contradicting the data in the second bar, the third bar data shows 56% reduced β-gal activity, indicating positive interaction between $DivIVA_{Ef}$ and full length MLJD1 (Fig 3.7). While the data depicted in the fourth and fifth bars ensure there is no background reduction of β-gal activity induced by either plasmid carrying $divIVA_{Ef}$, the data in

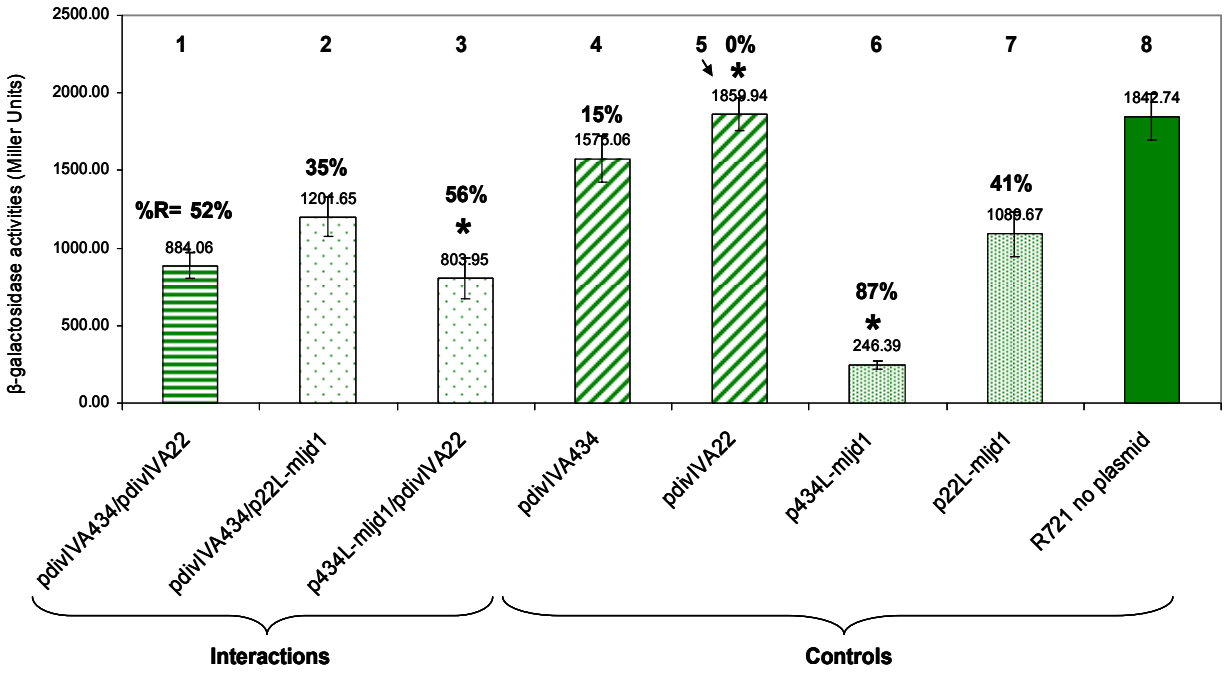

Figure 3.7: **DivIVA$_{Ef}$ Self-interaction and Interaction with Full Length MLJD1 in a Bacterial Two-hybrid system**. The *y-axis* is β-galactosidase activity measured in Miller Units. Along the *x-axis* bars represent β-gal activity within *E. coli* transformed with the indicated plasmids for examining the following protein-protein interactions: vertical lines- DivIVA$_{Ef}$ self interaction; spaced dots (bar 2 and 3)- DivIVA$_{Ef}$ interaction with full length MLJD1; thatched lines (bar 4 and 5)- single plasmid controls expressing DivIVA$_{Ef}$ fusion proteins; tight spaced dots (bar 6 and 7)- single plasmid controls expressing MLJD1 fusion proteins; and solid green (bar 8) is *E. coli* R721 with no transformed plasmids indicating maximum β-gal activity. %R = percent reduction of β-galactosidase activity**;** >50% indicates positive interaction. The B2H assays were performed as in section 2.5. The results represent four independent B2H assays; a (*****) indicates average of three B2H assays and each assay was performed in triplicates.

the data represented by the sixth and seventh bars do demonstrate background β-gal reduction for plasmids carrying *mljd1*. The plasmids p434L-mljd1and p22L-mljd1 induced 87% and 41% reduced β-gal activity, indicating that protein products from each plasmid alone could have been capable of reducing β-gal activity. The reduction observed in the data in bar 3 of Fig 3.7 could be a false positive due to background repression. For this reason, these results could not determine the interaction capabilities between $DivIVA_{Ef}$ and full length MLJD1.

3.3.2 $DivIVA_{Ef}$ Interaction with the CBS1 and CBS2 domains of MLJD1

MLJD1 is composed of a potential DNA binding helix-turn-helix (HTH) domain and two cystathionine-beta-synthase (CBS) domains (Fig 1.4). The potential for MLJD1 to bind DNA could have affected the B2H result of $DivIVA_{Ef}$ interaction with full length MLJD1 (Fig 3.7). This could have also affected the original Y2H, in which MLJD1 was discovered, where the fragment of MLJD1 containing the CBS1 and CBS2 domains and not the DNA binding domain showed interaction with $DivIVA_{Ef}$ (Liao *et al*., unpublished data). For this reason, the gene fragment containing the sequence for the two CBS domains (sequence encoding amino acids 79-199 of MLJD1) were cloned into the B2H plasmids and their interaction capabilities with $DivIVA_{Ef}$ studied. Figure 3.8 is the average of two B2H assays. From left to right, the data in bar one in Fig 3.8 again $DivIVA_{Ef}$ showed positive interaction, with reduced β-gal activity of 64%. Unlike with full length MLJD1 (ie: Fig 3.7), interaction of the MLJD1 fragment which included the CBS1CBS2 domains with $DivIVA_{Ef}$ indicated positive interaction for both plasmid combinations (Fig 3.8). The data in the second and third bars demonstrated a reduction of β-gal activity by 86% and 62%, respectively, both indicating strong interaction between $DivIVA_{Ef}$ and the CBS1CBS2 domain containing fragment of MLJD1 (Fig 3.8). Further more, data in bars 4-7 indicate there was no significant background repression induced

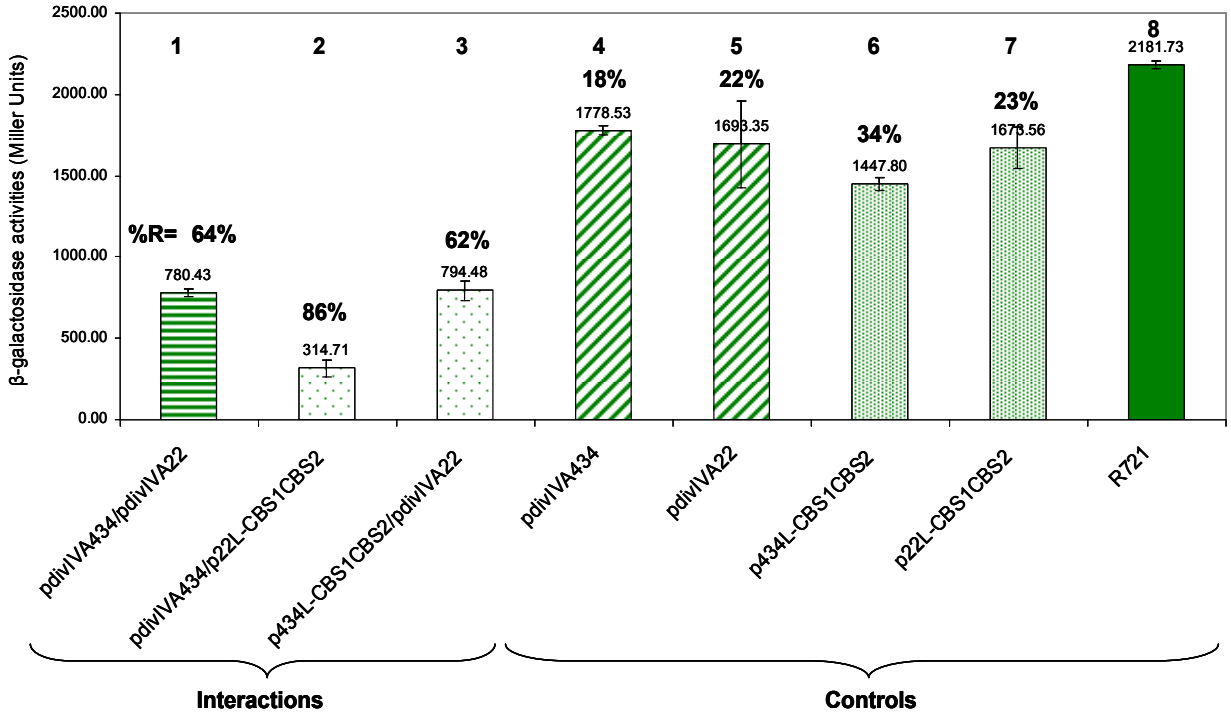

Figure 3.8: **DivIVA$_{Ef}$ interaction with MLJD1 CBS Domains using a Bacterial Two-hybrid system**. The *y-axis* is β-galactosidase activity measured in Miller Units. Along the *x-axis* bars represent β-gal activity within *E. coli* transformed with the indicated plasmids for examining the following protein-protein interactions: vertical lines- DivIVA$_{Ef}$ self interaction; spaced dots (bar 2 and 3)- DivIVA$_{Ef}$ interaction with the CBS containing fragment of MLJD1; thatched lines (bar 4 and 5)- single plasmid controls expressing DivIVA$_{Ef}$ fusion proteins; tight spaced dots (bar 6 and 7)- single plasmid controls expressing the CBS fragment of MLJD1 fusion proteins; and solid green (bar 8) is *E. coli* R721 with no transformed plasmids indicating maximum β-gal activity. %R = percent reduction of β-galactosidase activity as compared to *E. coli* R721**;** >50% indicates positive interaction. B2H assays were the results two independent β-galactosidase assays each done in triplicate. DivIVA$_{Ef}$ self-interaction was used as a positive control.

by any of the single plasmid controls for both $DivIVA_{Ef}$ self interaction and $DivIVA_{Ef}$ interaction with the fragment of MLJD1. The positive interaction between $DivIVA_{Ef}$ and the CBS domain containing fragment of MLJD1 can thus be recognized as a true positive interaction.

3.3.3 Interaction between the MR16 Mutant $DivIVA_{Ef}$ and the fragment of MLJD1 containing the two CBS domains

Previous work indicated that MLJD1 interacts between amino acids (aa) 60-130 of $DivIVA_{Ef}$, (Rigden, 2005). The first central coiled-coil is from aa 100-150 and is involved in oligomerization. So, MLJD1 most likely interacts with $DivIVA_{Ef}$ between aa 60-100. Due to the close proximity of this region to the central coiled-coil, $DivIVA_{Ef}$ oligomerization may be an important aspect of $DivIVA_{Ef}$ interaction with MLJD1. For this reason the $DivIVA_{Ef}$ mutant $MR16_{L104P,\ I115P,\ I125P,\ L143P}$, which disrupts oligomerization (Rigden *et al*., 2008), interaction capabilities with the fragment, containing the two CBS domains of MLJD1 was examined using the same B2H assay used to confirm $DivIVA_{Ef}$~MLJD1 (fragment) interaction (Fig 3.8).

One B2H assay was performed which demonstrated a potential loss of interaction between $DivIVA_{Ef}$ $MR16_{L104P,\ I115P,\ I125P,\ L143P}$ and the CBS containing MLJD1 fragment (Fig 3.9). In Fig 3.9, data represented in bar one indicated $DivIVA_{Ef}$ self-interaction with 66% reduced β-gal activity. The data in the second and third bars again demonstrated positive interaction between $DivIVA_{Ef}$ and the CBS fragment of MLJD1, with 91% and 70% reduced β-gal activity, respectively. Data in bar four, where wild type $DivIVA_{Ef}$ has been replaced with $DivIVA_{Ef}$ $MR16_{L104P,\ I115P,\ I125P,\ L143P}$, there appeared to be a loss of interaction with the MLJD1 fragment (Fig 3.9). However, data in the fifth bar, containing the opposite plasmid constructs, appeared to indicate $DivIVA_{Ef}$ $MR16_{L104P,\ I115P,\ I125P,\ L143P}$ and the CBS containing fragment conserved their interaction capabilities (with 61% reduced β-gal activity; Fig 3.9).

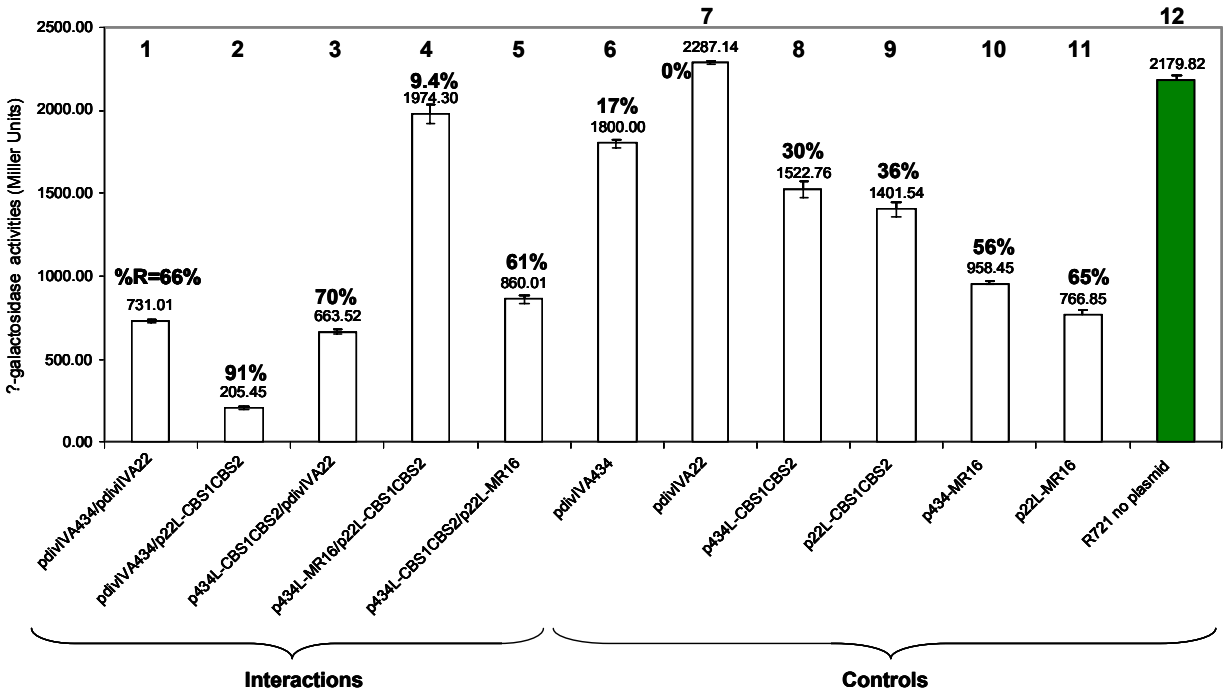

Figure 3.9: Interaction of mutant DivIVA$_{Ef}$ MR16$_{L104P, I115P, I125P, L143P}$ with MLJD1 CBS domains using Bacterial Two-hybrid system. The *y-axis* is β-galactosidase activity measured in Miller Units. Along the *x-axis* bars represent β-gal activity within *E. coli* transformed with the indicated plasmids for examining the following protein-protein interactions: bar 1- DivIVA$_{Ef}$ self interaction; bar 2 and 3- DivIVA$_{Ef}$ interaction with the CBS containing fragment of MLJD1; bar 4 and 5- DivIVA$_{Ef}$ MR16 mutant interaction with the CBS containing fragment of MLJD2; bars 6 and 7- single plasmid controls expressing wild type DivIVA$_{Ef}$ fusion proteins; bars 8 and 9- single plasmid controls expressing the CBS fragment of MLJD1 fusion proteins; bars 10 and 11- single plasmid controls expressing DivIVA$_{Ef}$ MR16 mutant fusion proteins; and solid green (bar 12) is *E. coli* R721 with no transformed plasmids indicating maximum β-gal activity. %R = percent reduction of β-galactosidase activity as compared to *E. coli* R721**;** >50% indicates positive interaction. The results represent a single B2H β-galactosidase assays done in triplicates. DivIVA$_{Ef}$ self-interaction and interaction with the CBS domains of MLJD1 was used as a positive control.

The single plasmid controls for $DivIVA_{Ef}$ self-interaction and interaction with the CBS containing fragment, data in bars 6-9 (Fig 3.9), demonstrated minimal background repression. Both single plasmid controls for $DivIVA_{Ef}$ $MR16_{L104P,\ I115P,\ I125P,\ L143P}$ had 56% and 65% background repression, data represented by bars 10 and 11 respectively. The repression observed by the data represented in bar 5 could thus be due to the effects of the background repression induced by the p22L-MR16 protein product. For this reason and because only one assay of results, no conclusions could be made regarding $DivIVA_{Ef}$ $MR16_{L104P,\ I115P,\ I125P,\ L143P}$ interaction with the fragment of MLJD1 containing the two CBS domains.

4.0 Discussion

4.1 The Essentiality of DivIVA$_{Ef}$ Oligomerization and the N-terminal Coiled-Coil for Proper Biological Function in *Enterococcus faecalis* Cell Division

DivIVA was first discovered and extensively studied as a cell division protein in *Bacillus subtilis* (Reeve *et al*., 1973). DivIVA is now recognized as a Gram-positive cell division protein with homologues in Gram-positive organisms such as *Streptomyces coelicolor*, *Streptococcus pneumoniae*, *Staphylococcus aureus*, *Brevibacterium lactofermentum* and *Enterococcus faecalis* (Ramirez-Arcos *et al*., 2005, Fadda *et al*., 2007, Pinho & Errington, 2004, Ramos *et al*., 2003, Flardh, 2003a). Predictions of the DivIVA structure in these and other Gram-positive organisms indicate a coiled-coil structure (Rigden *et al*., 2008, Edwards *et al*., 2000, Rigden, 2005, Fadda *et al*., 2007). Coiled-coil structures are responsible for oligomerization in a multitude of proteins and can be involved in interaction with heterologous proteins as well (Edwards *et al*., 2000, Fadda *et al*., 2007, Lupas, 1996b, Lupas, 1996a, Lupas *et al*., 1991). DivIVA in *E. faecalis* (DivIVA$_{Ef}$) was determined to have four coiled-coils, one at the N-terminal, two in the central region, and one at the C-terminal (Rigden *et al*., 2008, Rigden, 2005). The two central coiled-coils are involved in oligomerization, giving DivIVA$_{Ef}$ the capability of forming a complex comprised of 10-12 monomers (Rigden *et al*., 2008, Rigden, 2005). DivIVA in *B. subtilis* (DivIVA$_{Bs}$) also forms a complex of up to 10-12 monomers, although DivIVA$_{Bs}$ contains two coiled-coils, one at the N-terminal and one in the central region (Muchova *et al*., 2002b, Muchova *et al*., 2002a). A point mutation in DivIVA$_{Bs}$ at L120P resulted in reduced oligomerization capability by 50% (Muchova *et al*., 2002b). The corresponding mutation in DivIVA$_{Ef}$ L143P (MR10) formed a complex of 4 monomers instead of the typical 10-12 monomer complex, but was able to interact with wild type DivIVA$_{Ef}$ as determined by Y2H assays (Rigden *et al*., 2008, Rigden, 2005).

In the present study, *E. faecalis* MWMR10 contained an L143P point mutation in chromosomal *divIVA*$_{Ef}$, but required rescuing via *in trans* expression of wild type (wt) *divIVA*$_{Ef}$. Although *E. faecalis* MWMR10 was viable when rescued, wt DivIVA$_{Ef}$ was unable to restore the mutant to the wt phenotype. The inability of wt DivIVA$_{Ef}$ to fully restore the wt phenotype of *E. faecalis* MWMR10 could have been due to differences in expression levels of *divIVA*$_{Ef}$ compared to wt expression from the *E. faecalis* JH2-2 chromosome, which was also seen when *divIVA*$_{Ef}$ was inactivated by insertion of the kan cassette (Ramirez-Arcos *et al*., 2005). On the chromosome *divIVA*$_{Ef}$ expression might be controlled by two promoters, its own and the *ftsA*$_{Ef}$ promoter, while the rescue plasmid only carries the *divIVA*$_{Ef}$ promoter (Ramirez-Arcos *et al*., 2005). DivIVA$_{Ef}$ MR10$_{L143P}$ and wt DivIVA$_{Ef}$ would not occur in the same cell in nature because there is only one copy of *divIVA*$_{Ef}$ on the chromosome. In *E. faecalis* MWMR10, where both DivIVA$_{Ef}$ MR10$_{L143P}$ and wt DivIVA$_{Ef}$ are present, their interaction, as shown in Y2H assays (Rigden, 2005), could have been preventing wt DivIVA$_{Ef}$ from carrying out its functions in normal cell division. Thus, it is likely that with most of the small amount of wt DivIVA$_{Ef}$ bound and inactivated by DivIVA$_{Ef}$ MR10$_{L143P}$, the mutant phenotype could be observed. Differential Interference Contrast (DIC) microscopy and Transmission Electron Microscopy (TEM) showed that a significant percentage of *E. faecalis* MWMR10 cells had lost their typical lancet shape, formed short chains with irregular shaped cells, and presented asymmetrical division (Fig 3.1 and Fig 3.2) (Rigden *et al*., 2008).

Further disruption of DivIVA$_{Ef}$ oligomerization with multiple point mutations L104P, I115P, I125P (MR15) in the first central coiled-coil or L104P, I115P, I125P, L143P (MR16) in the first and second central coiled-coils, resulted in complete abolition of oligomerization (Rigden *et al*., 2008, Rigden, 2005). The MR15$_{L104P, I115P, I125P}$ DivIVA$_{Ef}$ mutant retained its ability to oligomerize with wt DivIVA$_{Ef}$, but was incapable of oligomerizing with itself

(Rigden, 2005, Rigden *et al*., 2008). The $MR16_{L104P, I115P, I125P, L143P}$ $DivIVA_{Ef}$ mutant was a combination of $MR10_{L143P}$ and $MR15_{L104P, I115P, I125P}$ point mutations which disrupted both central coiled-coils and resulted in loss of oligomerization with both wt and itself (Rigden *et al*., 2008, Rigden, 2005). Attempts to introduce the MR15 and MR16 point mutations into the *E. faecalis* JH2-2 chromosome proved to be lethal even with *in trans* expression of wild type $divIVA_{Ef}$. The dominant lethal phenotype of $MR15_{L104P, I115P, I125P}$ and $MR16_{L104P, I115P, I125P, L143P}$ mutant $DivIVA_{Ef}$ emphasizes the essentiality of the central coiled-coils and oligomerization of $DivIVA_{Ef}$ in *E. faecalis* bacterial cell division (Rigden *et al*., 2008).

Disruption of the N-terminal coiled-coil of $DivIVA_{Ef}$ in *E. faecalis* MWMR5, with point mutations E37P, N43P, L46D, L50E, and L57F (MR5), did not disrupt oligomerization, but was also unable to be introduced into the *E. faecalis* chromosomal $divIVA_{Ef}$ without rescuing by *in trans* supplementation with wt $DivIVA_{Ef}$ (Rigden *et al*., 2008). Again wt $DivIVA_{Ef}$ was not able to fully restore the wt phenotype and DIC and TEM microscopy showed that a significant percentage of *E. faecalis* MWMR5 mutant cells contained spherical and irregular shapes, short chains, and asymmetrical division (Fig 3.1; Fig 3.2) (Rigden *et al*., 2008). Previously, a mutation at A78T in the N-terminal of *B. subtilis* $DivIVA_{Bs}$, but outside its N-terminal coiled-coil, resulted in an anucleated minicell phenotype similar to the $DivIVA_{Bs}$ knockout (Cha & Stewart, 1997, Perry & Edwards, 2004, Rigden *et al*., 2008). The same mutation (A78T) at the same A78 N-terminal location in *S. pneumoniae* $DivIVA_{Sp}$ resulted in dispersed localization of $DivIVA_{Sp}$, a "chainy" phenotype, and loss of interaction with later divisome proteins FtsK, FtsL, FtsQ, FtsB, and FtsW (Fadda *et al*., 2007). The N-terminal of *B. subtilis* $DivIVA_{Bs}$ also possesses two polar targeting determinants R18 and G19, which are not in the N-terminal coiled-coil (Perry & Edwards, 2004). R18 and G19 are required by $DivIVA_{Bs}$ to sequester the MinCD FtsZ inhibitor complex to the cell poles; however, *E. faecalis* does not possess Min

proteins (Perry & Edwards, 2004, Rigden *et al*., 2008, Ramirez-Arcos *et al*., 2005). This present study focused on the N-terminal coiled-coil and demonstrates the N-terminal coiled-coil is essential for $DivIVA_{Ef}$ biological function in *E. faecalis* cell division.

Although research has previously demonstrated that DivIVA oligomerizes to form complexes of 10-12 monomers (Rigden, 2005, Rigden *et al*., 2008, Muchova *et al*., 2002b, Muchova *et al*., 2002a), this study is the first instance where DivIVA oligomerization has been proven to be essential for the proper biological function of DivIVA in bacterial cell division. The next step for developing a cell division model involving DivIVA would be to determine the exact functions which oligomerization and the N-terminal coiled-coil play. To elucidate if the N-terminal coiled-coil plays any role in localization of $DivIVA_{Ef}$, I would put a GFP tag on the $MR5_{E37P,\ N43P,\ L46D,\ L50E,\ L57F}$ $DivIVA_{Ef}$ mutant within *E. faecalis* MWMR5. This would allow the visualization of the localization of mutant $DivIVA_{Ef}$. Using GFP can be difficult due to the small size of *E. faecalis* cells, so immunofluorescence could be utilized instead. One could also study the interaction capabilities between divisome proteins FtsZ, FtsQ, or FtsW and $DivIVA_{Ef}$ $MR5_{E37P,\ N43P,\ L46D,\ L50E,\ L57F}$ to check if the N-terminal coiled-coil is involved in these interactions.

To further study the function of $DivIVA_{Ef}$ oligomerization I examined the interaction capabilities of $DivIVA_{Ef}$ MR16 with the novel putative division protein MLJD1 (discussed below).

4.2 $DivIVA_{Ef}$ Self Interaction and Interaction with MLJD1

The interaction between $DivIVA_{Ef}$ and a novel cell division protein MLJD1 was discovered in our laboratory through screening a DNA library in a yeast two-hybrid (Y2H), using $DivIVA_{Ef}$ as bait (Liao *et al.*, manuscript in preparation). Interaction between $DivIVA_{Ef}$ and full length MLJD1 was weak in the Y2H potentially due to the heterologous eukaryotic

background. Interaction between $DivIVA_{Ef}$ and an MLJD1 fragment including the CBS domains was also not very strong in the Y2H, but was stronger than with full length MLJD1 (Liao *et al*., manuscript in progress). Interaction between $DivIVA_{Ef}$ and MLJD1 was evident with *in vitro* and *in vivo* methods such as GST-pulldown and immunoprecipatation respectively (Liao *et al.*, manuscript in preparation). To further confirm that $DivIVA_{Ef}$ was interacting with MLJD1 I used a more sensitive *in vivo* Bacteria Two-hybrid (B2H) system (discussed in Appendix A) (Di Lallo *et al*., 2001). Using bacteria as the background in B2H could eliminate any problems seen in the heterologous Y2H system and help detect interactions otherwise missed in the Y2H. Again interaction between $DivIVA_{Ef}$ and full length MLJD1 was either not detected or very weak. Because the reciprocal results were contradicting, the weak interaction detected in one reciprocal could have been a false positive induced by bridging proteins (Di Lallo *et al*., 2003, Di Lallo *et al*., 2001). Unlike $divIVA_{Ef}$ expressed from either plasmid alone (single plasmid controls) the *mljd1* single plasmid controls demonstrated significant background repression of β-gal. Therefore, any repression of β-gal demonstrated between $DivIVA_{Ef}$ and full length MLJD1 could be due to repression induced by each plasmid's products alone, possibly through bridging proteins as mentioned, rather than a positive indication of interaction. The problem of high background repression of β-gal could also be due to the HTH region of MLJD1 potentially binding to DNA, which may cause repression of β-gal in the controls.

To solve the problem encountered with full length MLJD1, the sequence encoding a fragment of MLJD1 containing the CBS domains (a.a. 79-199) were cloned into the B2H plasmids. Without the HTH, the CBS domains should be free to interact directly with $DivIVA_{Ef}$. This hypothesis proved to be correct as there was a strong interaction between $DivIVA_{Ef}$ and the CBS domain fragment of MLJD1.

After I determined that $DivIVA_{Ef}$ interacts with the fragment of MLJD1 containing the CBS domains, the next step was to determine which regions of $DivIVA_{Ef}$ are involved. In previous Y2H experiments with truncations of $DivIVA_{Ef}$, it was predicted MLJD1 interacted with a region of $DivIVA_{Ef}$ close to the first central coiled-coil (Liao *et al*., manuscript in progress). This would be an interesting finding since the central coiled-coils are also involved in $DivIVA_{Ef}$ oligomerization. Again the Y2H results were only suggestive. To test this hypothesis of where $DivIVA_{Ef}$~MLJD1 interaction occurs I tested the interaction capabilities between $DivIVA_{Ef}$ carrying the $MR16_{L104P,\ I115P,\ I125P,\ L143P}$ mutations with the CBS domain containing fragment of MLJD1. Since the MR16 $_{L104P, I115P, I125P, L143P}$ mutations induce a loss of self interaction in $DivIVA_{Ef}$, I hypothesized it would also lose interaction with the CBS domain containing fragment. Preliminary results of one B2H assay studying the interaction of $DivIVA_{Ef}$ MR16 $_{L104P,\ I115P,\ I125P,\ L143P}$ with the CBS fragment were inconclusive. Wild type $DivIVA_{Ef}$ interaction with the CBS fragment was again detected, but when wt $DivIVA_{Ef}$ was replace by $DivIVA_{Ef}$ carrying MR16 $_{L104P,\ I115P,\ I125P,\ L143P}$ the results from the two plasmid combinations were conflicting. These contrasting results could indicate a false negative or a false positive, so interaction between the $DivIVA_{Ef}$ MR16 $_{L104P,\ I115P,\ I125P,\ L143P}$ mutant and the CBS containing fragment of MLJD1 could potentially be stronger or weaker compared to interaction with wt $DivIVA_{Ef}$. The difference between the two combinations could be due to differing levels of protein expression caused by the high and low copy plasmids (discussed in Appendix A). GST-pulldown and/or immunoprecipitation with $DivIVA_{Ef}$ MR16 $_{L104P,\ I115P,\ I125P,\ L143P}$ and the MLJD1 fragment containing the CBS domains could also be used to further determine if there is a stronger interaction or a loss of interaction between the two.

These results and the results of $DivIVA_{Ef}$ and full length MLJD1 indicate the B2H, although sensitive enough to prove interaction exists, may not be ideal for determining

interaction patterns of these two proteins, possibly due to a dynamic and complex mode of interaction. Recently, a protein in *B. subtlils*, which contains similar domains to MLJD1 from *E. faecalis*, YqzB (or CcpN) was shown to be involved in carbon catabolite repression (CCR) (Servant *et al*., 2005). During growth on a preferred carbon source, such as glucose, CcpN bindes to the promoters of *pckA* and *gapB*, which represses their transcription. CcpN thereby regulates gluconeogenisis (Servant *et al*., 2005, Tannler *et al*., 2008). $DivIVA_{Ef}$ and MLJD1 interaction could depend on the state of $DivIVA_{Ef}$ oligomerization and/or growth on different carbon sources, which would result in varying levels of ATP and other metabolites. The potential ATP and DNA binding capabilities of MLJD1 could indicate how and when MLJD1 interacts with $DivIVA_{Ef}$. Further research on potential ATP and DNA binding capabilities of MLJD1 needs to be performed in *E. faecalis* to further our understanding of the role of MLJD1 interaction with $DivIVA_{Ef}$ and thus in bacterial cell division. The role of MLJD1 in *E. faecalis* CCR should also be investigated.

In summary, the above B2H results indicate a novel interaction between the central coiled-coils of $DivIVA_{Ef}$ and the CBS domain containing fragment of MLJD1. These results will help devise a model for *E. faecalis* cell division, which may apply to other Gram-positive organisms possessing homologues of DivIVA and MLJD1. If MLJD1 plays a role in *E. faecalis* CCR as its *B. subtilis* homologue CcpN does, future research on MLJD1 and CcpN could identify a link between carbon metabolism and bacterial cell division.

4.3 $DivIVA_{Ef}$ and MLJD1 Localization in *Enterococcus faecalis*

DivIVA in *B. subtilis* and *S. pneumoniae* localizes to the cells poles and, at a later stage of cell division, the site of cell division (Fadda *et al*., 2007, Edwards & Errington, 1997). In both instances DivIVA remains at the nascent and new cell poles to help prevent division at these sites. Previous attempts to localize $DivIVA_{Ef}$ in *E. faecalis* using GFP tagged $DivIVA_{Ef}$

failed due to the formation of inclusion bodies (Rigden, 2005). I used immunofluorescence to show patterns of $DivIVA_{Ef}$ localization in *E. faecalis* JH2-2. I also used immunofluorescence to determine MLJD1 localization patterns in *E. faecalis* JH2-2.

Log phase *E. faecalis* JH2-2 cells were separated into five stages of cell division based on the state of septum formation and constriction, DNA staining of the chromosome, and the localization pattern of $DivIVA_{Ef}$ or MLJD1, as done for localization patterns of *S. pneumoniae* cell division proteins (Fadda *et al*., 2007, Lara *et al.*, 2005, Morlot *et al*., 2003). For localization of $DivIVA_{Sp}$ in *S. pneumoniae* six cell division stages were defined. Fadda *et al.* (2007) found $DivIVA_{Sp}$ to first localize to the cell poles at Stage 1 of cell division, where there is a single cell with a central stained chromosome. $DivIVA_{Sp}$ proceeded to localize to the cell poles and concurrently as an open ring and then as a closed ring at the center of the *S. pneumoniae* cells, in Stages 2 and 3 respectively (Fadda *et al*., 2007). The chromosome at Stages 2 and 3 appeared to elongate and then as two chromosomal masses still in close proximity, respectively (Fadda *et al*., 2007). At Stages 4 and 5, $DivIVA_{Sp}$ appeared as a band or disk at the cell center and remained at the cell poles (Fadda *et al*., 2007). At the final stage of cell division, Stage 6 for *S. pneumoniae*, the daughter cells were fully divided but still attached. The cells in Stage 6 of *S. pneumoniae* appear similar to cells in Stage 3 of cell division, the only difference between the two was the diplococci present in Stage 6 instead of single cells in Stage 3. The general findings indcated $DivIVA_{Sp}$ localized to the old and new cell poles in addition to the new division sites of the dividing daughter cells (Fadda *et al*., 2007).

$DivIVA_{Ef}$ localization in *E. faecalis* was similar to that of $DivIVA_{Sp}$ in *S. pneumoniae*. $DivIVA_{Ef}$ localized diffusely around the entire cell membrane during Stage 1 of *E. faecalis* cell division instead of being concentrated at the cell poles as seen for $DivIVA_{Sp}$. $DivIVA_{Ef}$, in

Stage 2 and 3 of *E. faecalis* cell division, localized to form caps at the lancet shaped poles of the dividing cells. The chromosome at Stages 2 and 3 in *E. faecalis* cell division was similar to *S. pneumoniae*, where it appeared to elongate and then replicate into two chromosomal masses still in close proximity, respectively. However, I did not detect $DivIVA_{Ef}$ to form an open or closed ring at the division site at these stages as reported for $DivIVA_{Sp}$. At Stage 4 of *E. faecalis* cell division, $DivIVA_{Ef}$ localized to the cell poles and at the central division site. In the final stage of *E. faecalis* cell division, Stage 5 where the cells were completely divided but still attached, $DivIVA_{Ef}$ localized as it did in Stage 1, diffused across the entire cell membrane.

Enterococcus faecalis $DivIVA_{Ef}$ localization patterns were similar to *S. pneunoniae* $DivIVA_{Sp}$ localization patterns, despite differences in cell division stages. In both cases DivIVA localizes to the cell poles and eventually concurrently to the cell division site in 80% of *S. pneumoniae* cells and 17% in *E. faecalis* cells. *Enterococcus faecalis* $DivIVA_{Ef}$ appears to localize to the cell division site later in cell division (i.e: Stage 4) than $DivIVA_{Sp}$ in *S. pneumoniae* (i.e: Stage 2 and 3). $DivIVA_{Sp}$ also remains at the cell poles after cell division, while $DivIVA_{Ef}$ tends to be more diffused along the entire cell membrane. Due to differing intensities and levels of background fluorescence as well as no quantitative measures to determine stages of cell division, the immunofluorescence localization of $DivIVA_{Sp}$ and $DivIVA_{Ef}$ are qualitative. As mentitioned previously, I could not differentiate $DivIVA_{Ef}$ localization as a ring, band or disk as the fluorescence was not always that clear (i.e: Stages 2-5 in *S. pneumoniae* cell division). This could be how Fadda *et al* (2007) was able to identify six stages of *S. pneumoniae* cell division whereas I could only identify five stages of *E. faecalis* cell division. Fadda *et al.* (2007) also studied co-localization of $DivIVA_{Sp}$ with $FtsZ_{Sp}$, which helped determine when $DivIVA_{Sp}$ localizes to the cell division site during cell division in reference to the development and progression of the divisome. In *B. subtilis* $DivVIA_{Bs}$ was

tagged with GFP and found to localize to old and new cell poles and concurrently to the division site (Edwards & Errington, 1997). So, in all three species of Gram-positive bacterium, DivVIA localizes to the cell poles and the division site at some point during cell division.

The novel putative cell division protein MLJD1 appeared to localize in a similar pattern as $DivIVA_{Ef}$ in *E. faecalis*, but only at the later stages of cell division. In Stage 1 and Stage 5 MLJD1 localized diffusely at the cell membrane as $DivIVA_{Ef}$ does. As cell division progressed into Stage 2 and 3, MLJD1 localized along the length of the cell, while $DiviVA_{Ef}$ localized to the cell poles. At Stage 4, MLJD1 localized to the cell poles and concurrently to the cell division site, just as $DivIVA_{Ef}$ had. Since the *E. faecalis* cells are so small it was difficult to definitively define where MLJD1 was localizing, particularly when comparing to $DivIVA_{Ef}$ localization. For this reason it would be useful to raise mouse polyclonal primary antibody to MLJD1 so co-immunofluorescence can be performed to further identify the localization of $DivIVA_{Ef}$ and MLJD1. Another issue with comparing $DivIVA_{Ef}$ and MLJD1 immunofluorescence was that the *E. faecalis* cultures fixed for each, $DivIVA_{Ef}$ and MLJD1 respectively, appeared to be in different stages of cell division. Co-immunofluorescence studies of this nature would help determine if $DivIVA_{Ef}$ and MLJD1 localize at the cell poles and cell division site during the same time point. DAPI staining would also be performed to investigate the location of the chromosome in conjunction with $DivIVA_{Ef}$ and MLJD1 localization. Calculating the replication time of the *E. faecalis* cells would also be useful for determining the stage of cell division. Knowing the replication time under specific growth conditions would help define the percentage of cells which are expected to be in the ”C period” or “D period” of chromosomal replication and cell division (Haeusser & Levin, 2008). One could even synchronize the culture, so at specific time points the majority of the cells would be at similar stages of cell division (Cutler & Evans, 1966). It would also be interesting to

investigate formation of the Z-ring in relation to MLJD1 localization as performed for DivIVA in *Streptococcus pneumoniae* (Fadda *et al*., 2007). Improvement of the immunofluorescent technique and co-immunofluorescence is being pursued in our laboratory.

4.4 Proposed Role of MLJD1 in *Enterococcus faecalis* Cell Division

Research of DivIVA interaction with other division proteins is a relatively new area of study. In *Streptococcus pneumoniae* $DivIVA_{Sp}$ was found to interact with cell division proteins FtsZ, FtsA, ZapA, FtsK, FtsL, and PcsB using the B2H assay (Fadda *et al*., 2007, Di Lallo *et al*., 2001). *Enterococcus faecalis* $DivIVA_{Ef}$ interacts with FtsA, FtsZ, FtsQ, and FtsW (Laio *et al*., manuscript in progress). Intriguingly, $DivIVA_{Sp}$ was also found to interact with Spo0J, which is involved in chromosome segregation (Fadda *et al*., 2007, Ben-Yehuda *et al*., 2003). In *B. subtilis*, $DivIVA_{Bs}$ also interacts indirectly with Spo0J; $DivIVA_{Bs}$ interacts with RacA, RacA interacts with Spo0J, and Spo0J interacts with the origin of replication to aid in positioning the chromosome during sporulation (Errington, 2001, Ben-Yehuda *et al*., 2003). Now, we have determined that $DivIVA_{Ef}$ in *E. faecalis* interacts with a novel division protein, MLJD1, which also possesses a potential DNA binding domain. MLJD1 could thus be a bridge between $DivIVA_{Ef}$ and the chromosome, aiding in segregation of the daughter chromosomes and migration towards opposite poles of the dividing cell.

In *B. subtilis* it is known that the interaction between $DivIVA_{Bs}$ and MinD is vital for normal cell division, but direct interaction between $DivIVA_{Bs}$ and MinD or MinC could not be detected. Two recent studies revealed the finding of a protein, MinJ, which interacts with $DivIVA_{Bs}$ and MinD (Patrick & Kearns, 2008, Bramkamp *et al.*, 2008). It was proposed that MinJ functions as a bridge between $DivIVA_{Bs}$ and MinD allowing $DivIVA_{Bs}$ to sequester the FtsZ inhibitor MinCD complex to the old and new cell poles of *B. subtilis* in order to constrict cell division to the midcell site (Bramkamp *et al*., 2008, Patrick & Kearns, 2008). *E. faecalis*

does not contain MinC, MinD, or MinJ, but we have demonstrated a direct interaction between $DivIVA_{Ef}$ and the novel putative division protein MLJD1. As mentioned previously, MLJD1 could potentially act as a bridge between $DivIVA_{Ef}$ and the chromosome much like MinJ acts as a bridge between $DivIVA_{Bs}$ and MinCD complex. This $DivIVA_{Ef}$~MLJD1~chromosome bridge model could explain how $DivIVA_{Ef}$ was previously described as essential for *E. faecalis* chromosome segregation (Ramirez-Arcos *et al*., 2005). MLJD1 could also be interacting with an additional yet undiscovered protein which, along with $DivIVA_{Ef}$, could in turn be responsible for midcell positioning of the division site in a similar manner as $DivIVA_{Bs}$~MinJ~MinCD performs this midcell site selection function.

MLJD1 in *E. faecalis* may also play a role in carbon catabolite repression (CCR) as does the *B. subtilis* homologue, CcpN. The role of CcpN or MLJD1 in cell division and CCR may depend on ATP levels and the presence of different metabolites during growth on varying carbon sources (Tannler *et al*., 2008, Servant *et al*., 2005). A link between bacterial cell division and carbon metabolism could help explain a dynamic mechanism used to control growth rates on various carbon sources. A knockout of *ccpN* in *B. subtilis* resulted in a reduced growth rate when grown on glucose because *pckA* and *gapB* were derepressed (Tannler *et al*., 2008, Servant *et al*., 2005). Derepression of these gluconeogenic genes caused a deficiency of TCA cycle intermediates and ATP levels (Tannler *et al*., 2008). Wild type growth rates were restored in a *ccpN pckA* double knockout or supplementation with various TCA cycle intermediates (Tannler *et al*., 2008). While the *B. subtilis ccpN* knockout demonstrated a decreased growth rate on glucose it showed an increased growth rate when grown on non-sugar alternative carbon sources (Servant *et al*., 2005). This may indicate CcpN controls the rate of *B. subtilis* cell division when growing on these alternative carbon sources. A potential role for CcpN in bacterial cell division was not reported as there were no reports of the physiological

phenotypes of the *ccpN* knockout. Our laboratory is currently working on a *B. subtilis ccpN* knockout to identify its chromosome segregation and cell division capabilities. This research will may provide a link between *B. subtilis* cell division and metabolism and help form future experiments to determine the role of MLJD1 in *E. faecalis*.

To determine if MLJD1 is forming a bridge between $DivIVA_{Ef}$ and the chromosome future research on MLJD1 DNA binding capabilities is vital. Once an association between MLJD1 and the chromosome can be made, mutations could be introduced in an attempt to disrupt this association to determine if MLJD1 is required for proper chromosome segregation. Due to the localization of MLJD1 along the length of *E. faecalis* cells during early cell division, MLJD1 could be acting as a nucleoid occlusion protein to prevent divisome formation and closure on replicating chromosomes. Further research can also be performed to determine if MLJD1 is capable of interacting with other known or hither to unknown division proteins and if MLJD1 plays a role in *E. faecalis* CCR.

4.5 Conclusions

The current study provides evidence that the N-terminal coiled-coil and oligomerization capabilities of $DivIVA_{Ef}$ are essential for its biological function in *Enterococcus faecalis* cell division. I also determined that $DivIVA_{Ef}$ localizes to the cell poles and eventually concurrently to the site of cell division. MLJD1 also appeared to localize along the length of *E. faecalis* during the first stages of cell division and eventually to the poles and concurrently to the site of cell division. These initial immunofluorescence experiments of MLJD1 localization provided evidence that MLJD1 and $DivIVA_{Ef}$ may co-localize during late cell division. Co-immunofluorescence of $DivIVA_{Ef}$ and MLJD1 in *E. faecalis* is currently being explored in our laboratory to refine our understanding of $DivIVA_{Ef}$ and MLJD1 localization.

Furthermore, I demonstrated the positive interaction between $DivIVA_{Ef}$ and a fragment of MLJD1 containing two CBS domains using the *in vivo* Bacterial Two-Hybrid (B2H) system (Di Lallo *et al*., 2001). However, I was not able to determine the region of $DivIVA_{Ef}$ which interacts with MLJD1 or detect interaction between $DivIVA_{Ef}$ and full length MLJD1 using the B2H system. The interaction between $DivIVA_{Ef}$ and MLJD1 could be quite dynamic given potential DNA binding, as shown for the *B. subtilis* homologue CcpN, and ATP binding capabilities of MLJD1, which will be investigated in future research. This research on *E. faecalis* $DivIVA_{Ef}$ and MLJD1 has set a strong base for future research, so a novel model of cell division in Gram-positive cocci can be developed. Determination of the involvement of MLJD1 in gluconeogenesis in *E. faecalis* and further research in the involvement of CcpN in *B. subtilis* cell division could help elucidate a potential link between bacterial cell metabolism and cell division in various Gram-positive organisms.

Appendix A

Bacterial Two-Hybrid Assay: How the System Works and Resolving Complications

The Bacterial two-hybrid (B2H) assay is a β-galactosidase (β-gal) assay which is utilized to study protein-protein interaction by determining the amount of β-gal produced in response to whether two proteins interact or not. In this system developed by Di Lallo *et al*. (2001), the *E. coli* R721 reporter strain contains a chimeric operator sequence controlling a *lacZ* gene in the chromosome (Fig A1). The plasmids used in this B2H system, pcI_{434} and pcI_{P22}, encoded for a fusion protein consisting of the N-terminal of the repressor protein from phage 434 or phage P22, respectively, with the protein being studied ("x" or "y" in Fig A1) whose gene is cloned into the pcI_{434} and pcI_{P22} plasmids. The N-terminal repressor portion recognizes and binds to the operator sequence. The reporter strain was transformed with pcI_{434} and pcI_{P22}, each plasmid carrying the genes of the proteins under study, to test either self-interaction or interaction with different proteins. Reciprocal cloned vectors should also be tested for interaction. If the proteins (s) under study interact they will dimerize causing the N-terminal repressors to match the chimeric operator sequence. In turn the *lacZ* gene will be repressed resulting in a decreased production of β-gal as compared to *E. coli* R721 background β-gal activity when no plasmid is present. Each B2H plasmids used in the study were also transformed seperately into *E. coli* R721 to check for significant background repression.

The B2H assay is not without its complications. First, the pcI_{434}-linker plasmid is a low copy plasmid while the pcI_{P22}-linker plasmid is a high copy plasmid (Di Lallo *et al*., 2001). *E. coli* R721 carrying the pcI_{P22}-linker plasmid typically grows slower, or sometimes not at all, after being sub-cultured from overnight culture to grow the log phase culture. For the slow

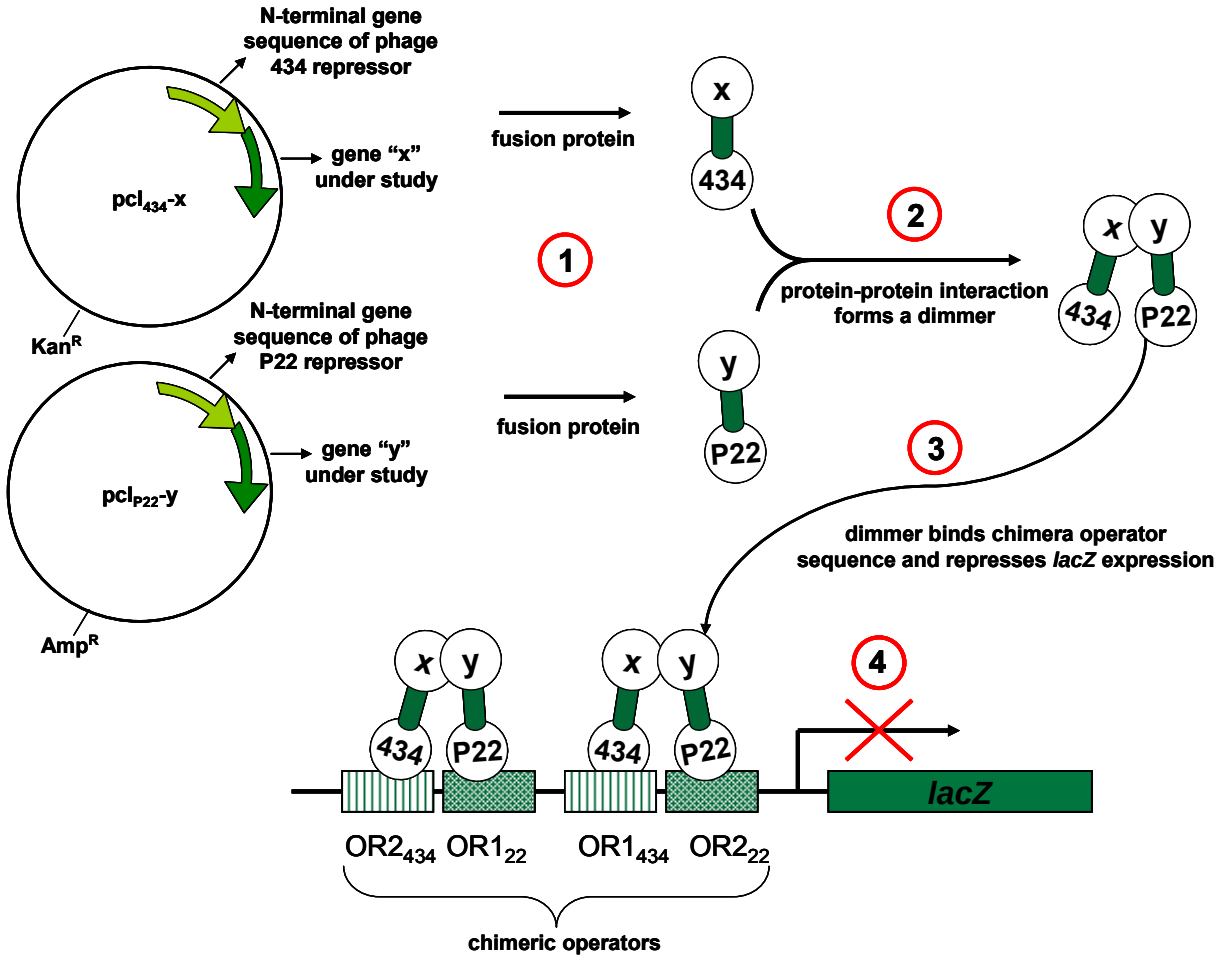

Figure A1: The Bacterial Two-Hybrid system developed by Di Lallo *et al*. (2001). Genes encoding proteins of interest, "x" or "y", are cloned into pcI434 and pcIP22 to 1) create a fusion with the N-terminal of the repressor proteins for phages 434 or P22, respectively. 2) If proteins "x" and "y" interact they form a dimmer which 3) binds to the chimeric operator located on the *E. coli* R721 chromosome and thus 4) represses *lacZ* expression. Detection of interaction is measured by a >50% reduction of β-galactosidase produced as compared to *E. coli* R721 containing no plasmids (Di Lallo *et al*., 2003, Di Lallo *et al*., 2001, Fadda *et al*., 2007).

growing cultures a 1:50 dilution was made instead of the 1:100 dilution used by Di Lallo *et al*. (2001). Some of the slow growing cultures would also be left to grow for 3-3.5 hr instead of the 2-2.5 hr for the samples growing at a normal rate, to improve the OD_{650}. All samples were also grown at 34 ^{0}C to slow down protein production as to not overwhelm the cells with protein and thus ensure cell survival.

DivIVA$_{Ef}$ is known to affect *E. coli* cell division, creating filamentous cells when over-expressed (Rigden *et al*., 2008). Overexpression of proteins from the high copy plasmids pcI$_{P22}$-linker could thus also affect growth rates of the cultures by impeding cell division in the host strain. The ratio of proteins may have also been affected by the expression from a high or low copy plasmid. Differences between reciprocal results may be due to the protein interaction reliability based on a particular ratio of one protein to the other. A Western blot was performed to ascertain DivIVA$_{Ef}$ levels in *E. coli* R721 transformed with pdivIVA434/pdivIVA22 (double transformation), pdivIVA434, pdivIVA22, and R721 with no plasmid (Fig A2). One would expect greater DivIVA$_{Ef}$ production from *E. coli* R721 transformed with pdivIVA22, the high copy plasmid, as compared to pdivIVA434, the low copy plasmid, upon induction with IPTG. However, the opposite was observed (Fig II.2). The *E. coli* R721 sample with pdivIVA434 and both pdivIVA434 and pdivIVA22 showed increased DivIVA$_{Ef}$ production when induced with IPTG, whereas the sample with pdivIVA22 alone did not produce more DivIVA$_{Ef}$ (Fig II.2). Because pdivIVA22 is a high copy plasmid DivIVA$_{Ef}$ (fused to N-terminal of phage P22) may be produced in high enough quantities to form inclusion bodies. The inclusion bodies would not be soluble and therefore the P22 N-terminal-DivIVA$_{Ef}$ fusion protein would not be detected in the Western blot. To check for inclusion bodies I would sonicate *E. coli* R721 carrying pdivIVA22 and centrifuge at 25000 rpm to collect insoluble fractions. I would keep a sample of the supernatant to check it for protein.

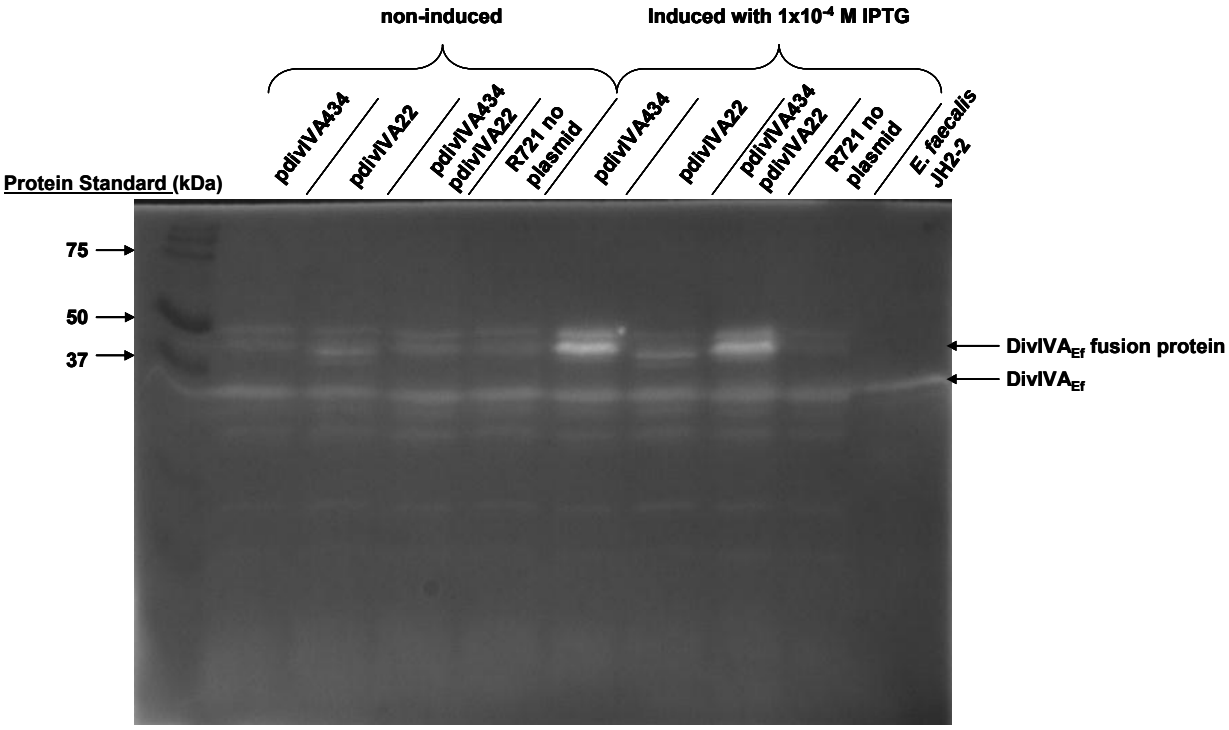

Figure A2: Western blot of *E. coli* R721 transformed with indicated B2H plasmids. The samples were grown to exponential phase by following the same method used for performing a bacterial two-hybrid β-galactosidase assay (see section 2.5). The experiment was repeated once.

I would then add 8M urea to the collected pellet to suspend potential inclusion bodies. I would do a Western blot of the supernatant sample and the inclusion body sample to compare. Inclusion bodies could also explain why *E. coli* R721 carrying pcI_{P22} or its derivatives did not typically grow well. Also note that $DivIVA_{Ef}$, predicted to have a molecular weight of 27 kDa appears to have a higher molecular weight after SDS-PAGE electrophoresis. This aberration in $DivIVA_{Ef}$ migration is most likely due to the charge of $DivIVA_{Ef}$ as described in Rigden *et al*. (Rigden *et al*., 2008).

To obtain reproducible results with repeated B2H assays it was important to use the same Z-buffer and prepare fresh assay reagents. The same stock of IPTG was also used for repeated experiments to reduce small variations of concentration. Due to damage of freeze-thawing of stock *E. coli* R721 it is also important to re-transform the B2H plasmids if the assay, which was previously working, starts yielding inconsistent results.

5.0 References

Addinall, S. G. & B. Holland, (2002) The tubulin ancestor, FtsZ, draughtsman, designer and driving force for bacterial cytokinesis. *J Mol Biol* **318**: 219-236.

Akiyama, T., S. Inouye & T. Komano, (2003) Novel developmental genes, *fruCD*, of *Myxococcus xanthus*: involvement of a cell division protein in multicellular development. *J Bacteriol* **185**: 3317-3324.

Bateman, A., (1997) The structure of a domain common to archaebacteria and the homocystinuria disease protein. *Trends Biochem Sci* **22**: 12-13.

Begg, K. J. & W. D. Donachie, (1985) Cell shape and division in *Escherichia coli*: experiments with shape and division mutants. *J Bacteriol* **163**: 615-622.

Ben-Yehuda, S., D. Z. Rudner & R. Losick, (2003) RacA, a bacterial protein that anchors chromosomes to the cell poles. *Science* **299**: 532-536.

Bernhardt, T. G. & P. A. de Boer, (2005) SlmA, a nucleoid-associated, FtsZ binding protein required for blocking septal ring assembly over Chromosomes in *E. coli*. *Mol Cell* **18**: 555-564.

Bi, E. F. & J. Lutkenhaus, (1991) FtsZ ring structure associated with division in *Escherichia coli*. *Nature* **354**: 161-164.

Biemans-Oldehinkel, E., N. A. Mahmood & B. Poolman, (2006) A sensor for intracellular ionic strength. *Proc Natl Acad Sci U S A* **103**: 10624-10629.

Bramkamp, M., R. Emmins, L. Weston, C. Donovan, R. A. Daniel & J. Errington, (2008) A novel component of the division site selection system of *Bacillus subtilis* and a new mode of action for the division inhibitor MinCD. *Mol Microbiol*.

Callegan, M. C., M. C. Booth, B. D. Jett & M. S. Gilmore, (1999) Pathogenesis of gram-positive bacterial endophthalmitis. *Infect Immun* **67**: 3348-3356.

Cetinkaya, Y., P. Falk & C. G. Mayhall, (2000) Vancomycin-resistant enterococci. *Clin Microbiol Rev* **13**: 686-707.

Cha, J. H. & G. C. Stewart, (1997) The divIVA minicell locus of *Bacillus subtilis*. *J Bacteriol* **179**: 1671-1683.

Clewell, D. B., (1981) Plasmids, drug resistance, and gene transfer in the genus *Streptococcus*. *Microbiol Rev* **45**: 409-436.

Cutler, R. G. & J. E. Evans, (1966) Synchronization of bacteria by a stationary-phase method. *J Bacteriol* **91**: 469-476.

de Boer, P. A., R. E. Crossley & L. I. Rothfield, (1989) A division inhibitor and a topological specificity factor coded for by the minicell locus determine proper placement of the division septum in *E. coli*. *Cell* **56**: 641-649.

Den Blaauwen, T., N. Buddelmeijer, M. E. Aarsman, C. M. Hameete & N. Nanninga, (1999) Timing of FtsZ assembly in *Escherichia coli*. *J Bacteriol* **181**: 5167-5175.

Di Lallo, G., L. Castagnoli, P. Ghelardini & L. Paolozzi, (2001) A two-hybrid system based on chimeric operator recognition for studying protein homo/heterodimerization in *Escherichia coli*. *Microbiology* **147**: 1651-1656.

Di Lallo, G., M. Fagioli, D. Barionovi, P. Ghelardini & L. Paolozzi, (2003) Use of a two-hybrid assay to study the assembly of a complex multicomponent protein machinery: bacterial septosome differentiation. *Microbiology* **149**: 3353-3359.

Edwards, D. H. & J. Errington, (1997) The *Bacillus subtilis* DivIVA protein targets to the division septum and controls the site specificity of cell division. *Mol Microbiol* **24**: 905-915.

Edwards, D. H., H. B. Thomaides & J. Errington, (2000) Promiscuous targeting of *Bacillus subtilis* cell division protein DivIVA to division sites in *Escherichia coli* and fission yeast. *EMBO J* **19**: 2719-2727.

Eisenberg, M. A. & S. C. Hsiung, (1982) Mode of action of the biotin antimetabolites actithiazic acid and alpha-methyldethiobiotin. *Antimicrob Agents Chemother* **21**: 5-10.

Eisenberg, M. A., O. Prakash & S. C. Hsiung, (1982) Purification and properties of the biotin repressor. A bifunctional protein. *J Biol Chem* **257**: 15167-15173.

Errington, J., (2001) Septation and chromosome segregation during sporulation in *Bacillus subtilis*. *Curr Opin Microbiol* **4**: 660-666.

Fadda, D., C. Pischedda, F. Caldara, M. B. Whalen, D. Anderluzzi, E. Domenici & O. Massidda, (2003) Characterization of *divIVA* and other genes located in the chromosomal region downstream of the *dcw* cluster in *Streptococcus pneumoniae*. *J Bacteriol* **185**: 6209-6214.

Fadda, D., A. Santona, V. D'Ulisse, P. Ghelardini, M. G. Ennas, M. B. Whalen & O. Massidda, (2007) *Streptococcus pneumoniae* DivIVA: localization and interactions in a MinCD-free context. *J Bacteriol* **189**: 1288-1298.

Flardh, K., (2003a) Essential role of DivIVA in polar growth and morphogenesis in *Streptomyces coelicolor* A3(2). *Mol Microbiol* **49**: 1523-1536.

Flardh, K., (2003b) Growth polarity and cell division in *Streptomyces*. *Curr Opin Microbiol* **6**: 564-571.

Francis, F., S. Ramirez-Arcos, H. Salimnia, C. Victor & J. R. Dillon, (2000) Organization and transcription of the division cell wall (*dcw*) cluster in *Neisseria gonorrhoeae*. *Gene* **251**: 141-151.

Goehring, N. W. & J. Beckwith, (2005) Diverse paths to midcell: assembly of the bacterial cell division machinery. *Curr Biol* **15**: R514-526.

Haeusser, D. P. & P. A. Levin, (2008) The great divide: coordinating cell cycle events during bacterial growth and division. *Curr Opin Microbiol* **11**: 94-99.

Hamoen, L. W. & J. Errington, (2003) Polar targeting of DivIVA in *Bacillus subtilis* is not directly dependent on FtsZ or PBP 2B. *J Bacteriol* **185**: 693-697.

Harry, E. J., (2001) Bacterial cell division: regulating Z-ring formation. *Mol Microbiol* **40**: 795-803.

Harry, E. J. & P. J. Lewis, (2003) Early targeting of Min proteins to the cell poles in germinated spores of *Bacillus subtilis*: evidence for division apparatus-independent recruitment of Min proteins to the division site. *Mol Microbiol* **47**: 37-48.

Hu, Z. & J. Lutkenhaus, (2001) Topological regulation of cell division in *E. coli*. spatiotemporal oscillation of MinD requires stimulation of its ATPase by MinE and phospholipid. *Mol Cell* **7**: 1337-1343.

Hu, Z., A. Mukherjee, S. Pichoff & J. Lutkenhaus, (1999) The MinC component of the division site selection system in *Escherichia coli* interacts with FtsZ to prevent polymerization. *Proc Natl Acad Sci U S A* **96**: 14819-14824.

Jacob, A. E. & S. J. Hobbs, (1974) Conjugal transfer of plasmid-borne multiple antibiotic resistance in *Streptococcus faecalis var. zymogenes*. *J Bacteriol* **117**: 360-372.

Jones, J. M., S. C. Yost & P. A. Pattee, (1987) Transfer of the conjugal tetracycline resistance transposon Tn916 from *Streptococcus faecalis* to *Staphylococcus aureus* and identification of some insertion sites in the staphylococcal chromosome. *J Bacteriol* **169**: 2121-2131.

Kemp, B. E., (2004) Bateman domains and adenosine derivatives form a binding contract. *J Clin Invest* **113**: 182-184.

Lara, B., A. I. Rico, S. Petruzzelli, A. Santona, J. Dumas, J. Biton, M. Vicente, J. Mingorance & O. Massidda, (2005) Cell division in cocci: localization and properties of the *Streptococcus pneumoniae* FtsA protein. *Mol Microbiol* **55**: 699-711.

Licht, A., R. Golbik & S. Brantl, (2008) Identification of ligands affecting the activity of the transcriptional repressor CcpN from *Bacillus subtilis*. *J Mol Biol* **380**: 17-30.

Lloyd, S. E., W. Gunther, S. H. Pearce, A. Thomson, M. L. Bianchi, M. Bosio, I. W. Craig, S. E. Fisher, S. J. Scheinman, O. Wrong, T. J. Jentsch & R. V. Thakker, (1997) Characterisation of renal chloride channel, CLCN5, mutations in hypercalciuric nephrolithiasis (kidney stones) disorders. *Hum Mol Genet* **6**: 1233-1239.

Lupas, A., (1996a) Coiled coils: new structures and new functions. *Trends Biochem Sci* **21**: 375-382.

Lupas, A., (1996b) Prediction and analysis of coiled-coil structures. *Methods Enzymol* **266**: 513-525.

Lupas, A., M. Van Dyke & J. Stock, (1991) Predicting coiled coils from protein sequences. *Science* **252**: 1162-1164.

Margolin, W., (2000) Themes and variations in prokaryotic cell division. *FEMS Microbiol Rev* **24**: 531-548.

Margolin, W., (2001) Spatial regulation of cytokinesis in bacteria. *Curr Opin Microbiol* **4**: 647-652.

Margolin, W., (2003) Bacterial division: the fellowship of the ring. *Curr Biol* **13**: R16-18.

Margolin, W., (2005) FtsZ and the division of prokaryotic cells and organelles. *Nat Rev Mol Cell Biol* **6**: 862-871.

Marston, A. L. & J. Errington, (1999) Selection of the midcell division site in *Bacillus subtilis* through MinD-dependent polar localization and activation of MinC. *Mol Microbiol* **33**: 84-96.

Marston, A. L., H. B. Thomaides, D. H. Edwards, M. E. Sharpe & J. Errington, (1998) Polar localization of the MinD protein of *Bacillus subtilis* and its role in selection of the mid-cell division site. *Genes Dev* **12**: 3419-3430.

Massidda, O., D. Anderluzzi, L. Friedli & G. Feger, (1998) Unconventional organization of the division and cell wall gene cluster of *Streptococcus pneumoniae*. *Microbiology* **144 (Pt 11)**: 3069-3078.

Miyagishima, S. Y., C. P. Wolk & K. W. Osteryoung, (2005) Identification of cyanobacterial cell division genes by comparative and mutational analyses. *Mol Microbiol* **56**: 126-143.

Morlot, C., A. Zapun, O. Dideberg & T. Vernet, (2003) Growth and division of *Streptococcus pneumoniae*: localization of the high molecular weight penicillin-binding proteins during the cell cycle. *Mol Microbiol* **50**: 845-855.

Muchova, K., E. Kutejova, L. Pribisova, A. J. Wilkinson & I. Barak, (2002a) *Bacillus subtilis* division protein DivIVA - screen for stable oligomer state conditions. *Acta Crystallogr D Biol Crystallogr* **58**: 1542-1543.

Muchova, K., E. Kutejova, D. J. Scott, J. A. Brannigan, R. J. Lewis, A. J. Wilkinson & I. Barak, (2002b) Oligomerization of the *Bacillus subtilis* division protein DivIVA. *Microbiology* **148**: 807-813.

Mukherjee, A. & J. Lutkenhaus, (1998) Dynamic assembly of FtsZ regulated by GTP hydrolysis. *EMBO J* **17**: 462-469.

Mulder, E. & C. L. Woldringh, (1989) Actively replicating nucleoids influence positioning of division sites in *Escherichia coli* filaments forming cells lacking DNA. *J Bacteriol* **171**: 4303-4314.

Patrick, J. E. & D. B. Kearns, (2008) MinJ (YvjD) is a topological determinant of cell division in *Bacillus subtilis*. *Mol Microbiol* **70**: 1166-1179.

Perry, S. E. & D. H. Edwards, (2004) Identification of a polar targeting determinant for *Bacillus subtilis* DivIVA. *Mol Microbiol* **54**: 1237-1249.

Pichoff, S. & J. Lutkenhaus, (2001) *Escherichia coli* division inhibitor MinCD blocks septation by preventing Z-ring formation. *J Bacteriol* **183**: 6630-6635.

Pinho, M. G. & J. Errington, (2004) A *divIVA* null mutant of *Staphylococcus aureus* undergoes normal cell division. *FEMS Microbiol Lett* **240**: 145-149.

Ponting, C. P., (1997) CBS domains in CIC chloride channels implicated in myotonia and nephrolithiasis (kidney stones). *J Mol Med* **75**: 160-163.

Poyart, C. & P. Trieu-Cuot, (1997) A broad-host-range mobilizable shuttle vector for the construction of transcriptional fusions to beta-galactosidase in gram-positive bacteria. *FEMS Microbiol Lett* **156**: 193-198.

Ramirez-Arcos, S., V. Greco, H. Douglas, D. Tessier, D. Fan, J. Szeto, J. Wang & J. R. Dillon, (2004) Conserved glycines in the C terminus of MinC proteins are implicated in their functionality as cell division inhibitors. *J Bacteriol* **186**: 2841-2855.

Ramirez-Arcos, S., M. Liao, S. Marthaler, M. Rigden & J. A. Dillon, (2005) *Enterococcus faecalis divIVA*: an essential gene involved in cell division, cell growth and chromosome segregation. *Microbiology* **151**: 1381-1393.

Ramirez-Arcos, S., H. Salimnia, I. Bergevin, M. Paradis & J. A. Dillon, (2001a) Expression of *Neisseria gonorrhoeae* cell division genes *ftsZ*, *ftsE* and *minD* is influenced by environmental conditions. *Res Microbiol* **152**: 781-791.

Ramirez-Arcos, S., J. Szeto, T. Beveridge, C. Victor, F. Francis & J. Dillon, (2001b) Deletion of the cell-division inhibitor MinC results in lysis of *Neisseria gonorrhoeae*. *Microbiology* **147**: 225-237.

Ramirez-Arcos, S., J. Szeto, J. A. Dillon & W. Margolin, (2002) Conservation of dynamic localization among MinD and MinE orthologues: oscillation of *Neisseria gonorrhoeae* proteins in *Escherichia coli*. *Mol Microbiol* **46**: 493-504.

Ramos, A., M. P. Honrubia, N. Valbuena, J. Vaquera, L. M. Mateos & J. A. Gil, (2003) Involvement of DivIVA in the morphology of the rod-shaped actinomycete *Brevibacterium lactofermentum*. *Microbiology* **149**: 3531-3542.

Real, G. & A. O. Henriques, (2006) Localization of the *Bacillus subtilis murB* gene within the *dcw* cluster is important for growth and sporulation. *J Bacteriol* **188**: 1721-1732.

Reeve, J. N., N. H. Mendelson, S. I. Coyne, L. L. Hallock & R. M. Cole, (1973) Minicells of *Bacillus subtilis*. *J Bacteriol* **114**: 860-873.

Reizer, J., V. Michotey, A. Reizer & M. H. Saier, Jr., (1994) Novel phosphotransferase system genes revealed by bacterial genome analysis: unique, putative fructose- and glucoside-specific systems. *Protein Sci* **3**: 440-450.

Rigden, M. D., (2005) Determining the role of coiled-coil domain interactions in the oligomerization of DivIVA from *Enterococcus faecalis*. In: Department of Biochemistry, Microbiology and Immunology; MSc. Thesis. Ottawa: University of Ottawa, pp. 96.

Rigden, M. D., C. Baier, S. Ramirez-Arcos, M. Liao, M. Wang & J. A. Dillon, (2008) Identification of the Coiled-coil Domains of *Enterococcus faecalis* DivIVA that

Mediate Oligomerization and their Importance for Biological Function. *J Biochem* **144**: 63-76.

Rothfield, L. I. & S. S. Justice, (1997) Bacterial cell division: the cycle of the ring. *Cell* **88**: 581-584.

Rothfield, L. I., Y. L. Shih & G. King, (2001) Polar explorers: membrane proteins that determine division site placement. *Cell* **106**: 13-16.

Sambrook, J., E.F. Fritschand and T. Maniatis, (1980) *Molecular Cloning: A Laboratory Manual*. Cold Spring Harbor Press, New York.

Sambrook, J., Russell, D., (2001) *Molecular Cloning: A Laboratory Manual,* p. 1.116-111.118. Cold Spring Harbor Laboratory Press, Cold Spring Harbor NY.

Servant, P., D. Le Coq & S. Aymerich, (2005) CcpN (YqzB), a novel regulator for CcpA-independent catabolite repression of *Bacillus subtilis* gluconeogenic genes. *Mol Microbiol* **55**: 1435-1451.

Shepard, B. D. & M. S. Gilmore, (1995) Electroporation and efficient transformation of *Enterococcus faecalis* grown in high concentrations of glycine. *Methods Mol Biol* **47**: 217-226.

Shih, Y. L., T. Le & L. Rothfield, (2003) Division site selection in *Escherichia coli* involves dynamic redistribution of Min proteins within coiled structures that extend between the two cell poles. *Proc Natl Acad Sci U S A* **100**: 7865-7870.

Shiomi, D. & W. Margolin, (2007) The C-terminal domain of MinC inhibits assembly of the Z ring in *Escherichia coli*. *J Bacteriol* **189**: 236-243.

Sintchak, M. D., M. A. Fleming, O. Futer, S. A. Raybuck, S. P. Chambers, P. R. Caron, M. A. Murcko & K. P. Wilson, (1996) Structure and mechanism of inosine monophosphate dehydrogenase in complex with the immunosuppressant mycophenolic acid. *Cell* **85**: 921-930.

Sun, Q., X. C. Yu & W. Margolin, (1998) Assembly of the FtsZ ring at the central division site in the absence of the chromosome. *Mol Microbiol* **29**: 491-503.

Tannler, S., E. Fischer, D. Le Coq, T. Doan, E. Jamet, U. Sauer & S. Aymerich, (2008) CcpN controls central carbon fluxes in *Bacillus subtilis*. *J Bacteriol* **190**: 6178-6187.

Thomaides, H. B., M. Freeman, M. El Karoui & J. Errington, (2001) Division site selection protein DivIVA of *Bacillus subtilis* has a second distinct function in chromosome segregation during sporulation. *Genes Dev* **15**: 1662-1673.

Tobisch, S., J. Stulke & M. Hecker, (1999) Regulation of the *lic* operon of *Bacillus subtilis* and characterization of potential phosphorylation sites of the LicR regulator protein by site-directed mutagenesis. *J Bacteriol* **181**: 4995-5003.

Vicente, M. & J. Errington, (1996) Structure, function and controls in microbial division. *Mol Microbiol* **20**: 1-7.

Weiss, D. S., (2004) Bacterial cell division and the septal ring. *Mol Microbiol* **54**: 588-597.

Wilson, K. P., L. M. Shewchuk, R. G. Brennan, A. J. Otsuka & B. W. Matthews, (1992) *Escherichia coli* biotin holoenzyme synthetase/bio repressor crystal structure delineates the biotin- and DNA-binding domains. *Proc Natl Acad Sci U S A* **89**: 9257-9261.

Woldringh, C. L., E. Mulder, P. G. Huls & N. Vischer, (1991) Toporegulation of bacterial division according to the nucleoid occlusion model. *Res Microbiol* **142**: 309-320.

Wu, L. J. & J. Errington, (2004) Coordination of cell division and chromosome segregation by a nucleoid occlusion protein in *Bacillus subtilis*. *Cell* **117**: 915-925.

Wu, L. J., A. H. Franks & R. G. Wake, (1995) Replication through the terminus region of the *Bacillus subtilis* chromosome is not essential for the formation of a division septum that partitions the DNA. *J Bacteriol* **177**: 5711-5715.

Yu, X. C. & W. Margolin, (1999) FtsZ ring clusters in min and partition mutants: role of both the Min system and the nucleoid in regulating FtsZ ring localization. *Mol Microbiol* **32**: 315-326.

Zhang, R., G. Evans, F. J. Rotella, E. M. Westbrook, D. Beno, E. Huberman, A. Joachimiak & F. R. Collart, (1999) Characteristics and crystal structure of bacterial inosine-5'-monophosphate dehydrogenase. *Biochemistry* **38**: 4691-4700.